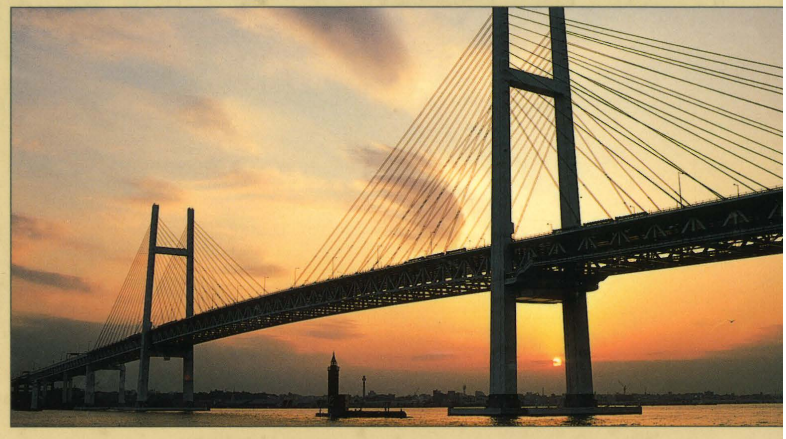


MACMILLAN TECHNOLOGY SERIES

ADSL/VDSL PRINCIPLES

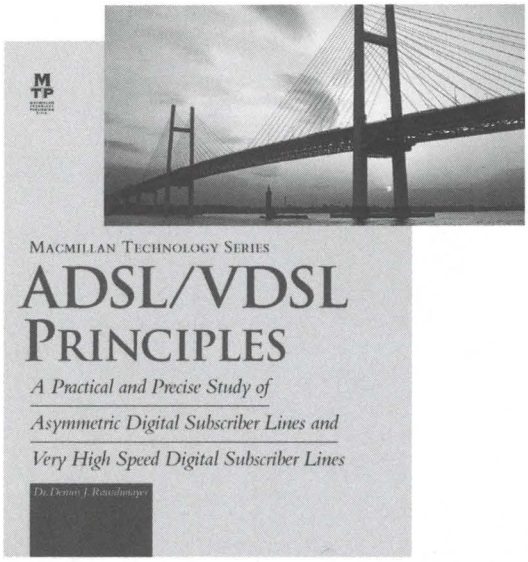
A Practical and Precise Study of

Asymmetric Digital Subscriber Lines and

Very High Speed Digital Subscriber Lines

Dr. Dennis J. Rauschmayer

ENTROPIC EXHIBIT 2017
DISH v. Entropic
IPR2024-00373



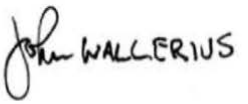
Copyright 1998

YOKOHAMA BAY BRIDGE

Yokohama, Japan

The Stock Market

Opened in 1989 as the gateway of the Port of Yokohama, the Yokohama Bay Bridge plays important roles in both waterfront development of the Bay of Tokyo and relaxation of the traffic situation of Yokohama City. A cable braced bridge of double girders with a 460 meter span between towers (total length of 860 meters), the Yokohama Bay Bridge is the second largest of its type in the world. The bridge is accented with a pedestrian walkway on the underbelly, which extends to an observation deck, called the Sky Walk, that offers breathtaking views of the harbor.


WALLERIUS

ADSL/VDSL PRINCIPLES:

A Practical and Precise Study of Asymmetric Digital Subscriber Lines and Very High Speed Digital Subscriber Lines

Dr. Dennis J. Rauschmayer

MTP
MACMILLAN TECHNICAL PUBLISHING U·S·A

ADSL/VDSL Principles

By Dr. Dennis J. Rauschmayer

Published by:
Macmillan Technical Publishing
201 West 103rd Street
Indianapolis, IN 46290 USA

All rights reserved. No part of this book may be reproduced or transmitted in any form or by any means, electronic or mechanical, including photocopying, recording, or by any information storage and retrieval system, without written permission from the publisher, except for the inclusion of brief quotations in a review.

Copyright © 1999 by Macmillan Technical Publishing

Printed in the United States of America 1 2 3 4 5 6 7 8 9 0

02 01 00 99 4 3 2 1

Library of Congress Cataloging-in-Publication Data

Library of Congress Cataloging Number: 96-80467

ISBN: 1-57870-015-9

Universal Product Code: 619472001592

Warning and Disclaimer

This book is designed to provide information about Digital Subscriber Line technology. Every effort has been made to make this book as complete and as accurate as possible, but no warranty or fitness is implied.

The information is provided on an "as is" basis. The authors and Macmillan Technical Publishing shall have neither liability nor responsibility to any person or entity with respect to any loss or damages arising from the information contained in this book or from the use of the disks or programs that may accompany it.

Trademark Acknowledgments

All terms mentioned in this book that are known to be trademarks or service marks have been appropriately capitalized. Macmillan Technical Publishing cannot attest to the accuracy of this information. Use of a term in this book should not be regarded as affecting the validity of any trademark or service mark.

Development Editor
Brad Miser
Christopher Cleveland

Project Editor
Dayna Isley

Copy Editors
Geneil Breeze
June Waldman

Technical Reviewer
Jacky Chow

Team Coordinator
Amy Lewis

Manufacturing Coordinator
Brook Farling

Book Designer
Anne Jones

Cover Designer
Sandra Schroeder

Cover Production
Aren Howell

Director of Production
Larry Klein

Production Manager
Laurie Casey

Graphics Image Specialist
Oliver Jackson

Production Team
Louis Porter, Jr.

Indexer
Bront Davis

Proofreader
Mary Ellen Stephenson

Acknowledgments

Writing this book was a great experience. Along the way, interactions with many of the people working on the standardization, design, and development of high-speed communications over copper increased my knowledge of the subject matter tenfold. I tip my hat to these engineers. This field truly has a bright future.

I must extend my thanks to the many folks who reviewed and contributed creative ideas to this text, including Chuck Stanski, Jeremy Nightingale, Debbie Wisniewski, and Jack Waller. A special thanks also goes out to Technical Editor Jacky Chow and Development Editor Brad Miser for playing an integral part in the development of this manuscript, as well as to the crew at Macmillan: Chris Cleveland, David Gibson, Tracy Hughes, and Dayna Isley.

Personally, I am indebted to many for the support I've received over the past year, including the fine folks at Pulsecom, especially Gerhard Pilcher, and my family—my sisters Eileen, Kathy, Joan, Nancy, Mary, Carol, and Linda; my brothers Joe and Rich; and most especially my mother.

About the Author

Dr. Dennis J. Rauschmayer received a B.S. (summa cum laude) degree in electrical engineering in 1992 from Wilkes University, an M.S.E.E. degree from The George Washington University in 1994, and a Ph.D. in electrical engineering from Temple University in 1997.

From 1992 to 1996, Dr. Rauschmayer was a design engineer with Pulsecom, where he designed voice-band line cards with automatic gain control and adaptive hybrid equalization to optimize performance against voice-band data modems and on-hook data transmission devices. Since 1996 he has been employed as principle scientist, broadband copper access, at Pulsecom. His work includes research, design, and development of high-speed copper access devices as well as network design of systems utilizing xDSL access devices.

Dr. Rauschmayer is an active member of ANSI Working Group T1E1.4, ITU-T, and the ADSL Forum, making numerous contributions assisting in the effort to standardize ADSL and VDSL technologies.

Dedication

To Jen

—for every single smile—

OVERVIEW

1 Introduction and Motivation, 1

2 Twisted Pair Environment, 23

3 Loop Analysis, 63

4 Power Spectral Densities and Crosstalk Models, 89

5 DSL Theoretical Capacity in Crosstalk Environments, 131

6 DSL Modulation Basics, 157

7 ADSL Modulation Specifics, 207

8 ADSL in WAN Networks, 253

9 VDSL Overview, 283

Index, 307

TABLE OF CONTENTS

1 *Introduction and Motivation* 1

Telephone and Data Systems 2
- Coexistence 2
- Subscriber Lines 4

Motivation for Higher Bit Rates 5
- Growth of the PC 5
- Bulletin Board Services 6
- Internet 6
- World Wide Web 6
- Internet Service Providers 7
- Video on Demand 8
- Small Office/Home Office 8

Modem Evolution 9

Why DSL Technology? 10

The Market Demand 11

The DSLs 12
- ADSL 13
- HDSL 13
- HDSL2 14
- IDSL 14
- MDSL 14
- RDSL and RADSL 14
- SDSL 15
- VDSL 15

Other High-Speed Data Options 15
- Cable Modems 15
- Wireless Technologies 16

End-to-End System Diagram 16
- Customer Interface 16
- The POTS Splitter 17
- The Twisted Pair 17
- xTU-R 17
- xTU-C 17
- DSLAM 18
- NSP Network 18
- Line Codes 18
- Data Link Framing and Encapsulation 19
- Backbone/ATM Cloud 19

ADSL and VDSL Standardization 19
ADSL Standardization 19
VDSL Standardization 22
Summary 22

2 *Twisted Pair Environment* 23

A Brief History of Twisted Pairs 23
Introduction to Twisted Pairs 25
Differential Mode and Common Mode Signals 25
Two-Wire Full-Duplex Systems 27
Physical Characteristics 28
Cable Bundles 28
Gauges and Line Characteristics 29
Electrical Characteristics of Twisted Pairs 30
Analytic RLCG Models 30
Numeric RLCG Models 31
Transmission Line Parameters 35
Propagation Constant 36
Characteristic Impedance 41
Crosstalk 42
Crosstalk Types 43
Unbalance Models 44
General Unbalance Expression 53
Near-end Crosstalk (NEXT) 53
Far-end Crosstalk (FEXT) 57
Summary 59
Exercises 60
Endnotes 60

3 *Loop Analysis* 63

ABCD Parameters 63
ABCD Parameters of a Lumped Impedance 65
ABCD Parameters of a Uniform Twisted Pair 66
Bridged Taps 70
Loop Analysis 71
Input Impedance, Transfer Functions, and Insertion Loss 72
Basic Loop Configurations 76
ADSL Loops 76
VDSL Loops 82

Summary 86
Exercises 86
Endnotes 87

4 *Power Spectral Densities and Crosstalk Models* 89

Introduction 90
Crosstalk Equations 91
Number of Crosstalkers 92
Types of Disturbers 92
ISDN and HDSL 94
T1 Lines 99
DMT ADSL (Downstream) 104
DMT ADSL (Upstream) 109
CAP/QAM ADSL 112
VDSL PSDs 121
Summary of PSDs 123
NEXT and FEXT Expressions 123
NEXT Disturbers 124
FEXT Disturbers 127
Summary 128
Exercises 129

5 *DSL Theoretical Capacity in Crosstalk Environments* 131

A Review of Capacity 132
Entropy and Information 132
Gaussian Channels 135
Channels with Memory and Interference 136
Framework for Capacity Calculations for ADSL and VDSL 141
ADSL Capacities 142
Loop Capacities with Identical Crosstalk 142
Comparison of Different Types of Crosstalk 143
Industry Standard Loop and Crosstalk Configurations 145
VDSL Capacities 145
Usable Frequencies on Crosstalk Channels 147
Summary 150
Exercises 150
Endnotes 151
Appendix 5A 152

6 DSL Modulation Basics 157

Modulation/Demodulation Blocks 158
QAM Modulation 158
CAP Modulation 164
Multitone Modulation 166
Forward Error Correction 172
Reed-Solomon Coding 173
Convolution Codes 174
Interleaving 182
Block Interleaving 182
Convolutional Interleaving 184
Scrambling 185
Equalization 187
Folded Spectrums 189
Linear Equalization 191
Decision Feedback Equalization 194
Tomlinson-Harashima Precoding 199
Frequency-Domain Equalization 201
Shaping 203
Summary 203
Exercises 203
Endnotes 204

7 ADSL Modulation Specifics 207

DMT ADSL Systems 207
Transmitter and Receiver Blocks 209
DMT ADSL Overhead 228
ADSL Reduced Overhead Modes 233
Physical Layer Training 235
ATM over ADSL 240
CAP/QAM ADSL Systems 240
Summary 249
Exercises 249
Endnotes 250

8 ADSL in WAN Networks 253

Protocol Basics 254
Ethernet 255

IP 256
TCP 263
ATM 263
PPP 265
Tunneling 266
End-to-End Players *268*
Users 269
Network Access Providers 269
Network Transport Providers 269
Network Service Providers 270
ILECs and CLECs 270
Architectures for DSL Networks *270*
Bridging Architectures 270
ATM End-to-End Architectures 273
Tunneling Architectures 276
Premise Network Considerations 278
Summary *280*
Exercises *280*
Endnotes *280*

9 *VDSL Overview* 283

VDSL Deployment Locations *283*
Crosstalk Issues 286
RFI Issues 288
VDSL Requirements *291*
Rate and Reach Goals 291
Frequency Allocation 292
Modulation Methods for VDSL *295*
TDD Approaches 295
FDD Approaches 302
VDSL in WAN Networks *304*
Video Services 304
Data Services 305
The Full-Service Network 305
Summary *305*
Endnotes *305*

***Index* 307**

CHAPTER 1

Introduction and Motivation

In this chapter:

- Overview of this book
- Basic discussion of the outside plant
- Motivation for higher bit rates
- Introduction to DSL technologies

This book discusses networks capable of delivering high-speed data to all end users. Specifically, the book discusses having widespread users connected to the network using traditional telephone lines with access rates in excess of 1 Mbps. Digital Subscriber Line (DSL) technologies, a family of relatively new and exciting high-speed access technologies using ordinary telephone lines, are especially well suited for the access portion or "on ramp" of such a network.

The principles of two specific DSL technologies, *Asymmetric Digital Subscriber Line* (ADSL) technology and *Very High Speed Digital Subscriber Line* (VDSL) technology, are the primary focus of this book, along with networks to which they allow access. ADSL provides an end user with data rates up to 8 Mbps in one direction and up to 800 Kbps in the other. VDSL provides even higher speeds as well as asymmetric or symmetric operation. This book presents in-depth discussions of ADSL and VDSL as well as how networks are designed to use them. Background discussion and theory are given for the issues faced by DSL technologies and the fundamental performance limits that can be achieved. Most of the discussions in this book are explained in terms suitable for both technical and nontechnical readers. In addition, detailed theory and extensive equations are provided for those who want to dive more deeply into the subject matter.

The book is logically divided into three main sections. The first section deals with the background necessary to understand the challenges and limits of DSL technologies. This section includes Chapter 1 through Chapter 5. Chapter 1 provides a basic introduction and motivation explaining why DSL technologies are important to widespread network access. Chapter 2 discusses physical and electrical characteristics of *twisted pairs* (telephone wires), including electrical and physical properties, and it discusses the basics of *crosstalk*. Chapter 3 continues this discussion by presenting tools used to analyze any type of twisted pair. Chapter 4 focuses on several different types of DSL technologies and the *Power Spectral Densities* (PSDs) used by each. From this, the crosstalk results of Chapter 2 are expanded to show mathematical models of how different technologies interact with one another. Chapter 5 takes this one step farther by combining these effects with the tools from Chapter 3 to predict the theoretical limits of performance of ADSL and VDSL.

The second part of the book deals with ADSL and consists of Chapter 6 through Chapter 8. Chapter 6 discusses, in general terms, the different blocks often present in DSL transmitters and receivers; the material in Chapter 6 is applicable to ADSL and VDSL as well as many other types of communications systems. Chapter 7 is dedicated to different types of ADSL transmitter and receiver systems. The specific implementations of the blocks discussed in Chapter 6 are explained. Real-world insight and issues are provided. Finally, Chapter 8 discusses how ADSL is integrated into *wide area networks* (WANs). Higher layer protocol issues are discussed as well as several network implementations.

The final part of the book deals with VDSL and consists of Chapter 9. There, candidate VDSL implementations (which are still under development) are discussed as well as some issues above and beyond ADSL. Finally, a brief discussion of possible VDSL WAN networks is provided.

Telephone and Data Systems

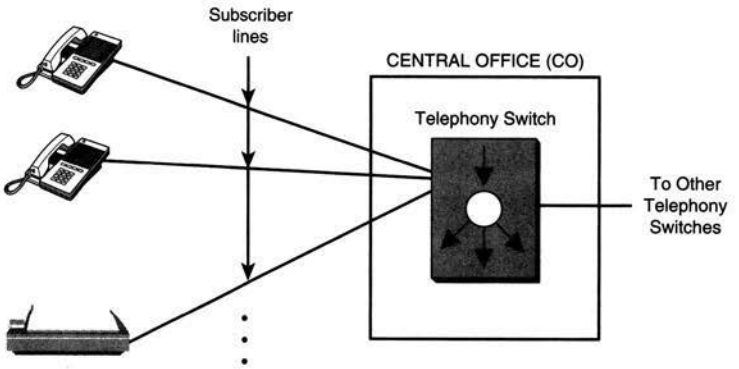
In the modern world, a telephone in every home and every building—and sometimes in every room—is the norm. This is relevant to DSL technology in that in each instance the telephone is connected to a pair of wires (or copper pair) that run out of the building and somewhere within the next 20,000 feet or so connect into telephone switching equipment. (This copper pair is also known as the *subscriber line.*) Thus, every home and building already has a physical means through which data can pass.

Coexistence

Figure 1.1 shows a typical section of the telephone system. The copper loops, or subscriber lines, could be serving a group of homes, an apartment building, an office building, or more generically, a subscriber. Common devices at the subscriber end of the subscriber line

include telephones, fax machines, and voice band modems. Generically, these will be referred to as *Plain Old Telephone Service* (POTS) devices.

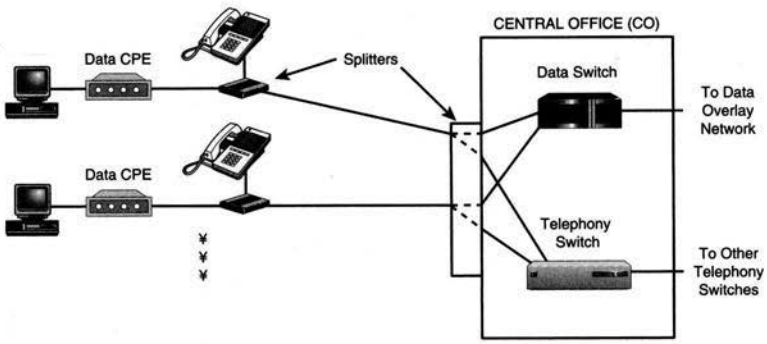
Figure 1.1 A typical example of subscriber lines and a Central Office (CO) housing a telephony switch.



The telephone switching equipment allows one end user to call another end user. Although the links between the telephone switches are typically high-bandwidth optical fibers, the links must be capable of serving many users simultaneously, and so each end user can only use a small portion of the data bandwidth. Furthermore, the switching equipment is designed to handle only small amounts of bandwidth per end user. Typically, the bandwidth available for POTS spans from about 200 Hz to around 3200 Hz and has a capability of carrying a maximum of 64 Kbps.

Now consider switching devices and terminal devices designed and optimized to handle large amounts of data rather than only voice signals for each end user. Further, consider that this new equipment should use the same subscriber lines that the telephone system previously used. Finally, add the criteria that this new system and the original telephone system both use the same subscriber line simultaneously without interfering with one another. This is the basis of DSL technology and is shown in Figure 1.2.

Figure 1.2 A conventional telephone system coexisting with a data overlay network.



In Figure 1.2, the data network is called a *data overlay network* because it essentially overlays the POTS signals on the subscriber lines. Both types of signals, the POTS signals and the data signals, are routed to their respective end terminals at the subscriber location and also to their respective switching equipment at the switching center, or central office (CO). A device called a *POTS splitter* is responsible for splitting and recombining the two types of signals at both ends of the subscriber line. Typical terminal equipment at the subscriber end for the data network are computers and set-top boxes.

Subscriber Lines

In all, about 560 million subscriber lines exist in the world (about 156 million are in the United States). Other common names for a subscriber line include a *copper pair*, *subscriber loop* or simply *loop*, and *twisted pair*. Although most lines have typically been used for voice or low-speed data, a typical loop can support much higher data rates depending on its type, length, and environment. Physical and electrical characteristics of twisted pairs are discussed in detail in Chapter 2.

Asymmetric Digital Subscriber Lines (ADSL) and Very High Speed Digital Subscriber Lines (VDSL), the main DSLs discussed in this book, are methods of transporting data over twisted pairs. As you will see, both technologies require considerable processing power, which normally increases cost and complexity. Much of this is due to the fact that twisted pairs, although capable, were never designed to carry high bit rates because they originally were designed and deployed for relatively low data content voice signals.

Given the differences between POTS and DSL technologies, a natural question might be, "Why try to piggyback a brand-new technology on old lines rather than install fiber or high-speed wireless connections to homes?" The simple answer is that the copper is already

there. It is an *installed base.* Installing a new base of any kind is costly and takes considerable time, so why not use what is already in place?

Copper loops provide one of the only means to deliver high bit rate data to many subscribers. Even though the switches and the POTS splitters must still be added, this is far less of a burden than installing a whole new infrastructure.

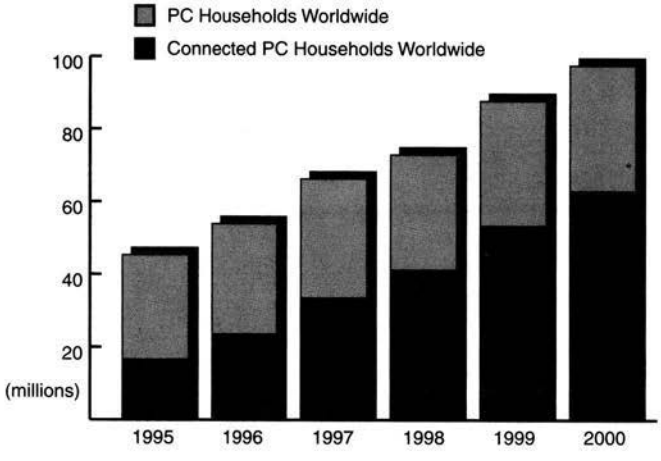
Motivation for Higher Bit Rates

Demand for new technologies needs a driver. Several drivers exist for ADSL, including the Internet and World Wide Web (WWW), video services, consumer services, and entertainment services. Synergy with other technological advances has also helped motivate for ADSL. The most noteworthy of these is the widespread deployment of personal computers (PCs) and an increasing awareness in the general public of how to use PCs. The following sections discuss motivations for ADSL and VDSL.

Growth of the PC

PCs are common in the home. In 1996 alone, more than 71 million PCs were shipped to retail distributors. PCs are becoming user friendly enough that no detailed technical knowledge is required to use many of the available software applications. The number of PC households is expected to continue to grow every year for the foreseeable future. Figure 1.3 shows the projected growth of PC households until the year 2000.

Figure 1.3 The growth of personal computers (PCs) worldwide.



Bulletin Board Services

Bulletin board services (BBSs) became popular in the 1980s. Although BBS systems do not presently provide impetus for higher bit rates, they are worthy of discussion because they are the predecessors to modern Internet service providers. Typically, a PC could dial into a BBS through a 300 to 2400 bps modem and access information (such as online encyclopedias and dictionaries) or enter into chat conversations with other users. Most early BBS systems had limited graphics so that 2400 bps was adequate.

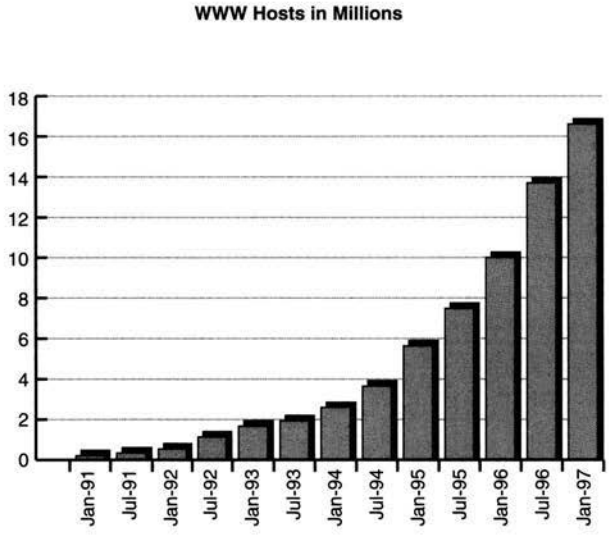
Internet

The Internet gained popularity in the late 1980s. At that time, Internet users were primarily universities and some businesses. Most users had a technical background, and there was little widespread interest in the Internet outside the scientific community. Email over the Internet as well as newsgroups started to spread interest into other disciplines. As more users started to regularly access the Internet, more diverse information and topics became available, creating an increased demand for wider access to the Internet.

World Wide Web

Originally, the Internet was primarily text based. The World Wide Web (WWW) changed this by allowing both text and graphics to be sent and received. This increased the need for higher access rates because graphics typically require larger data transfers than text. The WWW had a simple and attractive graphical user interface, requiring only the use of a mouse and little actual typing. The size of the WWW is growing dramatically. Figure 1.4 illustrates the growth of the number of WWW hosts over the past several years. With more than 16 million existing sites, the WWW's diversity in subject matter is astounding.

Figure 1.4 The growth of Internet hosts (courtesy of Network Wizards, http://www.nw.com/).



The size of a typical WWW page varies depending on the content. Some pages now contain multimedia, including text, graphics, audio, and video. Few high-quality graphics, even in compressed form (JPEG) are under 40 kilobits (kb) in size. Most audio clips run in the hundreds of kilobits range and most video clips in the several megabit range. As consumers continue to use and enjoy the WWW, the demand for higher bandwidth will grow because users do not want to wait for data transfers to take place and will demand faster response.

New WWW technology allows for real-time video and audio as well as three-dimensional graphics. As connection speeds increase, Web pages can become even more sophisticated. Games, shopping, entertainment, and educational applications will demand and use even more bandwidth as it becomes available, further increasing the demand for solutions providing higher bandwidths.

Internet Service Providers

Internet service providers (ISPs) and network service providers (NSPs) have become common in the 1990s. A typical NSP allows dial-up access to the WWW and Internet and provides other services such as email, educational tools, banking, and entertainment. Usually, a consumer connects to an NSP through a voice band modem over the Public Switched Telephone Network (PSTN). Some higher speed access technologies might also

be available to connect to NSPs including ISDN (128 Kbps), T1 (1.544 Mbps), and fractional T1 (n × 64 Kbps), but these are usually expensive and geared toward businesses rather than residential subscribers.

The popularity of ISPs and NSPs has grown tremendously in the 1990s. The number of subscribers to these services has grown to more than 20 million and is predicted to further increase.

Video on Demand

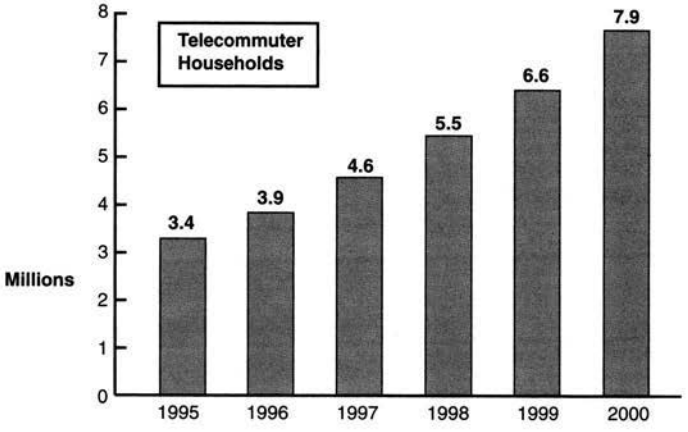
Video on demand (VOD) is another application for ADSL and VDSL technologies. A typical VOD channel requires around 3 Mbps of throughput. ADSL is one of the first technologies allowing the delivery of VOD over the telephone line, and VDSL could allow the delivery of multiple channels. In the United States, cable systems are widely accessible, and VOD might not be as popular an application for DSL technology as Internet access. However, it does give telephone companies (telcos) options they wouldn't otherwise have, which is important in a business and marketing sense. In other parts of the world, cable TV systems are not as available as in the United States, and DSL technologies could play a large role in delivering video to the home.

Small Office/Home Office

The small office/home office (SOHO) provides another good opportunity for DSL technology. In this application, DSL technology can be used to connect the SOHO to a corporate LAN, the Internet, or both. DSL technology would allow a telecommuter to access a LAN with similar perceived speed and efficiency as if she were at the corporate office. This could create a large demand for higher speed access. The number of telecommuters in the United States is also projected to grow into the year 2000 as shown in Figure 1.5.

A typical corporate LAN might have a 10 Mbps backbone connecting PCs and servers. Linking to this at a rate of several megabits per second via ADSL, although not optimal, would still provide an efficient means of connection, and the performance difference would most likely go unnoticed by most users. At VDSL speeds, even higher access rates are achievable.

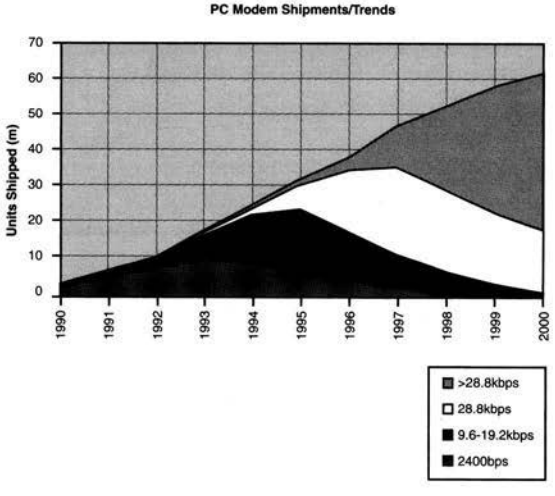
Figure 1.5 The increasing number of telecommuters in the United States will continue into the year 2000.



Modem Evolution

Voice band modems have evolved quite a bit in the 1990s. In a period of about four years, the speed of voice band modems increased by an order of magnitude. Figure 1.6 shows the trends in voice band modems for the PC since 1990 and predictions until the year 2000.

Figure 1.6 Personal computer modem shipment.



The rise and fall of lower speed voice band modems during the 1990s, including 2400 bps, 9.6 Kbps, and 28.8 Kbps modems, is apparent.

Modems with speeds greater than 28.8 Kbps include higher speed voice band modems such as 56 Kbps modems, Integrated Services Digital Network (ISDN) modems, different types of DSL modems, cable modems, and other types, such as wireless modems. Most likely, all these will be deployed in the future, although the types of modems dominating the deployment remain to be seen.

ISDN modems have struggled since the 1980s to achieve wide-scale deployment. ISDN modems use twisted pairs and can send and receive data up to 144 Kbps. Standardization discrepancies have made ISDN provisioning and installation difficult, thus impeding widespread use. Other factors have kept ISDN out of main stream usage, including cost and incompatibility with POTS service. Generally, the cost of ISDN was too high, and a POTS line cannot share the same twisted pair as ISDN. ISDN is typically switched through the telephone network and not through a data overlay network. Even with its faults, over the last decade, ISDN has been one of the only means of achieving data rates significantly greater than voice band modems.

Why DSL Technology?

With other broadband technologies in the running, several key attributes make DSL networks an attractive choice for high-bandwidth access. Although a reader of this book is likely to be aware of these technologies, a quick review of some key attributes will be beneficial.

As discussed earlier, xDSL technology can be deployed over existing twisted pairs. This installed base is widespread, and the total investment that telephone companies have placed in it over the years is immeasurable. Not only does using this copper further utilize this inherent vestment, but it also allows the delivery of new, high-speed service without investing in a brand-new infrastructure.

Most new technologies require considerable time even before feasibility trials can be done. For example, a wireless satellite system would require designing, building, and deploying the satellites before a trial could begin. DSL technology trials, on the other hand, can be much simpler due to the installed base of copper along with existing switching centers.

Many applications require high bandwidth, and new applications are sometimes created when high bandwidth is available. Applications in medicine, real estate, law, business, and many other fields can be supported with DSL technologies. Furthermore, DSLs can be deployed to many locations needing this bandwidth in a cost-efficient manner by using the existing infrastructure.

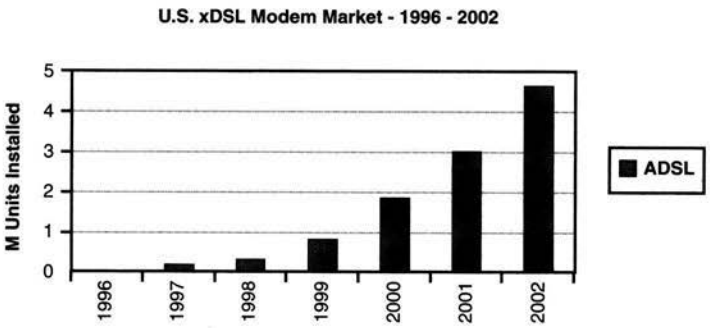
With the growing popularity of online services, the PSTN is being overrun with traffic. (This currently is a heated debate between Internet service providers who claim that the PSTN is in no danger of being overrun by data calls and the telephone companies who claim the opposite.) Originally, the PSTN was designed to handle voice traffic having patterns different from data traffic. For example, most voice calls are short in duration, whereas a data call to an Internet service provider might last several hours. The statistical models used to design the PSTN did not adequately consider the data call model. The data overlay network involved in xDSL technology will relieve the telephone switching system of some data traffic, avoiding major upgrades to the infrastructure.

The Market Demand

The market demand for a technology plays a large role in advancing the technology itself. This is because companies need to make a profit and often will only undertake projects that are predicted to generate income over in the future. The detailed justifications of a business case for DSL technologies are beyond the scope of this book; however, some of the more general arguments in favor of the DSL technology, such as the advantages of xDSL technology over competing options like cable modems and wireless data services, are worthy of discussion. The competing technologies are discussed later in this chapter.

Figure 1.7 depicts the predicted rollout of DSL modems over the next several years.

Figure 1.7 The predicted rollout volumes of xDSL modems through 2002.



The most significant growth is predicted from 1999 through 2002. In all, more than 10 million DSL units are predicted to be installed by the year 2002. If each had a cost of $300.00, probably a conservative estimate, xDSL would be a more than $3 billion industry over the four years! This is a good business case indeed.

The DSLs

This section discusses the various types of DSLs that have evolved over the past few years. Some of the technologies are driven by companies, whereas others are supported by the industry as a whole, including service providers and vendors. For these, standards bodies are defining or have defined specifications for implementation. Because of all the acronyms used for different DSL technologies, this section uses the generic term *xDSL* to generally refer to DSLs. Table 1.1 shows a summary of many xDSL technologies.

Table 1.1 Capabilities of Various DSL Technologies

DSL	Upstream Rates	Downstream Rates	Symmetric/ Asymmetric	POTS Coexistence	Standardization
ADSL	100–800 Kbps	1–8 Mbps	Asymmetric	Yes	Yes
HDSL	Fixed 784, 1544, 2048 Kbps	Fixed 784, 1544, 2048 Kbps	Symmetric	No	Yes
HDSL2	Fixed 1544, 2048 Kbps	Fixed 1544, 2048 Kbps	Symmetric	No	Yes
IDSL	Fixed 128 Kbps	Fixed 128 Kbps	Symmetric	No	No[1]
MDSL	64–200 Kbps	800–2000 Kbps	Asymmetric	Yes	No
SDSL	384 Kbps	384 Kbps	Symmetric	Yes	No
VDSL	Up to 25 Mbps	Up to 25 Mbps	Both	Yes	Under development

[1]IDSL itself has no standard, but is similar to ISDN, for which a standard does exist.

ADSL

As stated earlier, Asymmetric Digital Subscriber Lines (ADSL) technology is one of the main topics of this book. ADSL is characterized by a different data rate from the service provider to the customer (the downstream direction) as compared to the data rate from the customer to the service provider (the upstream direction). This difference is the origin of the name Asymmetric. Data rates are typically about 10 times as high in the downstream direction and range anywhere from around 1 Mbps to around 8 Mbps—the maximum rate can depend on the length and condition of the loop determined during initialization or on a maximum provisioned rate.

For example, consider a loop capable of supporting 4 Mbps in the downstream direction and 440 Kbps in the upstream direction. A modem having the capability to operate at 6 Mbps downstream will realize during initialization and training that 6 Mbps cannot be supported on the particular loop and will negotiate the rate downward to 4 Mbps. This is an example of a rate determined by the length and condition of the loop. The service provider might, however, have provisioned the modem to run even slower than this (for example, at a maximum of 2 Mbps). (It is not yet clear whether network providers such as telcos will provision modems to limit the data rate, but it is expected to be a desired option. A telco might want to do this to provide various tiers of service with, of course, higher pricing for higher bandwidth capable tiers.) In this case, even though the modem could operate at the higher speed of 4 Mbps, it will limit the downstream bit rate to 2 Mbps.

ADSL is typically geared to support applications such as Internet access, LAN bridging, and VOD. ADSL has been in many technology trials since the early to mid-1990s.

HDSL

High Bit Rate Digital Subscriber Line (HDSL) technology provides symmetric bit rates. Typically, HDSL modems are designed to run at fixed speeds. Some common operating speeds are 768 Kbps, 1.544 Mbps, and 2.048 Mbps. The latter two values correspond to T1 and E1 lines, respectively. HDSL usually needs two separate twisted pairs, and both must be full duplex. Applications for HDSL are growing, but the original driver was the replacement of T1 and E1 lines because HDSL had a longer range than these older technologies. HDSL uses 2B1Q modulation and cannot coexist on the same twisted pair with POTS.

Note

The code 2B1Q is a four-level baseband code; 2B1Q stands for two binary, one quatenary signal. That is, each symbol is one of four possible symbols and conveys two bits of data.

HDSL2

HDSL2 is a follow-on technology to HDSL. Essentially, it is meant to transmit T1 and E1 rate signals over a single twisted pair. Currently, HDSL2 is undergoing the standardization process. POTS cannot be run on the same twisted pair as HDSL2.

IDSL

IDSL is one of the new abbreviations to come along, and it stands for ISDN Digital Subscriber Line. IDSL uses the same 2B1Q line code technology as used in ISDN. IDSL is a symmetric service and cannot share a twisted pair with POTS. Initial rates for IDSL include 56 Kbps, 64 Kbps, 128 Kbps, and 144 Kbps.

MDSL

Medium Bit Rate Digital Subscriber Line (MDSL) technology is basically a watered down version of ADSL. MDSL is an asymmetric technology running at slower speeds than ADSL—typically 800 Kbps to 1 Mbps downstream and 100 Kbps upstream. MDSL was proposed to reduce the cost and complexity of a DSL modem while still providing reasonably high data rates. Applications for MDSL include Internet access and LAN bridging. MDSL is currently under study but is not being standardized.

RDSL and RADSL

RDSL and RADSL can stand for two different things. The first is Rate Adaptive ADSL, meaning an ADSL line that can automatically select an optimum operating rate for a twisted pair. Originally, ADSL was not thought of as adaptive in rate. This name was coined when vendors began proposing rate adaptive functionality. This name is seldom used because ADSL itself is usually assumed to be rate adaptive.

The second technology denoted by RDSL and RADSL is Reverse ADSL. Reverse ADSL was proposed as an ADSL system in which the asymmetry of data rate is reversed. Thus, the upstream direction runs faster than the downstream direction. The proposed main application for Reverse ADSL was for subscribers wanting to provide WWW servers. Typically, a WWW server provides more data than it receives, motivating the need for a higher upstream data rate and a slower downstream data rate. Because of spectrum incompatibilities, Reverse ADSL has received little attention by vendors or standards bodies.

SDSL

Symmetric Digital Subscriber Line technology is the little brother to HDSL. As the name implies, data rates in the upstream and downstream direction are symmetric. Typical data rates are 384 Kbps and 768 Kbps. SDSL can be used to provide fractional T1 services or LAN and Internet access. No standard currently exists for SDSL.

VDSL

Very High Speed Digital Subscriber Line (VDSL) technology is the other major topic of this book. VDSL can be viewed as ADSL's big brother. VDSL can run with either symmetric or asymmetric rates. The highest symmetric rate being proposed for VDSL is 26 Mbps in each direction. Other typical VDSL rates being proposed are 13 Mbps symmetric, 52 Mbps downstream and 6.4 Mbps upstream, 26 Mbps downstream and 3.2 Mbps upstream, and finally, 13 Mbps downstream and 1.6 Mbps upstream. VDSL can coexist with POTS on a twisted pair.

The maximum possible length of a VDSL loop is much less than for that of an ADSL loop. VDSL is planned for use as the last link in fiber in the loop (FITL) and fiber to the curb (FTTC) networks. FITL and FTTC networks have small access nodes, are remote from the CO, and are fed by high bandwidth fiber. A typical node might reside on a curb in a neighborhood and serve 10 to 50 homes. Thus, the loop lengths from the node to the subscriber tend to be shorter than loops from the CO to the subscriber. Although the applications are not yet clear, VDSL could be used as the last link in a full-service multimedia network delivering voice, video, and data to a subscriber.

Other High-Speed Data Options

xDSL is not the only option available to provide high-bandwidth solutions. Several others offer formidable competition to xDSL.

Cable Modems

Cable television delivered via coaxial cable (coax) is available throughout most of the United States and much of Europe. Coax can handle high bandwidths, and cable modems take advantage of this. Cable systems are traditionally a broadcast medium with one line serving many subscribers. Because of this, the subscribers must share the bandwidth of the coax cable. Also, the upstream direction from the subscriber back to the coax distribution point traditionally has not been used to transfer information and, in many areas, does not support transmission. Reconditioning the infrastructure to support upstream transmission is costly and time consuming, and deployment in a geographical area cannot be done until

the entire infrastructure in that area is upgraded. Despite this, cable modem standards are under development, and cable modems will continue to be a significant competitor to xDSL.

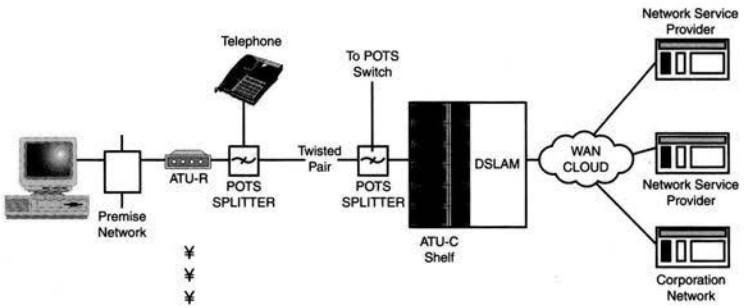
Wireless Technologies

Several wireless technologies also have the capability to distribute data to subscribers. Direct Broadcast Satellite (DBS) relies on geostationary satellites to supply data—primarily programming in broadcast form—to subscribers. Multichannel Multipoint Distribution Systems (MMDS) can send 33 television channels in analog form or around 100 channels in digital form to subscribers. These technologies require a satellite dish receiver and a set-top box at the subscriber location. Although primarily geared for broadcast at the present time, these technologies might become players in the high-speed interactive data world in the future.

End-to-End System Diagram

Many companies throughout the world are developing products based on ADSL and VDSL. Specialized chipsets are available for ADSL and should be available for VDSL in 1999. To better discuss all the aspects of ADSL and VDSL systems, a generic model on which to base the discussion will be helpful. Figure 1.8 shows this model for an ADSL access network, and the various components, including hardware equipment, line codes, and protocols are discussed in the following sections.

Figure 1.8 An end-to-end system diagram of an ADSL or VDSL network.



Customer Interface

Many possible options are available for the customer interface. Common interfaces include 10BaseT and a 25.6 Mbps ATM interface (sometimes simply called an ATM-25 interface). These are more common types of high-speed interfaces to the PC. Also for a PC interface,

an internal card sometimes called a *network interface card* (NIC) is used. Certain other interfaces, such as a V.35 interface to a set-top box and newer types of high-speed interfaces, such as Universal Serial Bus (USB), are also possibilities for the customer interface.

The POTS Splitter

The POTS splitter allows ADSL or VDSL signals to coexist on a twisted pair with telephony signals. One POTS splitter is needed on each end of the twisted pair. In one direction, the POTS splitter combines the two kinds of signals, whereas in the other direction it properly splits the signals.

The POTS splitter is basically a three-port device containing a bidirectional high-pass filter and a bidirectional low-pass filter. The POTS splitter might be fully or partially integrated into the ATU-R and ATU-C.

The Twisted Pair

The twisted pair is made up of two copper conductors twisted around one another; these are usually less than 18,000 feet in length for ADSL and less than 4,500 feet in length for VDSL. (In both cases, the loop length varies over a wide range up to the maximum. The actual length dictates what data rates can be supported; longer loops support only lower data rates.) The physical and electrical properties of twisted pairs are discussed in detail in Chapter 2.

xTU-R

The xTU-R modem resides at a customer's location (house or business). The xTU-R might be an external modem, a card plugging into a PC, or, in some cases, part of a bigger piece of network equipment such as a router. For ADSL, this modem is called the ATU-R and for VDSL is called the VTU-R.

xTU-C

The xTU-C is the counterpart to the xTU-R and resides at the central office. Generally, the xTU-C is part of the network access equipment. The xTU-C normally consists of cards plugging into an access shelf. More than one modem can exist on each card, or the modem functions can be distributed among several cards, but an xTU-C connects only to one xTU-R at a time. For ADSL, this modem is called the ATU-C, and for VDSL, it is called the VTU-O (the O represents the fact that the VDSL node normally resides at an optical node).

Note

Note that the xTU-C may reside outside the central office and the data traffic backhauled over high-speed links such as OC-3 optical fiber.

DSLAM

DSLAM has become one of the more popular abbreviations in xDSL technology; it stands for Digital Subscriber Line Access Multiplexer. The DSLAM aggregates subscriber line traffic onto higher speed links for the backbone switching equipment.

NSP Network

The network service provider (NSP) network is an important part in achieving of an overall service network. NSP is a generic term for an Internet service provider, entertainment provider, corporate network, or any other type of provider whose customers gain access to services via the xDSL network.

Line Codes

The line code is the physical layer modulation scheme used by the xDSL technology. This book discusses line codes for both ADSL and VDSL technologies. For ADSL, discrete multitone modulation (DMT) is the standard line code. Carrierless amplitude and phase (CAP) modulation and quadrature amplitude modulation (QAM) are other line codes competing with DMT as ADSL modulation schemes. CAP and QAM produce similar signals under certain conditions and are lobbying for standardization. CAP- and DMT-based ADSL modems have been successful in field trials, and both, along with QAM, are discussed in detail in later chapters. CAP and QAM are often referred to as single carrier modulation schemes, whereas DMT is referred to as a multicarrier modulation scheme.

Note

The reader may note that referring to CAP as a single carrier modulation scheme contradicts the "C" in its acronym, which stands for carrierless. CAP is generated using digital filters instead of by modulating a carrier, thus the name carrierless. In the most widely used implementation, the digital filters generate sine and cosine waves, and the result is a signal very similar (and sometimes identical) to a carrier modulation scheme such as QAM.

A line code has not yet been standardized for VDSL. Codes in competition include single carrier systems based on CAP and QAM, multicarrier systems based on symmetric DMT (SDMT), and also a DMT technique called Zipper. All these line codes are discussed in later chapters.

Note

One proposal for a VDSL line code is actually a hybrid approach with a single carrier downstream scheme and a multicarrier upstream scheme based on Discrete Wavelet Multitones (DWMT).

Data Link Framing and Encapsulation

Different types of data link framing and encapsulation techniques being standardized for ADSL include ATM-based approaches and frame-based approaches. VDSL framing is not as far along, although initial applications make ATM a strong candidate. Chapter 8 discusses framing and encapsulation methods for ADSL; Chapter 9 covers proposed framing and encapsulation methods for VDSL.

Backbone/ATM Cloud

In discussing ADSL and VDSL systems, it is assumed that a network backbone exists linking the subscriber lines to network services. In many cases, *Asynchronous Transfer Mode* (ATM) will be the underlying transport mechanism in the backbone, although the protocols running on top of ATM may vary. For example, in some cases, protocols that encapsulate Internet protocol (IP) data might be discussed, whereas in other cases, tunnel protocols might be used. It is also possible to have other types of backbone WAN networks including an IP routed network or a frame relay network.

ADSL and VDSL Standardization

Standardization is an important aspect in the xDSL marketplace. Service providers deploying equipment like to have the assurance that what they are purchasing from one will properly interoperate with what they might purchase from other vendors. The voice band modem market is an example of the benefits of standardization as almost any pair of off-the-shelf modems interoperate with one another.

ADSL Standardization

Several different standardization organizations (sometimes referred to as standards bodies) play a role in ADSL specifications. The following sections discuss the various standards bodies involved.

Committee T1

The original body studying ADSL was committee T1, which is an open group of industrial participants that create standards for the United States. The American National Standards Institute (ANSI) accredits committee T1. Several subcommittees exist within the committee. These subcommittees are dedicated to different areas of standardization and include the following:

- T1A1 is dedicated to performance and signal processing
- T1E1 is dedicated to interfaces, power, and protection for networks
- T1M1 is dedicated to internetwork operations, administration, maintenance, and provisioning
- T1P1 is dedicated to wireless/mobile services and systems
- T1S1 is dedicated to services architecture and signaling
- T1X1 is dedicated to digital hierarchy and synchronization

The subcommittee relevant to ADSL is T1E1, with xDSL falling under the interfaces category. T1E1 is further broken down into working groups. The working group assigned to DSL access (including ADSL) is T1E1.4. The scope of working group T1E1.4 includes the development of standards for the physical layer including transmission techniques and interface functionalities. The T1E1.4 working group developed the T1.413 standard for ADSL. This standard was published in 1995.

The ADSL Forum

The ADSL Forum is a group of industry participants formed in 1994 to promote ADSL with both marketing and technical efforts. The marketing effort is primarily to educate the public on ADSL. On the technical front, committees exist to work in implementation issues not covered by T1E1.4 (primarily layers above the physical layer as well as the management and signaling planes). Several subgroups exist in the ADSL Forum including the following:

- A packet mode protocols group dedicated to defining ADSL functionality with a packet-based (non-ATM) access
- An ATM mode group dedicated to defining ADSL functionality within ATM networks
- A network migration group dedicated to defining the evolution of networks implementing ADSL

- A network management group dedicated to defining the management methods for ADSL including the management information base (MIB)
- A test group dedicated to defining test requirements for ADSL systems

The ADSL Forum publishes technical specifications in many of the areas listed previously. Further information and updates of work in progress are available at `http://www.adsl.com`.

The ITU

In 1998, the International Telecommunications Union (ITU) joined the effort to standardize ADSL. This is the same standardization body that has published specifications for voice band modems including V.34. The ITU is working on many items related to ADSL including the following:

- **G.DMT**. a project based largely on T1.413
- **G.lite**. a project aimed at lower speed, reduced complexity ADSL applications
- **G.test**. a project aimed at specifying test specifications for xDSL technologies
- **G.OAM**. a project aimed at specifying operations, administration, and maintenance aspects of xDSL systems
- **G.HS**. a project aimed to define handshaking protocols to allow startup negotiation among xDSL modems

Many items being worked on by the ITU overlap work being done by T1E1.4 or the ADSL Forum. In most cases, cooperation between the groups exists to facilitate convergence of xDSL technology.

ETSI

The European Technical Standards Institute (ETSI) is an open European body dedicated to determining and producing telecommunications standards. A technical body within ETSI known as TM is responsible for transmission and multiplexing. A subgroup of technical body TM known as TM6 is responsible for xDSL standards development including ADSL. TM6 is very much a European counterpart to T1E1.4. Cooperation between T1E1.4 and ETSI TM6 on ADSL standards development is common.

VDSL Standardization

T1E1.4 and ETSI TM6 also study projects dedicated to VDSL. From 1996 to 1998, the bodies individually drafted technical requirements documents. In the future, it is expected that an actual standard will be developed, most likely with cooperation between the groups. It is likely in the future that other groups will begin work on aspects of VDSL as well.

Summary

This chapter provided an introduction to xDSL technology as well as a guide to what can be found in subsequent chapters of this book. The chapter also discussed drivers for high-bandwidth access to various types of networks. It also reviewed the benefits of xDSL technology, as well as how xDSL technology uses the existing PSTN infrastructure.

The chapter also explained the different flavors of xDSL technology and key characteristics of each. The chapter explored the role and importance of standardization bodies in ADSL and VDSL technologies and described several bodies along with the area of ADSL and VDSL that they cover.

CHAPTER 2

Twisted Pair Environment

In this chapter:

- History of twisted pairs
- Physical and electrical characteristics of twisted pairs
- Transmission line parameters
- Derivation of basic crosstalk equations

This chapter is devoted to the physical and electrical characteristics of twisted pairs. A twisted pair channel is noisy, lossy, and prone to crosstalk. ADSL and VDSL modulation schemes are designed to overcome and mitigate these impairments. Thorough understanding of ADSL and VDSL begins with thorough understanding of the environment in which they must exist.

This chapter discusses the physical and electrical properties of common twisted pairs. The transmission line characteristics and basic crosstalk equations in twisted pair bundles will be derived. This information becomes useful in subsequent chapters dealing with transmission performance. But first, an introduction to twisted pairs is in order.

A Brief History of Twisted Pairs

The history of telephone wires is more than a century old and has roots in the wires originally used to carry information from the telephone's predecessor, the telegraph.

Samuel F. B. Morse constructed the first commercial telegraph line between Baltimore, Maryland, and Washington, D.C., in 1844. After failing to successfully install underground lines due to high leakage from the environment, Morse decided that an aerial approach

would be better. Morse proceeded to install 700 wooden poles spaced about 300 feet apart for the 40-mile span. A 2-foot cross arm was nailed to the top of each pole, and a wire was run through a slot at the end of each cross arm. Thus, the groundwork was laid for the deployment of twisted pairs.

After the telephone began to gain popularity, the need for many more wires was necessary, and the telephone cable—consisting of many wires bound in a sheath—was developed. One of the biggest problems at first was crosstalk between wires, as the two-wire metallic circuit had not yet been employed. In New York City, in 1879, cable was laid across the Brooklyn Bridge, years before it was even open. In 1880, an electrician speaking for the Metropolitan Telephone and Telegraph Company reported:

> We have over the East River Bridge at the present time, four cables, 3800 feet long, each cable with seven conductors.... In using the cables and talking on one wire, you could hear whatever was said on another wire.[1]

In the following years, many schemes were employed to reduce crosstalk, most dealing with shielding the individual wires or providing grounding at intervals. Finally in 1881, a patent for the metallic twisted pair circuit, which worked well in suppressing crosstalk, was given to Alexander Graham Bell, who testified to the Honorable Commissioner of Patents about his experiments as follows:

> The methods by which I sought to accomplish this result, on the 26th of November, 1876 was to employ a metallic circuit, the direct and return wires which should be parallel to the disturbing wires and to one another.... The improvements in the arrangement that I devised in England were:
>
> To place the direct and return lines close together...and
>
> To twist the direct and return lines around one another so that they should be absolutely equidistant from the disturbing wires.[1]

Thus, the twisted pair was born. Since that time, the deployment of twisted pair lines has been extensive and includes many types and sizes of cable.

Several surveys have been conducted on deployed twisted pair subscriber loop statistics with some results including average lengths, impedances, and losses.[2,3]

Note

For an interesting history of all methods of mass communications in the United States, including the rise of the telegraph and telephone and the development of the twisted pair, I highly recommend visiting the communications exhibits at the Smithsonian American History Museum in Washington, D.C.

Introduction to Twisted Pairs

Before getting into the technical and mathematical details regarding twisted pairs, let's review exactly what the term twisted pair means and why, in nontechnical terms, twisted pairs are used for communications.

As described in the previous section, a twisted pair is made up of two wires twisted around one another. The two wires are electrically driven and sensed differentially, and neither is connected to a common ground point. Because the wires are physically close and geometrically symmetric to one another, any outside signal influencing one of the wires influences the other wire in the same way. If a receiver senses only the difference between the two wires, the outside influence subtracts out. Historically, the two wires making up a twisted pair are called tip and ring.

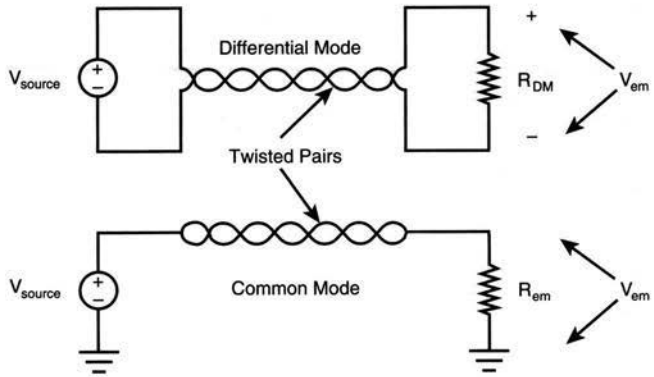
Note

The names *tip* and *ring* come from connector cables used by operators in which one wire terminated at the tip of the connector, and one wire terminated in a ring around the connector. The names are still widely used today.

Differential Mode and Common Mode Signals

An important concept to understand about twisted pairs is the difference between differential mode and common mode signals. A *differential mode signal* is applied between the two wires making up the twisted pair. A *common mode signal* is applied between the two individual wires of the twisted pair and ground. Differential mode signals are sometimes called *metallic signals*, and common mode signals are sometimes called *longitudinal signals*. Figure 2.1 illustrates differential mode signals and common mode signals.

Figure 2.1 Differential mode and common mode signals.



Data and voice signals on a twisted pair are always transmitted as differential signals. Common mode signals are typically due to outside influences such as 60 Hz induction from nearby power lines, RF interference from radio stations and other active operating bands, and disturbances from signals on other twisted pairs.

Note

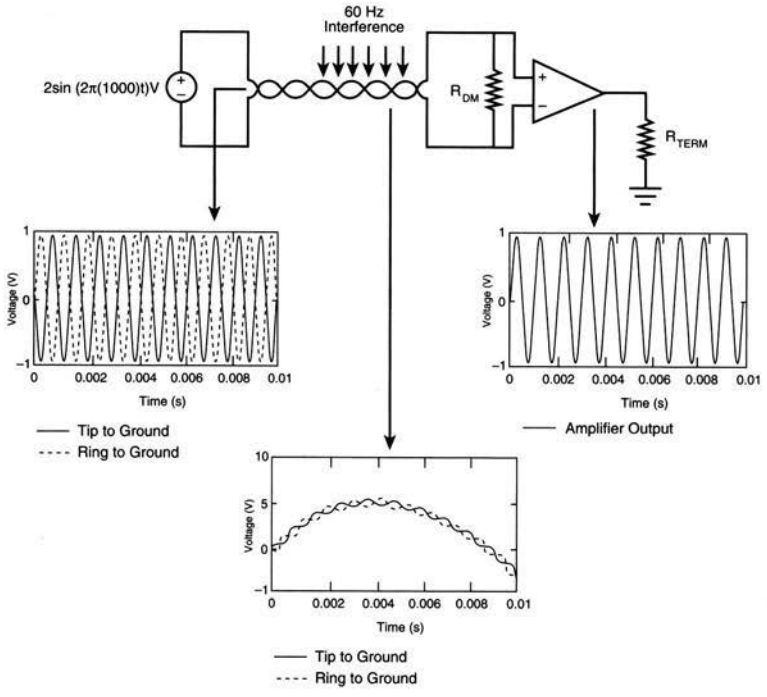
In some systems, such as HDSL powering units, the common mode is used to transmit D.C. power for remote unit powering.

At the receiver of a twisted pair system, only the differential voltage of the twisted pair is processed for information. The common mode signal is rejected by transformers and well-balanced differential amplifiers, which effectively subtract the voltage on the individual wires of the twisted pair.

For example, consider the twisted pair shown in Figure 2.2.

Voltages of each wire are shown along the length of the pair with respect to ground. Note that the voltage on the twisted pair appears as a 1000 Hz, 1 V peak sine wave riding on a 60 Hz wave. The 60 Hz is in phase on each wire, and the 1000 Hz wave is 180 degrees out of phase on each wire. After the differential amplifier, which essentially subtracts the voltage on one wire from the voltage on the other, the 60 Hz voltage subtracts away and is no longer present, and only the 1000 Hz waveform remains (in this simple example, loss on the twisted pair is ignored). This is sometimes referred to as common mode rejection.

Figure 2.2 An example of common mode rejection on a twisted pair.

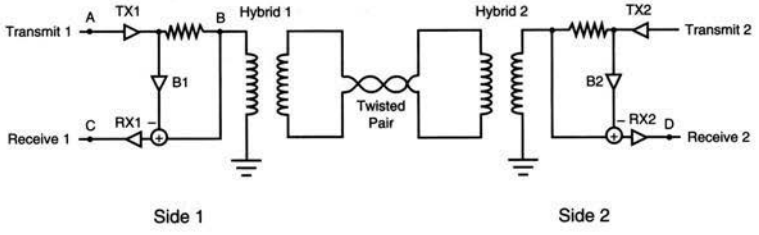


Two-Wire Full-Duplex Systems

If you don't have experience with twisted pair applications, the use of two wires to send signals in both directions simultaneously, or full-duplex operation, might seem extraordinary. If fact, full duplex use of a twisted pair is common and simple. Figure 2.3 shows a basic scheme.

Here, the twisted pair part of the circuit is called the *two-wire path*, and the transmit and receive portion on each end is called the *four-wire path.* The conversion at each end of the twisted pair between two-wire and four-wire paths is called *the two-wire to four-wire hybrid*, or simply the *hybrid*. Signals arriving at point A pass through TX1 and on through the transformer to the twisted pair. Some portion of the signal at point B will enter the receive path of side 1. This signal is called the *echo signal.* The echo signal is canceled by a balance filter B1 and thus will not pass to point C. The original signal will arrive and pass through side 2's transformer and into the receive path of side 2. If side 2 is simultaneously transmitting a signal, any echo from that signal will be canceled by B2 and will not affect the signal proceeding to point D.

Figure 2.3 A full-duplex twisted pair circuit with two-wire to four-wire hybrids on each end.



Note

Take note that different hybrid designs exist, including designs using transformers to cancel the anticipated echo, using analog or digital amplifiers to cancel the "average expected" echo, and using adaptive filters to measure the echo and adjust to do cancellation. Most high-speed data systems use the latter method.

Using a hybrid to achieve full-duplex communications on a twisted pair is typical of voice systems and some *echo canceled systems* including ISDN, HDSL, and some ADSL systems. Other systems, especially high bit rate systems, do not use echo cancellation because they often require complex echo cancellation filters and front-end analog-to-digital converters. Instead, these systems may use *frequency division multiplexing* (FDM) or *time division multiplexing* (TDM). Such systems are discussed in detail in later chapters.

Physical Characteristics

With the massive number of twisted pairs deployed over many years, care must be taken not to mix generalizations of the characteristics of common twisted pairs with the characteristics of all deployed twisted pairs. In other words, some twisted pairs have characteristics different from those described in this chapter. This fact is especially important when troubleshooting "real world" issues and problems.

Cable Bundles

Twisted pairs are usually deployed in *cable bundles* containing multiple twisted pair lines in a cable sheath. The number of pairs contained in the cable varies from as little as one pair to as many as 4,200 pairs. Common cables used in the subscriber loops contain 25 to 100 twisted pairs. A color coding scheme is used to identify specific twisted pairs within a bundle.[4,5]

Each wire in a twisted pair has an insulator coating. Older wires used a paper-based insulation—these are called *pulp-insulated twisted pairs.* Newer twisted pairs use various types of plastics as insulators. The plastics used include polyethylene, polypropylene, and PVC. These types of twisted pairs are generically referred to as *plastic-insulated cables* or PIC. Some cables might also be packed with gel to increase resistance to moisture.

Cable bundles normally have an outer metallic shield. This shield is grounded at the cable ends to help reduce interference from outside sources. The type of shield varies from cable to cable. Cables may also contain support structures such as coated steel armor and galvanized steel supporting strands.

Individual twisted pairs encountered in the outside plant normally do not have dedicated shields. The twisting along the length of a specific pair is constant, but the amount of twist varies between pairs from 2 to 6 inches in length. The varying twist length of neighboring twisted pairs helps further reduce crosstalk between the pairs.

Gauges and Line Characteristics

Twisted pairs are most often characterized by their gauge using the American Wire Gauge (AWG) designations; the gauge is indicative of the diameter of the copper wires making up the twisted pair. Typical twisted pair gauges include #19, #22, #24, and #26 with diameters ranging from 0.03589 inches (0.912 mm) to 0.01594 inches (0.404 mm) with the smaller gauge number corresponding to the larger diameter. Gauges #24 and #26 are most common in DSL applications. Table 2.1 shows the preceding gauges along with the diameters and DC resistance per 1,000 feet of each.

Table 2.1 Common Twisted Pair Wire Gauges and Characteristics

AWG	Diameter (in)	DC Resistance 20° (ohms/kft)
19	0.03589	16.9
22	0.02535	33.8
24	0.02010	53.4
26	0.01594	85.8

Twisted pairs are also defined by categories specifying electrical tolerances of the pair. Installations for high-speed data are typically required to be category 3 or higher cables. Higher category numbers correspond to higher performance twisted pairs in terms of the loss and crosstalk properties of each. Table 2.2 lists the different cable categories, the approximate bit rates supported, and the target applications of each category.

Table 2.2 Twisted Pair Categories and Characteristics

Category	Bit Rates	Applications
1	Unspecified	
2	1 Mbps	Some low-speed data circuits (DDS)
3	16 Mbps	16 Mbps Used for 10BaseT and 4 Mbps Token Ring
4	20 Mbps	10BaseT and 16 Mbps Token Ring
5	100 Mbps	10/100BaseT, other high-speed copper technologies

For DSL technologies, category 3 or higher twisted pair is preferred. As discussed in Chapter 1, reuse of the existing copper plant is a major driver for ADSL and VDSL. Existing cable is normally as good as or better than category 3 specifications.[6] Detailed specifications for typical wiring categories can be found in *Telecommunications Wiring for Commercial Buildings, A Practical Guide.*[7]

Electrical Characteristics of Twisted Pairs

For any transmission line, the basic parameters of interest are resistance, inductance, capacitance, and admittance. These parameters are also called the *RLCG parameters.* In the voice band, the RLCG parameters are close to constant for #24 and #26 gauge twisted pairs. At frequencies above the voice band, resistance, inductance, and admittance vary with frequency. These three parameters also vary with gauge. Capacitance tends to be constant over both frequency and gauge.

Depending on the situation, one of two assumptions can be made when discussing line parameters. The first assumption ignores the effects of admittance and assumes that inductance and capacitance are constant with frequency. Also, resistance is assumed to be proportional to $f^{1/2}$ where f is frequency in Hz. This approximation is used when deriving near-end and far-end crosstalk models. Later in this chapter, and in Chapter 3, you will see that this approximation makes for a simple and accurate model for crosstalk on DSLs.

The second approximation is used for actual numeric calculations of twisted pair characteristics. This approximation will be used when finding the transfer function and insertion losses of a twisted pair as well as the characteristic impedance. This approximation was numerically determined for #24 and #26 twisted pairs.[8]

Analytic RLCG Models

Analytic RLCG models have been accepted and used in literature for many years. The parameters are given in Eqtn. 2.1–2.4 and the constants in Table 2.3. The resulting RLCG

parameters are with respect to 1,000 feet, or 1 kft, a common measure of distance for twisted pairs.

Eqtn. 2.1

$$R = R_0 f^{\frac{1}{2}}$$

Eqtn. 2.2

$$L = L_0$$

Eqtn. 2.3

$$C = C_0$$

Eqtn. 2.4

$$G = 0$$

Table 2.3 Parameters for the Analytic Twisted Pair Model

Parameter	#24 Gauge	#26 Gauge
R^0 (ohms/kft)	0.15	0.195
L^0 (mH/kft)	0.188	0.205
C^0 (nF/kft)	15.7	15.7

Numeric RLCG Models

The numeric RLCG models for #24 and #26 gauge twisted pairs are valid over the frequency range from D.C. to 10 MHz. The model parameters were found by curve fitting to measured cable.[8] Eqtns. 2.5–2.8 are the general equations for all four parameters; the constant values applicable to #24 and #26 gauge pairs are given in Table 2.4. The resulting RLCG parameters in Table 2.4 are with respect to 1 km.

Eqtn. 2.5

$$R(f) = \sqrt[4]{r_{oc}^4 + a_c f^2}$$

Eqtn. 2.6

$$L(f) = \frac{l_o + l_\infty \left(\frac{f}{f_m}\right)^b}{1 + l_\infty \left(\frac{f}{f_m}\right)^b}$$

Eqtn. 2.7

$$G(f) = g_o f^{g_e}$$

Eqtn. 2.8

$$C(f) = c_\infty$$

Table 2.4 Parameters for the Numeric Twisted Pair Model

Parameter	#24 Gauge	#26 Gauge
r_{oc} (ohms/km)	174.55888	286.17578
a_c (ohms^4/km^{4}Hz^2)	0.053073481	0.14769620
l_o (H/km)	6.1729593*10$_{-6}$	675.36888*10$_{-6}$
l_∞ (H/km)	478.97099*10$_{-6}$	488.95186*10$_{-6}$
f_m (Hz)	553760.63	806338.63
b	1.1529766	0.92930728
g_o (Siemen/Hz*km)	0.23487476*10$_{-12}$	4.3*10$_{-8}$
g_e	1.38	0.70
c_∞ (nF/km)	50*10$_{-9}$	49*10$_{-9}$

The RLCG parameters for both the analytic models and the numeric models are graphed in Figures 2.4–2.7.

In Figure 2.7, only the numeric model is shown because the analytic admittance is assumed to be zero. As frequency increases past 100 kHz, note the closeness of the numeric resistance model to the analytic model dependent on $f^{1/2}$. This is largely due to skin effect of the copper wires at high frequency, which for a cylindrical conductor, is known to exhibit such a dependence on frequency.[9]

Figure 2.4 Resistance models for #24 and #26 gauge twisted pairs.

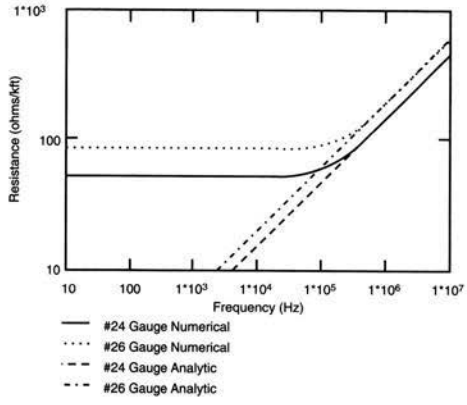


Figure 2.5 Inductance models for #24 and #26 gauge twisted pairs.

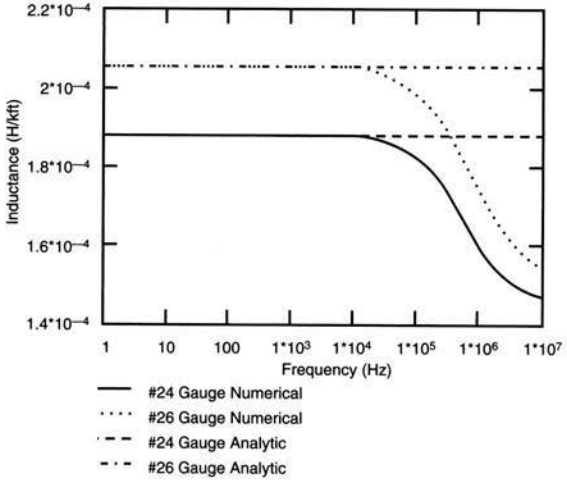


Figure 2.6 Capacitance models for #24 and #26 gauge twisted pairs.

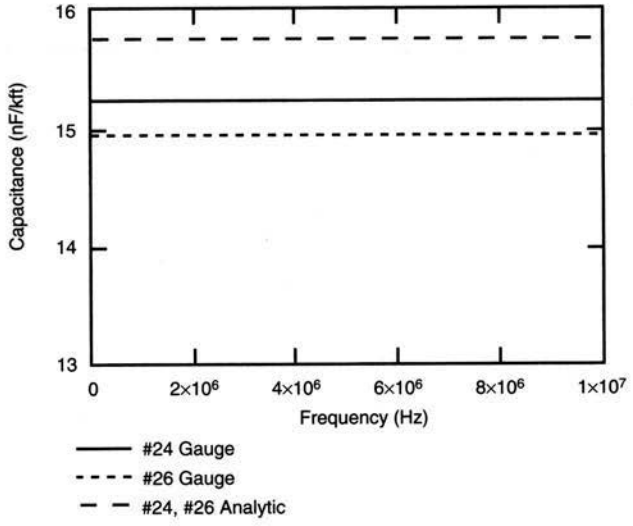
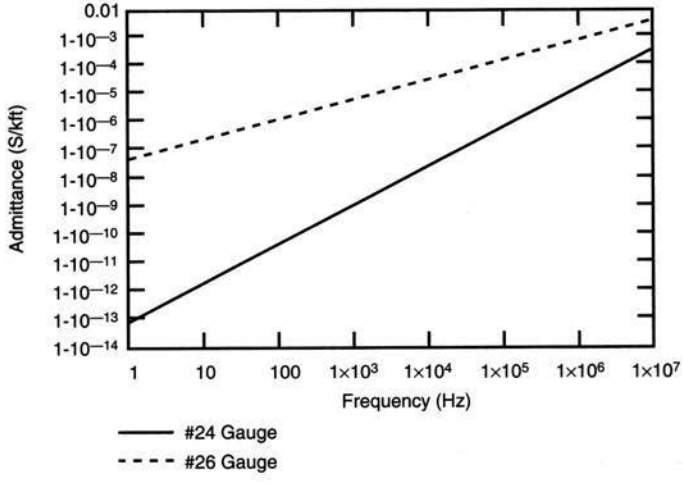


Figure 2.7 Admittance models for #24 and #26 gauge twisted pairs.



Note that in Figure 2.5, the inductance for both #24 and #26 wires varies by about 20 percent in the region above 100 kHz. Assuming that inductance is constant in the analytic model is certainly incorrect, but the choice to trade off error for simplicity is reasonable. The following sections show that the assumption of zero admittance in the analytic model,

although not accurate according to the numeric model, is reasonable at frequencies above 100 kHz. At these frequencies, the admittance needs to compare to jωC where j is the imaginary unit vector and ω is the radian frequency variable (2πf).

Transmission Line Parameters

The RLCG parameters of a transmission line define two common parameters useful in characterizing voltage and current along the line. These are the *propagation constant* (γ) and *characteristic impedance* ($Z_0(f)$). With these parameters, the voltage at some point z on a transmission line of length l with a load $Z_L(f)$ is given by Eqtn. 2.9. (The assumption is made that z=0 at the source voltage and increases positively until z=l at the termination load.)

Eqtn. 2.9

$$V(f,z) = V_0(f)\left(e^{-\gamma(f)z} + \Gamma_L(f)e^{\gamma(f)z}\right)$$

In Eqtn. 2.9, $V_0(f)$ is the source voltage, and $\Gamma_L(f)$ is the reflection coefficient of the line given by Eqtn. 2.10.

Eqtn. 2.10

$$\Gamma_L(f) = \frac{Z_L(f) - Z_o(f)}{Z_L(f) + Z_o(f)}$$

Note that for a known source voltage, termination impedance, and position, the voltage on the line is a function of only propagation constant and characteristic impedance.

Maximum power is delivered to a termination load on a transmission line when the characteristic impedance of the line and the load impedance are equal. This is desired in the case of a DSL because the termination load is the front of the channel receiver; delivering the maximum possible power to the receiver is necessary to optimize performance.

Under this condition, the expression for voltage on the line is simplified as the reflection coefficient in Eqtn. 2.10 becomes zero and the second exponential term in Eqtn. 2.9 drops out of the equation. When the load impedance is the same as the transmission line characteristic impedance, we say that the transmission line is matched. Hereafter, unless otherwise stated, it will be assumed that the twisted pair transmission lines under investigation are always matched, and the expression for voltage at some point z along the line is given by Eqtn. 2.11.

Eqtn. 2.11

$$V(f,z) = V_0(f)e^{-\gamma(f)z}$$

Note

Later in the chapter, you will see that this is a reasonable assumption over the frequencies of interest. Even when the characteristic impedance and load impedance are slightly different, the second term in Eqtn. 2.9 is negligible compared to the first term.

Knowledge of the propagation constant of a twisted pair is key to understanding the effect that a twisted pair has on signals. The propagation constant can further be broken down resulting in Eqtn. 2.12.

Eqtn. 2.12

$$\gamma = \alpha + j\beta = \sqrt{(R + j\omega L)(G + j\omega C)}$$

In Eqtn. 2.12, dependence of all quantities on frequency has been dropped only for notational simplicity. The terms α and β are the real and imaginary parts of the propagation constant, respectively. Substituting these into Eqtn. 2.11 yields the following in Eqtn. 2.13.

Eqtn. 2.13

$$V(f,z) = V_0(f)e^{-(\alpha + j\beta)z} = V_0(f)e^{-\alpha z}e^{-j\beta z}$$

The transfer function between the source voltage and some point z on the twisted pair is given by $H(f)$ as defined in Eqtn. 2.14.

Eqtn. 2.14

$$H(f) = \frac{V(f,z)}{V_0(f)} = e^{-\alpha z}e^{-j\beta z} = \left|e^{-\alpha z}\right| \angle \beta z$$

The last part of Eqtn. 2.14 is valid because the exponential involving β has unity magnitude and only contributes to phase shifting the voltage. On the other hand, the term involving α affects only the magnitude of the voltage. Thus, from Eqtn. 2.14, you can see that the real part of the propagation constant determines by how much the voltage will change over a length of twisted pair and the imaginary part how much the phase will change.

Propagation Constant

Later in this chapter, you will see that crosstalk between two twisted pairs becomes worse as frequency increases. Also, propagation loss of a twisted pair increases as frequency increases. In this section, an expression will be derived for the propagation constant of a twisted pair at these high frequencies. Two basic assumptions will aid in characterizing the propagation constant: first, $j\omega C >> G$, or equivalently, $G=0$; and second, $j\omega L > R$. Note that the second condition is less strict than the first. These approximations are valid for #24 AWG twisted pairs at frequencies above 100 kHz.

Using the approximations set forth, the propagation constant of a twisted pair can be written as shown in Eqtn. 2.15.

Eqtn. 2.15

$$\gamma = \sqrt{(R + j\omega L)(G + j\omega C)} \approx \sqrt{j\omega C}\sqrt{(R + j\omega L)}$$

In Eqtn. 2.15, the first assumption was used to eliminate the admittance term. Factoring the equation yields the result in Eqtn. 2.16.

Eqtn. 2.16

$$\gamma = \sqrt{j\omega C}\sqrt{(R + j\omega L)} = j\omega\sqrt{LC}\sqrt{\left(\frac{R}{j\omega L} + 1\right)}$$

$$\approx j\omega\sqrt{LC}\left(\frac{R}{j\omega L} + 1\right)$$

$$= R\sqrt{\frac{C}{L}} + j\omega\sqrt{LC}$$

In this equation, the final approximation is based on the second assumption $(x+1)^{1/2}=(x+1)$ for small x.

In terms of α and β, the real and imaginary parts of the propagation constant, the result from Eqtn. 2.16 yields these terms as shown in Eqtn. 2.17 and Eqtn. 2.18.

Eqtn. 2.17

$$\alpha = R\sqrt{\frac{C}{L}} = \alpha_o f^{1/2}$$

Eqtn. 2.18

$$\beta = \omega\sqrt{LC} = \beta_o f$$

In Eqtns. 2.17 and 2.18, α_o and β_o are introduced as constants. The final result for α comes from using the analytic approximation for the RLCG parameters. α is proportional to the square root of frequency because capacitance and inductance are both assumed constant, and R is assumed proportional to $f^{1/2}$ due to skin effect. The final result for β shows that β is proportional to frequency due to the $\omega(2\pi f)$ term.

Figures 2.8 and 2.9 show the real and imaginary part of propagation constant of a #24 and #26 gauge twisted pair. At frequencies above 100 kHz, both plots are consistent with Eqtn. 2.17 and Eqtn. 2.18. Note that the real part of the propagation constant, which was already established to have a direct effect on loss, increases with frequency and is higher for #26 wire than for #24.

Figure 2.8 Real part of the propagation constant for #24 and #26 twisted pairs.

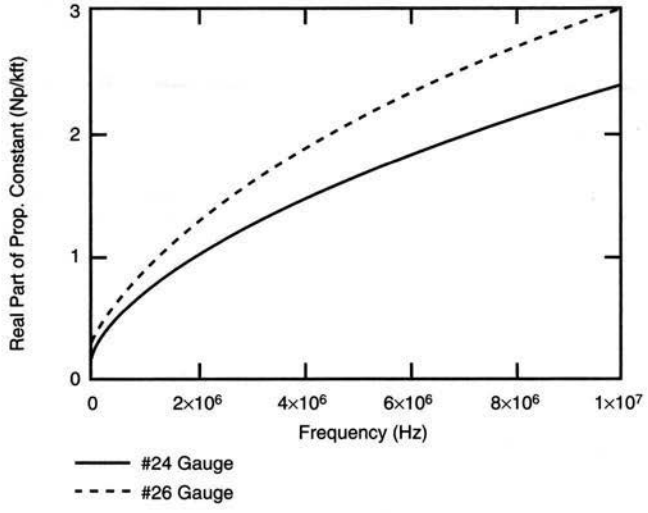
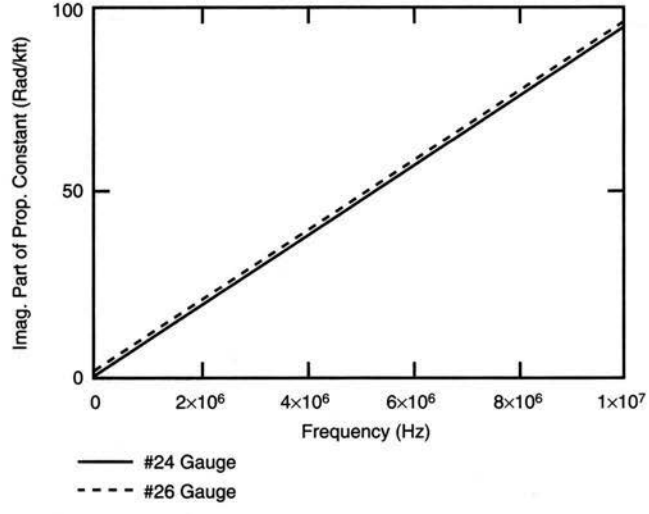


Figure 2.9 Imaginary part of the propagation constant for #24 and #26 twisted pairs.



In Eqtn. 2.11, an expression for the transfer function of a twisted pair was given in terms of the propagation constant. Figures 2.10–2.13 show the transfer function magnitude and phase for both #24 and #26 gauge cables.

Figure 2.10 Transfer function magnitude for various #24 gauge twisted pairs.

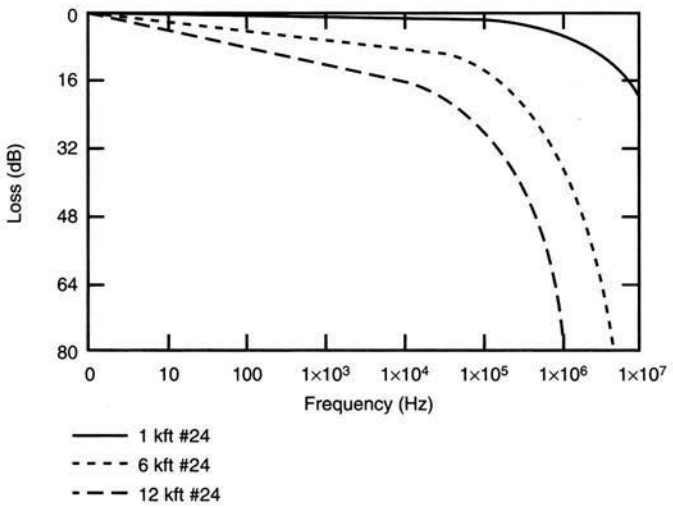


Figure 2.11 Transfer function phase for various #24 gauge twisted pairs.

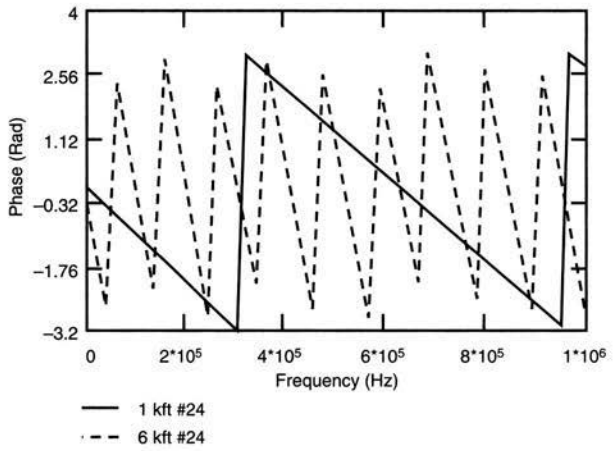


Figure 2.12 Transfer function magnitude for various #26 gauge twisted pairs.

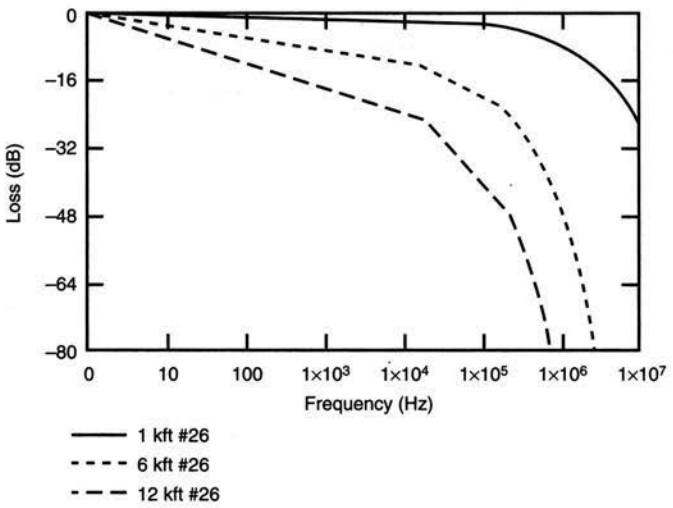
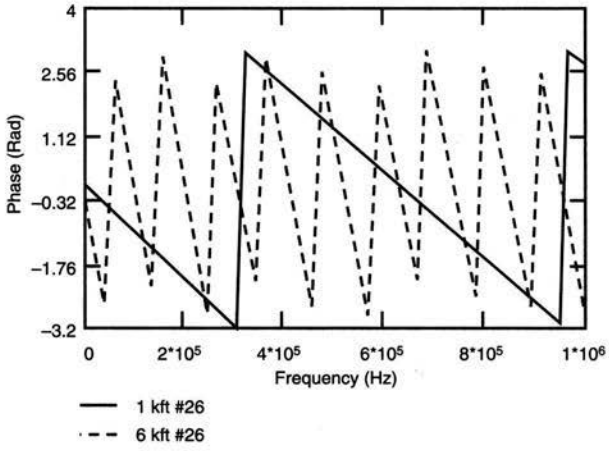


Figure 2.13 Transfer function phase for various #26 gauge twisted pairs.



Figures 2.10–2.13 show various cable line lengths. Note that the loss of the cable increases as line length increases and that it also increases with higher frequencies. Intuitively, these behaviors make sense. Longer lines have more loss than shorter lines, and higher frequencies are attenuated more by a pair of wires. Note also in Figures 2.11 and 2.13, where

phase is shown for only a 1,000 ft. and 6,000 ft. loop, the greater phase slope of the longer line. This trend continues as the loop length is further increased.

Characteristic Impedance

The preceding analysis assumes that the twisted pair was terminated in its characteristic impedance, Z_o. The characteristic impedance of any transmission line is defined in terms of the transmission line RLCG parameters and is given by Eqtn. 2.19.

Eqtn. 2.19

$$Z_o = \sqrt{\frac{R + j\omega L}{G + j\omega C}}$$

Note that the characteristic impedance does not depend on the length of the twisted pair. Figure 2.14 shows the characteristic impedance magnitude for a #24 and #26 gauge twisted pair. The respective phases are shown in Figure 2.15.

Figure 2.14 The characteristic impedance magnitude for #24 and #26 gauge twisted pairs.

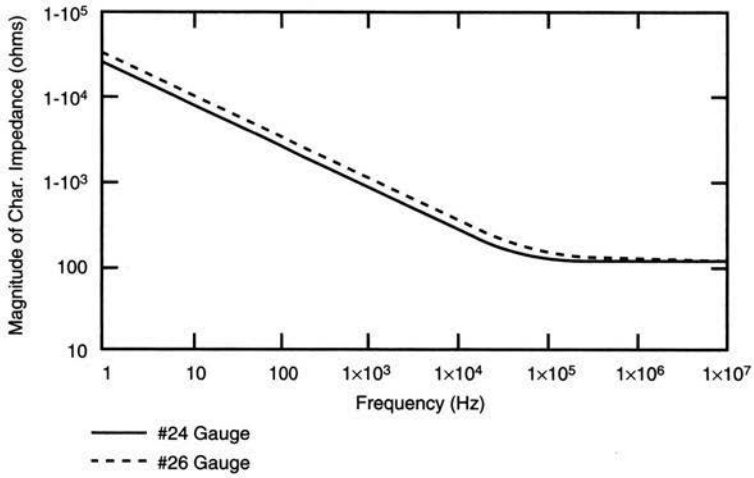
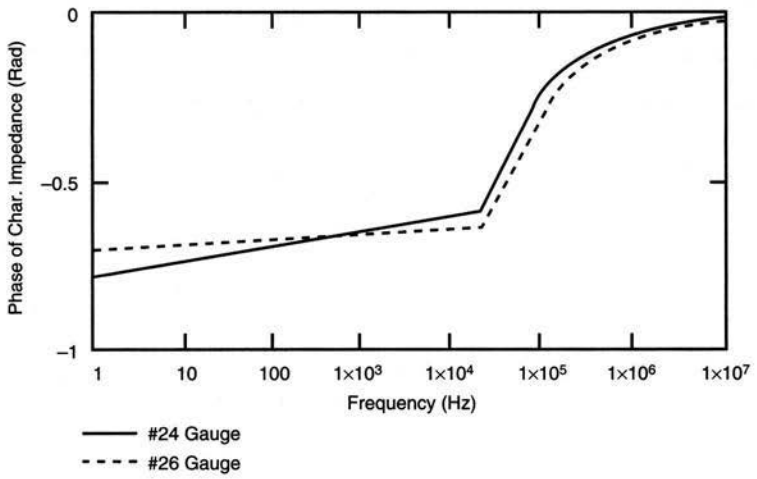


Figure 2.15 The characteristic impedance phase for #24 and #26 gauge twisted pairs.



Although the characteristic impedances vary with frequency, a 100 ohm purely resistive impedance is often assumed. (In some cases, especially in Europe, 135 ohms is assumed.) The error of this assumption is negligible in many cases because the reflection coefficient further reduces the effect of small mismatches as indicated in Eqtn. 2.10.

Note
In an actual implementation, it might be reasonable to design a terminating impedance to better favor either a #24 gauge or a #26 gauge twisted pair.

Crosstalk

This section is dedicated to defining crosstalk on twisted pairs and creating a mathematical model for it.

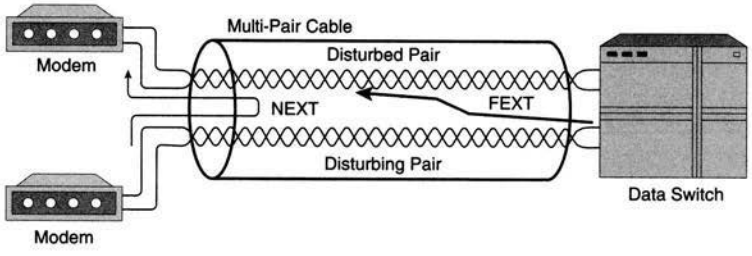
Crosstalk refers simply to disturbance on one twisted pair due to signals on another twisted pair. Usually, the twisted pairs are in the same cable or *binder group*. This text refers to the twisted pair being disturbed as the *disturbed pair* and to the twisted pair causing the disturbance as the *disturber* or *disturbing pair*. In cables with many pairs, it is common to have multiple disturbers. This also is addressed.

Note
If you have ever been on the telephone and faintly heard someone else's conversation on your line, you have experienced crosstalk firsthand.

Crosstalk Types

Crosstalk is generally characterized as either *near-end crosstalk* (NEXT) or *far-end crosstalk* (FEXT). NEXT is characterized by the disturbing pair's source being local to the disturbed pair's receiver. In this case, the disturbing signal starts down the disturbing pair, couples into the disturbed pair, and then propagates back to the disturbed pair's receiver. FEXT is characterized by the disturbing pair's source being distant from disturbed pair's receiver. In this case, the disturbing signal propagates down the disturbing pair, crosstalks into the disturbed pair, and propagates the rest of the distance along the disturbed pair into the disturbed pair's receiver. Figure 2.16 illustrates NEXT and FEXT.

Figure 2.16 Near-end crosstalk (NEXT) and far-end crosstalk (FEXT).



As shown in Figure 2.16, disturbing signals due to NEXT usually have to travel over less length of the twisted pair before entering a disturbed pair's receiver as compared to FEXT. For this reason, NEXT from a particular disturber is usually more damaging than FEXT. Note that either NEXT or FEXT or both might exist for a disturbed pair, and furthermore, more than one NEXT or FEXT disturber might exist.

NEXT or FEXT from a disturber whose line code is the same as that of the disturbed pair creates self-NEXT or self-FEXT, respectively. This type of disturbance is often present as similar services are often deployed from a central location. Later, you will see that ADSL and VDSL systems avoid self-NEXT, although self-FEXT is inevitable. Other common disturbers (both NEXT and FEXT) for ADSL systems include ISDN, HDSL, and T1 systems.

Unbalance Models

The following sections break the derivation of a mathematical model for NEXT and FEXT into two parts. The first part derives a mathematical model for crosstalk between two very short twisted pair sections. The second part takes that generic result and applies it to integrals specific to either NEXT or FEXT. It is interesting to note that the models stem from work done just after the turn of the 20th century by George Campbell[10,11] and also from work done in the 1960s by Cravis and Carter.[12] Both works are considered classics in crosstalk modeling and referenced in many journal articles on crosstalk.

For two twisted pairs located near one another, capacitive and inductive components exist between each of the four wires and also between each wire and ground. Analysis shows that crosstalk occurs when an unbalance exists among the capacitive and inductive components. The following assumptions are made while deriving the crosstalk models:

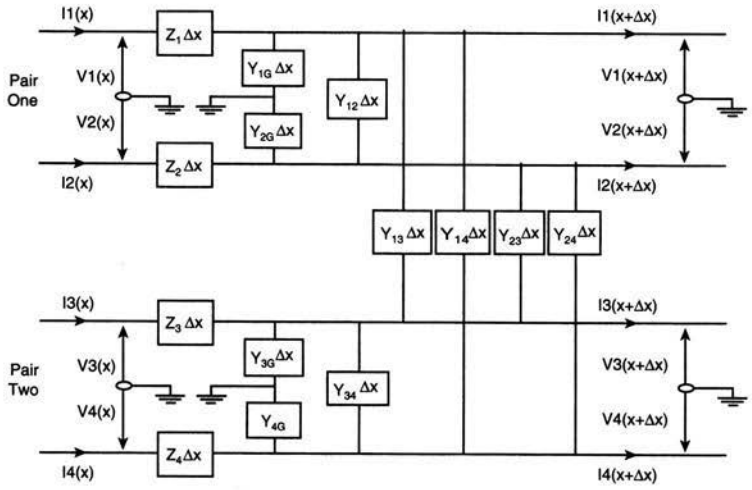
- The total crosstalk is a sum of the crosstalk due to capacitive and inductive crosstalk.
- Secondary effects (or crosstalk due to crosstalk) can be ignored.

Capacitive Unbalance Model

The capacitive unbalance analysis follows the derivation done by Miller.[13] Figure 2.17 shows a model of a portion of length of two twisted pair circuits in reasonably close proximity (for example, in a cable or binder group).

The four wires that compose the model each have some self-impedance, an admittance to one another, and a capacitance to ground. Furthermore, it is assumed that resistance between wires is negligible due to the plastic insulation. Thus, all admittances are purely capacitive (consistent with the analytic RLCG model).

Figure 2.17 Capacitive model of a short section of two twisted pairs.



For convenience, you can write all capacitances as admittances (Y=jωC). You can then write equations for the voltage and current on each of the four wires at the location x+Δx using basic circuit theory as in Eqtns. 2.20–2.27.

Eqtn. 2.20

$$V_1(x+\Delta x) = V_1(x) - I_1(x)Z_1\Delta x$$

Eqtn. 2.21

$$V_2(x+\Delta x) = V_2(x) - I_2(x)Z_2\Delta x$$

Eqtn. 2.22

$$V_3(x+\Delta x) = V_3(x) - I_3(x)Z_3\Delta x$$

Eqtn. 2.23

$$V_4(x+\Delta x) = V_4(x) - I_4(x)Z_4\Delta x$$

Eqtn. 2.24

$$I_1(x+\Delta x) = I_1(x) - V_1(x)Y_{1G}\Delta x - \left[V_1(x) - V_2(x)\right]Y_{12}\Delta x \\ -\left[V_1(x) - V_3(x)\right]Y_{13}\Delta x - \left[V_1(x) - V_4(x)\right]Y_{14}\Delta x$$

Eqtn. 2.25

$$I_2(x+\Delta x) = I_2(x) - V_2(x)Y_{2G}\Delta x - \left[V_2(x) - V_1(x)\right]Y_{12}\Delta x \\ -\left[V_2(x) - V_3(x)\right]Y_{23}\Delta x - \left[V_2(x) - V_4(x)\right]Y_{24}\Delta x$$

Eqtn. 2.26

$$I_3(x+\Delta x) = I_3(x) - V_3(x)Y_{3G}\Delta x - \left[V_3(x) - V_1(x)\right]Y_{13}\Delta x \\ -\left[V_3(x) - V_2(x)\right]Y_{23}\Delta x - \left[V_3(x) - V_4(x)\right]Y_{34}\Delta x$$

Eqtn. 2.27

$$I_4(x+\Delta x) = I_4(x) - V_4(x)Y_{4G}\Delta x - \left[V_4(x) - V_1(x)\right]Y_{14}\Delta x \\ -\left[V_4(x) - V_2(x)\right]Y_{24}\Delta x - \left[V_4(x) - V_3(x)\right]Y_{34}\Delta x$$

In Eqtns. 2.20–2.27, you can divide through by Δx, and as Δx approaches zero, the definition of the derivative can be invoked. The eight simultaneous equations can then be rearranged and placed in matrix form as shown in Eqtn. 2.28.

Eqtn. 2.28

$$\frac{d}{dx}\begin{bmatrix} V_1 \\ V_2 \\ V_3 \\ V_4 \\ I_1 \\ I_2 \\ I_3 \\ I_4 \end{bmatrix} = \begin{bmatrix} 0 & 0 & 0 & 0 & -Z_1 & 0 & 0 & 0 \\ 0 & 0 & 0 & 0 & 0 & -Z_2 & 0 & 0 \\ 0 & 0 & 0 & 0 & 0 & 0 & -Z_3 & 0 \\ 0 & 0 & 0 & 0 & 0 & 0 & 0 & -Z_4 \\ -\begin{pmatrix} Y_{1G}+Y_{12} \\ +Y_{13}+Y_{14} \end{pmatrix} & 0 & 0 & 0 & 0 & 0 & 0 & 0 \\ Y_{12} & -\begin{pmatrix} Y_{2G}+Y_{12} \\ +Y_{23}+Y_{24} \end{pmatrix} & 0 & 0 & 0 & 0 & 0 & 0 \\ Y_{13} & 0 & -\begin{pmatrix} Y_{3G}+Y_{13} \\ +Y_{23}+Y_{34} \end{pmatrix} & 0 & 0 & 0 & 0 & 0 \\ Y_{14} & 0 & 0 & -\begin{pmatrix} Y_{4G}+Y_{14} \\ +Y_{24}+Y_{34} \end{pmatrix} & 0 & 0 & 0 & 0 \end{bmatrix} \cdot \begin{bmatrix} V_1 \\ V_2 \\ V_3 \\ V_4 \\ I_1 \\ I_2 \\ I_3 \\ I_4 \end{bmatrix} = A \cdot S$$

In Eqtn. 2.28, for convenience of notation only, the dependence on x from all voltages and currents has been dropped, and S and A have been introduced to denote the 8×8 impedance matrix and the 8×1 voltage and current vector, respectively.

At this point, it is helpful to transform the voltages and currents on the four lines to metallic and longitudinal voltages and currents. A simple set of linear transformations shown in Eqtns. 2.29–2.36 accomplishes this.

Eqtn. 2.29

$$V_{1M} = V_1 - V_2$$

Eqtn. 2.30

$$V_{2M} = V_3 - V_4$$

Eqtn. 2.31

$$V_{1L} = \frac{V_1 + V_2}{2}$$

Eqtn. 2.32

$$V_{2L} = \frac{V_3 + V_4}{2}$$

Eqtn. 2.33

$$I_{1M} = \frac{I_1 - I_2}{2}$$

Eqtn. 2.34

$$I_{2M} = \frac{I_3 - I_4}{2}$$

Eqtn. 2.35

$$I_{1L} = I_1 + I_2$$

Eqtn. 2.36

$$I_{2L} = I_3 + I_4$$

In these equations, the first subscript $_{(1 \text{ or } 2)}$ identifies the twisted pair, and the second subscript $_{(M \text{ or } L)}$ indicates metallic or longitudinal signal type, respectively. Thus for example, V_{1M} would represent the metallic voltage on twisted pair 1.

To transform Eqtn. 2.28 to be in terms of metallic and longitudinal signals, Eqtns. 2.30–2.36 must be solved for the original voltages and currents. By letting S be a column vector of the metallic and longitudinal voltages and currents, it can easily be shown that Eqtn. 2.37 is true.

Eqtn. 2.37

$$S = T \cdot \begin{bmatrix} V_{1M} \\ V_{1L} \\ V_{2M} \\ V_{2L} \\ I_{1M} \\ I_{1L} \\ I_{2M} \\ I_{2L} \end{bmatrix} = T \cdot S'$$

In Eqtn. 2.37, S is the column vector of voltage and currents, and T is a transformation matrix given by Eqtn. 2.38.

Eqtn. 2.38

$$T = \begin{bmatrix} \frac{1}{2} & 1 & 0 & 0 & 0 & 0 & 0 & 0 \\ \frac{-1}{2} & 1 & 0 & 0 & 0 & 0 & 0 & 0 \\ 0 & 0 & \frac{1}{2} & 1 & 0 & 0 & 0 & 0 \\ 0 & 0 & \frac{-1}{2} & 1 & 0 & 0 & 0 & 0 \\ 0 & 0 & 0 & 0 & 1 & \frac{1}{2} & 0 & 0 \\ 0 & 0 & 0 & 0 & -1 & \frac{1}{2} & 0 & 0 \\ 0 & 0 & 0 & 0 & 0 & 0 & 1 & \frac{1}{2} \\ 0 & 0 & 0 & 0 & 0 & 0 & -1 & \frac{1}{2} \end{bmatrix}$$

You can then transform the system of equations given in Eqtn. 2.28 as in Eqtn. 2.39.

Eqtn. 2.39

$$\frac{d}{dx} S' = T^{-1} A T S'$$

The result of this transformation shows that the derivatives with respect to x of the metallic and longitudinal voltages depend only on the metallic and longitudinal currents, and the derivative with respect to x of the metallic and longitudinal currents depends only on the metallic and longitudinal voltages. Concentration will be placed only on the latter, simplifying the system of equations to four equations and four unknowns. Thus, the simplified set of equations in terms of metallic and longitudinal signals is shown in Eqtn. 2.40.

Eqtn. 2.40

$$\frac{d}{dx} \begin{bmatrix} I_{1M} \\ I_{1L} \\ I_{2M} \\ I_{2L} \end{bmatrix} = \frac{-j \cdot \omega}{4} \begin{bmatrix} a_{11} & a_{12} & a_{13} & a_{14} \\ a_{21} & a_{22} & a_{23} & a_{24} \\ a_{31} & a_{32} & a_{33} & a_{34} \\ a_{41} & a_{42} & a_{43} & a_4 \end{bmatrix} \cdot \begin{bmatrix} V_{1M} \\ V_{1L} \\ V_{2M} \\ V_{2L} \end{bmatrix}$$

The elements of the four-by-four matrix are given by Eqtns. 2.41–2.50.

Eqtn. 2.41

$$a_{11} = C_{1G} + C_{2G} + 4C_{12} + C_{13} + C_{14} + C_{23} + C_{24}$$

Eqtn. 2.42

$$a_{21} = a_{12} = 2C_{1G} - 2C_{2G} + 2C_{13} + 2C_{14} - 2C_{23} - 2C_{24}$$

Eqtn. 2.43

$$a_{31} = a_{31} = -C_{13} + C_{14} + C_{23} - C_{24}$$

Eqtn. 2.44

$$a_{41} = a_{14} = -2C_{13} - 2C_{14} + 2C_{23} + 2C_{24}$$

Eqtn. 2.45

$$a_{22} = 4C_{1G} + 4C_{2G} + 4C_{13} + 4C_{14} + 4C_{23} + 4C_{24}$$

Eqtn. 2.46

$$a_{23} = a_{32} = -2C_{13} + 2C_{14} - 2C_{23} + 2C_{24}$$

Eqtn. 2.47

$$a_{24} = a_{42} = -4C_{13} - 4C_{14} - 4C_{23} - 4C_{24}$$

Eqtn. 2.48

$$a_{33} = C_{3G} + C_{4G} + C_{13} + C_{14} + C_{23} + C_{24} + 4 \cdot C_{34}$$

Eqtn. 2.49

$$a_{34} = a_{43} = 2C_{3G} - 2C_{4G} + 2C_{13} - 2C_{14} + 2C_{23} - 2C_{24}$$

Eqtn. 2.50

$$a_{44} = 4C_{3G} + 4C_{4G} + 4C_{13} + 4C_{14} + 4C_{23} + 4C_{24}$$

In these equations, capacitance has been used instead of admittance to further stress that the impedances between all wires is capacitive. For crosstalk between twisted pairs, you should be most concerned with the coupling from the metallic signal of the disturbing pair into the metallic signal of the disturbed pair. The parameter a_{31} from Eqtn. 2.43 defines this coupling, metallic voltage in the disturbing pair (V_{1M}) to metallic current in the disturbed pair (I_{2M}). Parameter a_{31} is referred to as the *capacitance unbalance* of a twisted pair. For notational purposes, a_{31} will be renamed as C_{M1M2}. Thus, crosstalk resulting from capacitance unbalance is given by Eqtn. 2.51.

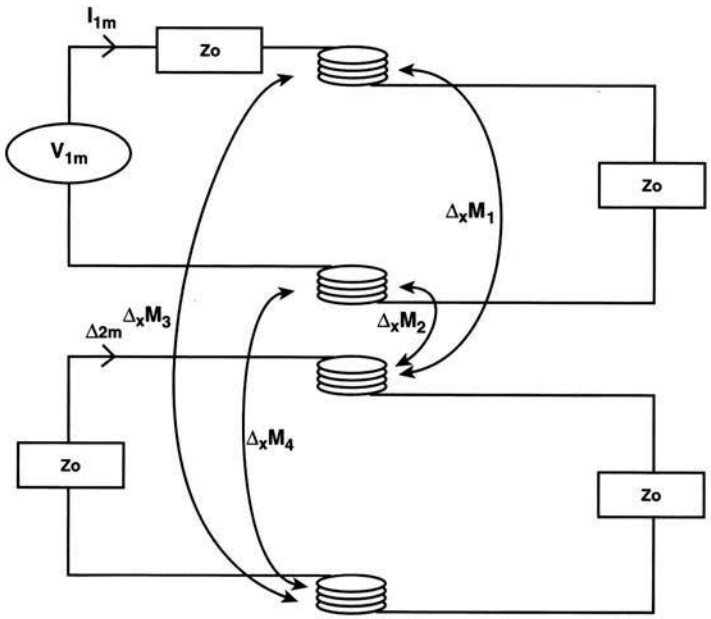
Eqtn. 2.51

$$I_{2M} = \frac{-d}{dx}\frac{j\omega}{4} C_{M1M2} V_{1M}$$

Inductive Unbalance Model

Crosstalk due to mutual inductance unbalance is a bit easier to derive than capacitive unbalance. Consider a small section of two twisted pairs as shown in Figure 2.18.

Figure 2.18 Mutual inductance model of a short section of two twisted pairs.

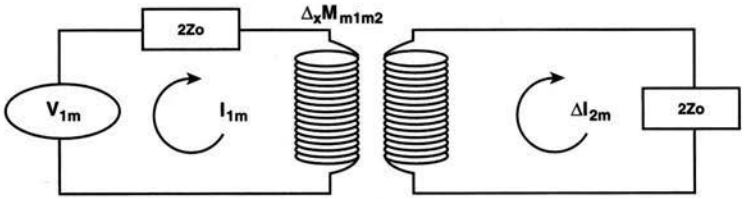


Mutual inductance exists pair-wise between each of the wires in the two twisted pairs. The effective termination at each end of the two pairs is the characteristic impedance. No

crosstalk occurs if the couplings are balanced with respect to one another. For example, if M_1 and M_3 produce exactly opposite currents in the disturbed pair and M_2 and M_4 do the same, then all the coupled currents will cancel one another, and no net crosstalk will be present on the disturbed pair.

To mathematically analyze Figure 2.18, it is helpful to draw the equivalent circuit shown in Figure 2.19.

Figure 2.19 Equivalent circuit for the mutual inductance unbalance of a short section of two twisted pairs.



The mutual inductance denoted by M_{M1M2} is given by Eqtn. 2.52.

Eqtn. 2.52

$$M_{M1M2} = M_1 + M_2 + M_3 + M_4$$

Note that M_{M1M2} will be zero when the mutual inductances are balanced. In Figure 2.19, the current ΔI_{2M} is the current generated on the disturbed twisted pair on the small section shown.

The circuit in Figure 2.19 can be analyzed by writing the following loop equations (Eqtn. 2.53 and Eqtn. 2.54) for I_{1M} and ΔI_{2M}:

Eqtn. 2.53

$$2ZI_{1M} - M\Delta xI_{2M} = V_{1M}$$

Eqtn. 2.54

$$-M\Delta xI_{1M} + 2ZI_{2M} = 0$$

These equations can then be solved simultaneously, and the resulting ΔI_{2M} is in Eqtn. 2.55.

Eqtn. 2.55

$$I_{2M} = \frac{j\omega M \Delta x V_{1M}}{4Z^2 - M^2\omega^2\Delta x^2}$$

Because M is usually very small and Δx is a very small portion of line, the second term in the denominator is small with respect to the first term and can be dropped. Also, the definition of derivative can be invoked as Δx approaches zero, so Eqtn. 2.55 can be written as Eqtn. 2.56.

Eqtn. 2.56

$$\frac{dI_{2M}}{dx} \approx \frac{j\omega M V_{1M}}{4Z^2}$$

Thus, the result of inductive coupling here gives a similar result to the earlier result for capacitive coupling in that the current induced on a disturbed line due to a voltage on a disturbing line is proportional to the frequency. (This assumes that the characteristic impedance is constant with frequency as was shown earlier in this chapter.)

General Unbalance Expression

From the capacitive and inductive unbalance expressions, the total crosstalk on a small portion of twisted pair can be written as in Eqtn. 2.57.

Eqtn. 2.57

$$\frac{dI_{2M}}{dx} = \left(\frac{j\omega M}{4Z^2} + \frac{j\omega C_{M1M2}}{4}\right) V_{1M}$$

If the characteristic impedance of the line is a constant over frequency, then the current in Eqtn. 2.57 is proportional to frequency for a given voltage. With this in mind, all the constants of Eqtn. 2.57 can be grouped together to form a new unbalance constant, Q_{M1M2} such that Eqtn. 2.58 holds.

Eqtn. 2.58

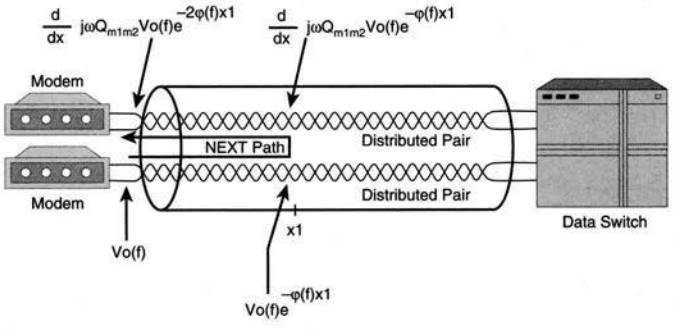
$$\frac{dI_{2M}}{dx} = \left(\frac{j\omega M}{4Z^2} + \frac{j\omega C_{M1M2}}{4}\right) V_{1M} = j\omega Q_{M1M2} V_{1M}$$

Near-end Crosstalk (NEXT)

Now that a generic expression has been obtained for the crosstalk from a very short segment of a disturbing pair to a very short segment of a disturbed pair, attention can be

turned to the specific cases of NEXT and FEXT. Consider a signal V traveling along a disturbing pair. At some distance x1 along a disturbing pair, it couples into a disturbed pair due to unbalance and then travels back to the receiver of the disturbed pair as shown in Figure 2.20.

Figure 2.20 An example of near-end crosstalk due to only one unbalance point (x1).



If the signal exciting the disturbing pair is V_o, then from Eqtn. 2.11 the signal on the disturbing pair at x1 is as shown in Eqtn. 2.59.

Eqtn. 2.59

$$V_1(f, x1) = V_o(f)e^{-\gamma(f)x1}$$

This signal couples due to unbalance onto the disturbed pair at x1. From the unbalance term of Eqtn. 2.58, the resulting current on the disturbed pair is shown by Eqtn. 2.60.

Eqtn. 2.60

$$I_2(f, x1) = \frac{d}{dx} j\omega Q_{M1M2} V_1(f, x1) = \frac{d}{dx} j\omega Q_{M1M2} V_o(f)e^{-\gamma(f)x1}$$

To reach the disturbed pair's receiver, the signal must propagate the distance x1 along the disturbed pair. This introduces further attenuation of $e_{ms\gamma x1}$. The current arriving at the disturbed pair's receiver can thus be written as in Eqtn. 2.61.

Eqtn. 2.61

$$I_2(f,0) = I_2(f, x1)e^{-\gamma(f)x1} = \frac{d}{dx} j\omega Q_{M1M2} V_o(f)e^{-2\gamma(f)x1}$$

The expression in Eqtn. 2.61 gives the current that NEXT will produce if only one unbalance point existed along the twisted pairs. Usually, unbalance will exist at many points along the pairs, and furthermore, the unbalance coefficient, Q_{M1M2} might be different at

each point. To find the total current at the disturbed pair's receiver due to all the unbalance points along the pairs, you can let the unbalance coefficient be a function of position on the line, Q_{M1M2}, and integrate along the length of the line. The total current is then given by Eqtn. 2.62.

Eqtn. 2.62

$$I_2(f) = \int_0^L j\omega Q_{M1M2}(x) V_o(f) e^{-2\gamma(f)x1} dx$$

For performance analysis, the concern is more with the power due to NEXT than with the current. Given a current and a termination impedance, Z_{term}, power can be found by Eqtn. 2.63.

Eqtn. 2.63

$$P(f) = I(f)I^*(f)Z_{term} \; P(f) = I(f)I^*(f)Z_{term}$$

In Eqtn. 2.63, * is the complex conjugate operator. For the NEXT expression, still in integral form, explicit calculation of the current, and therefore power, would be impossible because knowledge of Q_{M1M2} at every point x on the pairs is not known. Assuming that the termination impedance is equal to the line's characteristic impedance, from Eqtn. 2.62, the NEXT power at the disturbed receiver can be written as in Eqtn. 2.64.

Eqtn. 2.64

$$E[P(f)] = E\left[|Z_o| I_2(f) I_2(f)^*\right]$$
$$= E\left[|Z_o| \int_0^L j\omega Q_{M1M2}(x) V_o(f) e^{-2\gamma(f)x} dx \int_0^L - j\omega Q_{M1M2}(y) V_o(f) e^{-2\gamma^*(f)y} dy\right]$$

The operator E* is used here to denote the expected value. All terms that do not involve x or y can be pulled outside the integral so that Eqtn. 2.64 simplifies to Eqtn. 2.65.

Eqtn. 2.65

$$E[P(f)] = E\left[|Z_o| I_2(f) I_2(f)^*\right]$$
$$= E\left[|Z_o| \omega^2 V_o^2(f) \int_0^L \int_0^L Q_{M1M2}(x) Q_{M1M2}(y) e^{-2\gamma(f)x} e^{-2\gamma^*(f)y} dxdy\right]$$

The double integration in Eqtn. 2.65 can be simplified by assuming that the unbalance at some point x1 on the twisted pair is independent of the unbalance at another point x2. Using this assumption leads to the expression in Eqtn. 2.66.

Eqtn. 2.66

$$E\left[Q_{M1M2}(x)Q_{M1M2}(y)\right] = k \cdot \delta(x-y)$$

Here, k is the second moment of the random variable Q_{M1M2}, and δ is the khroniker delta function such that Eqtn. 2.67 is true.

Eqtn. 2.67

$$\delta(x) = \begin{cases} 1 & \text{if } x = 0 \\ 0 & \text{otherwise} \end{cases}$$

Because Q_{M1M2} is the only random variable in Eqtn. 2.65, the expectation can be taken inside, and the first integration performed such that the result in Eqtn. 2.68 is obtained.

Eqtn. 2.68

$$\begin{aligned} E[P(f)] &= |Z_o|\omega^2 V_o^2(f)\int_0^L \int_0^L E\left[Q_{M1M2}(x)Q_{M1M2}(y)\right] e^{-2\gamma(f)x} e^{-2\gamma^*(f)y}\,dxdy \\ &= |Z_o|\omega^2 V_o^2(f)\int_0^L \int_0^L k\delta(x-y) e^{-2\gamma(f)x} e^{-2\gamma^*(f)y}\,dxdy \\ &= |Z_o|\omega^2 V_o^2(f)\int_0^L k e^{-2\gamma(f)x} e^{-2\gamma^*(f)x}\,dx \end{aligned}$$

The sifting property was used to obtain the last line of Eqtn. 2.68.

If the exponential terms in Eqtn. 2.68 are combined and the propagation constant expressed in terms of α and β, Eqtn. 2.69 results.

Eqtn. 2.69

$$\begin{aligned} E[P(f)] &= |Z_o|\omega^2 V_o^2(f)\int_0^L k e^{-2\gamma(f)x} e^{-2\gamma^*(f)x}\,dx \\ &= |Z_o|\omega^2 V_o^2(f)\int_0^L k e^{-2x[(\alpha(f)+j\beta(f))+(\alpha(f)-j\beta(f))]}\,dx \\ &= |Z_o|\omega^2 V_o^2(f)\int_0^L k e^{-4x\alpha(f)}\,dx \end{aligned}$$

The final integration can now be carried out. The result is in Eqtn. 2.70.

Eqtn. 2.70

$$E[P(f)] = |Z_o|\omega^2 V_o^2(f)\int_0^L k e^{-4x\alpha(f)}dx$$
$$= |Z_o|\omega^2 V_o^2(f)k\frac{e^{-4x\alpha(f)}}{-4\alpha(f)}\Big|_0^L$$
$$= \frac{|Z_o|\omega^2 V_o^2(f)k}{-4\alpha(f)}\left(e^{-4L\alpha(f)} - 1\right)$$

For long lines, the exponential in the result will be small compared to 1, and Eqtn. 2.70 can be simplified. In addition, Eqtn. 2.70 can be divided by the power of the disturbing transmitter ($|V_o|^2/Z_o$) to obtain the power transfer function between the disturbing transmitter and the disturbed receiver, denoted as H_{NEXT} as in Eqtn. 2.71.

Eqtn. 2.71

$$H_{NEXT}(f) = \frac{|Z_o|^2\omega^2 k}{4\alpha(f)} = \frac{k' f^2}{\alpha_o f^{1/2}} = K_{NEXT} f^{3/2}$$

In Eqtn. 2.71, K_{NEXT} is a constant of proportionality encompassing all the constants in the first two terms of Eqtn 2.71. Thus, for a disturber with a *flat power spectral density* (PSD), you have an expression showing that NEXT is proportional to $f^{3/2}$. Eqtn. 2.71 is sometimes called a *crosstalk loss function*. It is more generic than a general NEXT power equation because it does not depend on the PSD of the disturber. Instead, it can be multiplied by any PSD to give the expected NEXT power that the disturber would cause.

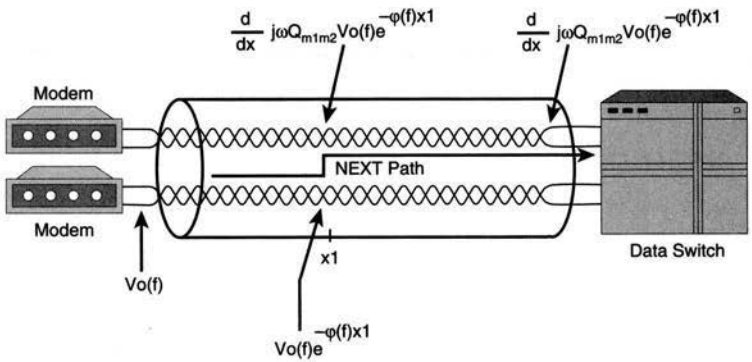
Note that NEXT does not depend on the length of the twisted pair. This is because the interference due to NEXT, although a sum of crosstalk at every point along the pair, will be dominated by the unbalance points nearest to the receiver. The crosstalk from the nearer unbalance points will dominate the crosstalk from distant unbalance points due simply to the length of twisted pair that each must propagate through.

Note also that K_{NEXT} is a random variable. For many different disturbers into a disturbed pair, K_{NEXT} will tend toward a Gaussian distribution due to the central limit theorem.[14,15,16]

Far-end Crosstalk (FEXT)

FEXT will be derived using a similar method as used in the NEXT derivation. Figure 2.21 shows an example of FEXT due to an unbalance point at x1 only.

Figure 2.21 An example of far-end crosstalk due to only one unbalance point (x1).



The signal expressions on the disturbing pair are the same as for the NEXT case, and the current at x1 on the disturbed pair is also the same as in the NEXT derivation. Repeating the expression for this current from Eqtn. 2.60 yields Eqtn. 2.72.

Eqtn. 2.72

$$I_2(f,x1) = \frac{d}{dx} j\omega Q_{M1M2} V_1(f,x1) = \frac{d}{dx} j\omega Q_{M1M2} V_o(f) e^{-\gamma(f)x1}$$

To reach the disturbed pair's receiver, the signal must propagate over the remainder of the disturbed pair (a distance of L-x1). Upon reaching the disturbed pair's receiver, the resulting expression for current on the disturbed line is shown in Eqtn. 2.73.

Eqtn. 2.73

$$I_2(f,L) = \frac{d}{dx} j\omega Q_{M1M2} V_o(f) e^{-\gamma(f)x1} e^{-\gamma(f)(L-x1)}$$
$$= \frac{d}{dx} j\omega Q_{M1M2} V_o(f) e^{-\gamma(f)L}$$

Just as in the NEXT case, the total crosstalk signal on the disturbed pair will be a summation of crosstalk due to unbalance points all along the twisted pairs and not just the one at x1. Eqtn. 2.73 can be integrated to find this expression. Moving one step farther, one can write an expression for the total FEXT power similar to Eqtn. 2.64 as in the following Eqtn. 2.74.

Eqtn. 2.74

$$E[P(f)] = E\left[|Z_o| I_2(f) I_2(f)^*\right]$$
$$= E\left[|Z_o| \int_0^L j\omega Q_{M1M2}(x) V_o(f) e^{-\gamma(f)L} dx \int_0^L - j\omega Q_{M1M2}(y) V_o(f) e^{-\gamma^*(f)L} dy\right]$$
$$= |Z_o| \omega^2 V_o^2(f) e^{-\gamma(f)L} e^{-\gamma^*(f)L} \int_0^L \int_0^L E[Q_{M1M2}(x) Q_{M1M2}(y)] dx dy$$

The relationship given in Eqtn. 2.66 can again be used to help carry out the integral in Eqtn. 2.74 so that the expression for FEXT simplifies to Eqtn. 2.75.

Eqtn. 2.75

$$E[P(f)] = |Z_o| \omega^2 V_o^2(f) e^{-2\alpha(f)L} \int_0^L k dx = |Z_o| \omega^2 V_o^2(f) e^{-2\alpha(f)L} L$$

The constants in Eqtn. 2.75 can be grouped together in a single constant, and the average FEXT transfer function can be written as Eqtn. 2.76.

Eqtn. 2.76

$$H_{FEXT}(f) = K_{FEXT} f^2 e^{-2\alpha(f)L} L$$

Note that K_{FEXT}, like K_{NEXT} is also a random variable. When multiple disturbers exist, K_{FEXT} can be expected to tend toward a Gaussian random variable due to the central limit theorem. Note also that FEXT, unlike NEXT, is a function of the length of the twisted pair. This fact is intuitively satisfying because FEXT disturbances due to any unbalance point along the twisted pairs must propagate the entire length of the pair to disturb the receiver. (At this point, the reader should realize that both NEXT and FEXT increase with frequency, and thus a twisted pair designed for low frequency signals presents challenges when high frequency signals are involved.)

Summary

This chapter was dedicated to better understanding twisted pair physical and electrical properties. The primary line constants, RLCG, of a twisted pair were discussed. Numeric and analytic models of a twisted pair's propagation constant and characteristic impedance were derived. The attenuation of various twisted pair cables was also illustrated.

Crosstalk between twisted pairs was discussed in some detail. The basic cause of crosstalk, unbalance between neighboring pairs, was derived from basic circuit theory. From the unbalance expressions, expressions for near-end crosstalk (NEXT) power and far-end crosstalk (FEXT) power were derived.

Understanding the challenges that a twisted pair environment poses to an ADSL or a VDSL environment will help the reader understand the motivation for some of the modulation and coding schemes presented in later chapters. Also, the models developed here will be used directly in later chapters to predict and bound the performance of certain ADSL and VDSL examples.

Exercises

1. For #24 and #26 gauge twisted pairs, plot over frequency the characteristic impedance and propagation constant using the analytic and numeric models.
2. Find the loss at 500 kHz of a 10 kft, #26 gauge twisted pair using both the analytic and numeric models.
3. For a #26 loop, plot Eqtn. 2.70 for various lengths. At what length does the approximation of Eqtn. 2.71 become valid?
4. Graph the NEXT and FEXT loss functions on the same set of axes for different lengths of #24 and #26 twisted pair. At what length does NEXT become dominant over FEXT?
5. Plot the loss of a #26 twisted pair at 500 kHz against the length of the pair. At what length is the loss equal to the NEXT loss at 500 kHz?

Endnotes

1. Rhodes, Frederick Leland, *Beginnings of Telephony.* New York: Harper and Brothers, 1929.
2. Manhire, L. M., "Physical and Transmission Characteristics of Customer Loop Plant." *Bell System Technical Journal* 57 (January 1978): 35–39.
3. Chin, Wu-Jhy, et al, "Loop Survey in the Taiwan Area and Feasibility Study for HDSL." IEEE Selected Areas in Communications 9, no. 6 (August 1991): 801–809.
4. Reeve, Whitham D., *Subscriber Loop Signalling and Transmission Handbook.* New York: IEEE Press, 1992.
5. Bellamy, John, *Digital Telephony.* New York: John Wiley and Sons, 1991.
6. Gang, Huang, and J.J. Werner, "Cable Characteristics." *ANSI Contribution T1E1.4/97-169*, Clearwater, FL, May 12, 1997.
7. Gilbert, Elliot and John Nellist, *Telecommunications Wiring for Commercial Buildings, A Practical Guide.* New York: IEEE Press, 1996.

8. Pickering, Ashley, "Primary Line Constants for US 24 and 26 AG Twisted Pair Cables." *ANSI Contribution T1E1.4/96-074.* Colorado Springs, CO, April 22, 1996.

9. Sadiku, M., *Elements of Electromagnetics.* Philadelphia: Saunders College Publishing, 1989.

10. Campbell, G., "Dr. Campbell's Memoranda of 1907 and 1912." *Bell System Technical Journal* 14, no. 4 (October 1935): 558–472.

11. AT&T Company, *Collected Papers of George A. Campbell.* New York: AT&T, 1937.

12. Cravis, H. and T.V. Carter, "Engineering of T1 Carrier System Repeated Lines." *Bell System Technical Journal* 42, no. 1 (March 1963): 431–486.

13. Miller, G., "The Effect of Longitudinal Imbalance on Crosstalk." *Bell System Technical Journal* 54, no. 7 (September 1975): 1227–1251.

14. Kerpez, K., "Near End Crosstalk Is Almost Gaussian." *IEEE Transactions on Communications* 41, no. 1 (January 1993): 670–672.

15. Werner, J.J., "The HDSL Environment." *IEEE Journal on Selected Areas in Communications* 9, no. 6 (August 1991): 785–800.

16. Gallager, Robert, *Information Theory and Reliable Communications.* New York: John Wiley and Sons, 1968.

CHAPTER 3

Loop Analysis

In this chapter:

- A review of ABCD parameters
- Discussion of bridged taps
- Application of ABCD parameters to twisted pair characteristics
- Discussion of ADSL and VDSL test loops

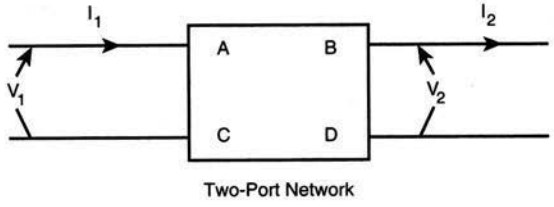
This chapter presents methods to analyze transmission parameters of twisted pairs. This chapter provides a generic procedure using ADCD parameters that is applicable to almost every type of loop. Understanding the properties of twisted pairs is necessary for understanding many aspects of ADSL and VDSL modulation methods. Being able to characterize different types of loops is also necessary for benchmarking the limits of performance for a modulation. In this spirit, a discussion is given on the various test loops to be used when characterizing theoretical performance achievable on a twisted pair, as well as actual performance of different modulation schemes. Various standards bodies have defined these loops to benchmark proposed modulation schemes and define the performance goals of DSL technologies.[1,2] In addition, several sections deal with the definition and use of ABCD parameters, providing the tools to characterize virtually any loop configuration.

ABCD Parameters

Before discussing various test loops, a review of *ABCD transmission parameters* will be helpful. ABCD parameters are useful in characterizing *two-port networks.* A two-port network is generically defined to have a single unique input port and a single unique output port with some transfer function between the two. These parameters mathematically relate the input voltage and current to the output voltage and current. Figure 3.1 shows a generic two-port

network. In this figure, the output voltage and current V_2 and I_2 are related to the input voltage and current V_1 and I_1 in terms of ABCD parameters as in Eqtn. 3.1.

Figure 3.1 A generic two-port network.



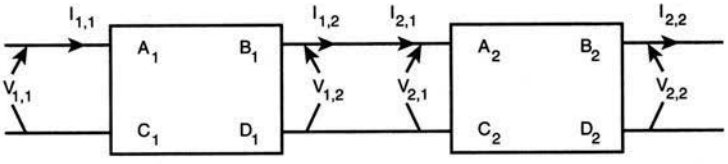
Eqtn. 3.1

$$V_1 = AV_2 + BI_2$$
$$I_1 = CV_2 + DI_2$$

Note that Eqtn. 3.1 characterizes the network without making any assumptions about the network's termination. The parameters A, B, C, and D are specific to the transfer function of the network.

Figure 3.2 shows two networks in tandem. Each network is independently characterized by its own ABCD parameters (denoted by subscript 1 and subscript 2).

Figure 3.2 Two two-port networks in tandem; each network has unique ABCD parameters.



The effective ABCD parameters for the entire system can be given by a simple matrix multiplication of the individual parameters such that Eqtn. 3.2 is true.[3]

Eqtn. 3.2

$$\begin{bmatrix} A & B \\ C & D \end{bmatrix} = \begin{bmatrix} A_1 & B_1 \\ C_1 & D_1 \end{bmatrix} \begin{bmatrix} A_2 & B_2 \\ C_2 & D_2 \end{bmatrix}$$
$$= \begin{bmatrix} A_1A_2 + B_1C_2 & A_1B_2 + B_1D_2 \\ C_1A_2 + D_1C_2 & C_1B_2 + D_1D_2 \end{bmatrix}$$

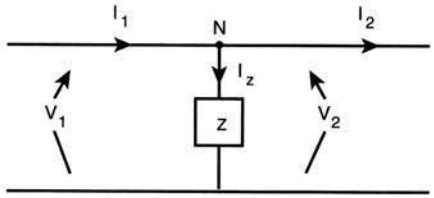
If another two-port network was added to that in Figure 3.2 to the right of the existing networks, the new equivalent ABCD parameters of the entire system could be found by matrix multiplication of the ABCD matrix for the new network by the result of Eqtn. 3.2. Thus, if the parameters of each individual network are given in ABCD form, it is a trivial task to find the characteristics of the network as a whole.

ABCD parameters are useful for characterizing twisted-pair loops because not all loops consist of a uniform gauge and a perfect termination. For example, a loop might consist of 9 kft of #26 gauge cable followed by 2 kft of #24 gauge cable. The insertion loss analysis in Chapter 2 did not account for such a case.

ABCD Parameters of a Lumped Impedance

One of the simplest cases of ABCD parameters is for a lumped impedance as shown in Figure 3.3.

Figure 3.3 A two-port network consisting of a lumped parallel impedance.



In this case, V_2=V_1 independent of I_2. Thus, the ABCD parameter equations can be written as in Eqtn. 3.3.

Eqtn. 3.3

$$V_1 = AV_2 + BI_2 = AV_1 + BI_2$$
$$I_1 = CV_2 + DI_2 = CV_1 + DI_2$$

Solving the first equation is trivial and yields Eqtn. 3.4.

Eqtn. 3.4

$$A = 1$$
$$B = 0$$

Eqtn. 3.3 is best solved using Kirkoff's current law at point N. This results in Eqtn. 3.5.

Eqtn. 3.5

$$I_1 = I_Z + I_2$$
$$= \frac{V_1}{Z} + I_2$$

Comparing Eqtn. 3.5 and Eqtn. 3.3, it should be clear that Eqtn. 3.6 is true.

Eqtn. 3.6

$$C = \frac{1}{Z}$$
$$D = 1$$

Thus, the ABCD matrix for a two-port network consisting only of a shunt impedance is given by Eqtn. 3.7.

Eqtn. 3.7

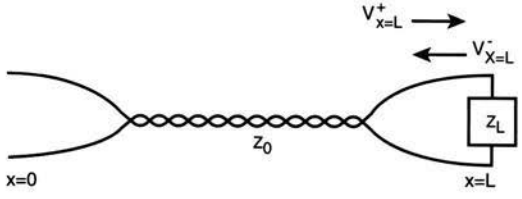
$$\begin{bmatrix} 1 & 0 \\ \frac{1}{Z} & 1 \end{bmatrix}$$

Z in Eqtn. 3.7 represents the shunt impedance. Note that Z may be complex because no restriction is placed on it to be real.

ABCD Parameters of a Uniform Twisted Pair

For a uniform twisted pair, finding the ABCD parameters is a bit more involved than for a simple lumped element. Chapter 2 showed that a wave traveling on a twisted pair is attenuated exponentially with distance and that the exponential depends on the pair's propagation constant. The voltage at a point on the line is the sum of a forward traveling wave at that point and the backward traveling wave. Figure 3.4 shows a twisted pair with the forward and backward traveling waves labeled at the end of the pair (x=L). Eqtn. 3.8 gives the voltage at the other end of the twisted pair (x=0).

Figure 3.4 A twisted pair transmission line; the forward (V+) and backward (V–) traveling waves are labeled.



Eqtn. 3.8

$$V(f,0) = \left(V^{+}_{x=L} e^{\gamma(f)L} + V^{-}_{x=L}(f) e^{-\gamma(f)L}\right)$$
$$= V^{+}_{x=L}\left(e^{\gamma(f)L} + \Gamma_L e^{-\gamma(f)L}\right)$$

The reflection coefficient in Eqtn. 3.8 was given in Eqtn. 2.10 and is repeated in Eqtn. 3.9.

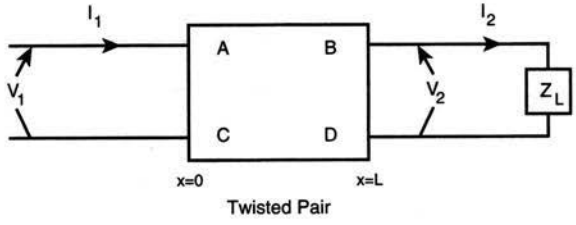
Eqtn. 3.9

$$\Gamma_L(f) = \frac{Z_L(f) - Z_o(f)}{Z_L(f) + Z_o(f)}$$

Note that in Eqtn. 3.8, the voltage at x=0 is the sum of a forward and backward traveling wave seen at x=L. The forward traveling wave will be larger at x=0 because it propagates from x=0 to x=L (indicated by the positive exponent in Eqtn. 3.8). The backward traveling wave will be larger at x=L because it propagates from x=L to x=0 (indicated by the negative exponential exponent in Eqtn. 3.8).

For ABCD parameters, it is helpful to write Eqtn. 3.8 in terms of the two-port output voltage and current rather than in terms of the positive traveling wave voltage, $V^{+}_{x=L}$. Figure 3.5 shows the equivalent two-port network representation of the uniform twisted pair.

Figure 3.5 An equivalent two-port network for a twisted pair.



Dependence of all values on frequency has been dropped for notational simplicity. Because the output voltage is the sum of forward and backward wave voltages at x=L, you can immediately find the expression for V_2 given in Eqtn. 3.10.

Eqtn. 3.10

$$V_2 = V^+_{x=L} + V^-_{x=L}$$
$$= V^+_{x=L}\left(1+\Gamma_L\right)$$

Solving for $V^+_{x=L}$ is then relatively straightforward as shown in Eqtn. 3.11.

Eqtn. 3.11

$$V^+_{x=L} = \frac{V_2}{1+\Gamma_L}$$

To find V_1, Eqtn. 3.11 can be substituted into Eqtn. 3.8 and upon simplifying, results in Eqtn. 3.12.

Eqtn. 3.12

$$V_1 = \frac{V_2}{1+\Gamma_L}\left(e^{\gamma(f)L} + \Gamma_L e^{-\gamma(f)L}\right)$$

To further simplify Eqtn. 3.12, Eqtn. 3.9, the definition of reflection coefficient, is used. After substituting and simplifying, Eqtn. 3.12 can be rewritten as Eqtn. 3.13.

Eqtn. 3.13

$$V_1 = V_2\left(\left(\frac{1}{2}+\frac{Z_o}{2Z_L}\right)e^{\gamma(f)L}+\left(\frac{1}{2}-\frac{Z_o}{2Z_L}\right)e^{-\gamma(f)L}\right)$$
$$= V_2\left(\left(\frac{1}{2}+\frac{Z_o I_2}{2V_2}\right)e^{\gamma(f)L}+\left(\frac{1}{2}-\frac{Z_o I_2}{2V_2}\right)e^{-\gamma(f)L}\right)$$
$$= \left(\frac{e^{\gamma(f)L}+e^{-\gamma(f)L}}{2}\right)V_2 + Z_o\left(\frac{e^{\gamma(f)L}-e^{-\gamma(f)L}}{2}\right)I_2$$

Recall that Z_o is the characteristic impedance of the transmission line at x=L, and Z_L is the load impedance. The second line in Eqtn. 3.13 results from simply using Ohm's law and the third line from combining like terms. Note that the definitions of hyperbolic cosine (cosh) and hyperbolic sine (sinh) are present in the last line of Eqtn. 3.13. Substituting for these yields Eqtn. 3.14.

Eqtn. 3.14

$$V_1 = (\cosh(\gamma L))V_2 + Z_o(\sinh(\gamma L))I_2$$
$$= AV_2 + BI_2$$

Similarly, the second two ABCD parameters can be found (the details are left to you in Exercise 2 at the end of the chapter) as in Eqtn. 3.15.

Eqtn. 3.15

$$I_1 = \left(\frac{\sinh(\gamma L)}{Z_o}\right)V_2 + (\cosh(\gamma L))I_2$$
$$= CV_2 + DI_2$$

Thus, the ABCD parameters for a uniform twisted pair (or any generic uniform transmission line) are as shown in Eqtn. 3.16.

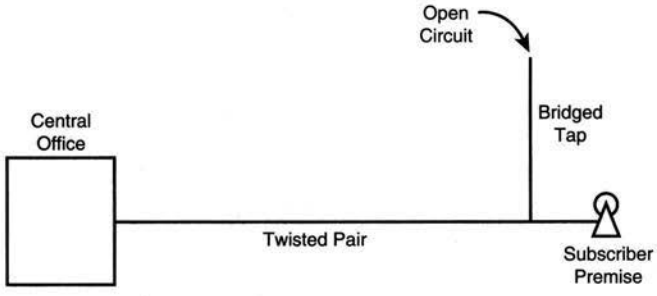
Eqtn. 3.16

$$\begin{bmatrix} A & B \\ C & D \end{bmatrix} = \begin{bmatrix} \cosh(\gamma L) & Z_o \sinh(\gamma L) \\ \dfrac{\sinh(\gamma L)}{Z_o} & \cosh(\gamma L) \end{bmatrix}$$

Bridged Taps

Sometimes, a twisted pair running to a subscriber might have another, unused twisted pair section connected at some point along its length. The other end of the unused section is left open circuited (see Figure 3.6). The unused section of twisted pair is called a *bridged tap.*

Figure 3.6 A common bridged tap configuration on a twisted pair.



The purpose of a bridged tap is usually to leave flexibility in the location of a subscriber using the loop. This flexibility is necessary when twisted pairs are installed prior to being used because in many cases the actual location of the subscriber is not yet known (for example, when cables are laid in a neighborhood under development). A bridged tap causes reflections at the open circuit end producing dips in the transfer function of the loop to which it is attached. Note that the propagation constant and characteristic impedance of the bridged tap might or might not be the same as the loop to which the tap is connected. Also note that the main loop itself might have different line characteristics on each side of the bridged tap.

The ABCD parameters of a bridged tap are the same as any other uniform twisted pair as given in Eqtn. 3.16. In the bridged tap case, however, you do not need to be concerned with the transfer function of the tap (because the signal does not propagate along the bridged tap) but rather the effect that the tap's presence has on the main loop's transfer function. Using Eqtn. 3.16, a bridged tap's ABCD equations are shown in Eqtn. 3.17.

Eqtn. 3.17

$$V_1 = \cosh(\gamma L_{tap})V_2 + Z_{o,tap}\sinh(\gamma L_{tap})I_2 = \cosh(\gamma L_{tap})V_2$$

$$I_1 = \frac{\sinh(\gamma L_{tap})}{Z_{o,tap}}V_2 + \cosh(\gamma L_{tap})I_2 = \frac{\sinh(\gamma L_{tap})}{Z_{o,tap}}V_2$$

The simplification in both equations comes because the bridged tap, by definition, is open circuited at one end, and thus, $I_2=0$.

Dividing the two equations in Eqtn. 3.17 yields Eqtn. 3.18.

Eqtn. 3.18

$$Zin_{tap} = \frac{V_1}{I_1} = \frac{\cosh(\gamma L_{tap})V_2}{\frac{\sinh(\gamma L_{tap})}{Z_{o,tap}}V_2}$$
$$= Z_{o,tap}\coth(\gamma L_{tap})$$

In Eqtn. 3.18, the hyperbolic cotangent (coth) is used. From the main loop's point of view, the effect of the bridged tap would be the same as the effect of a lumped impedance across the loop with a value of Zin_{tap}. The ABCD parameters of a lumped impedance were derived in Eqtn. 3.7. Substituting the effective shunt impedance of a bridged tap from Eqtn. 3.17 into Eqtn. 3.5 yields Eqtn. 3.19.

Eqtn. 3.19

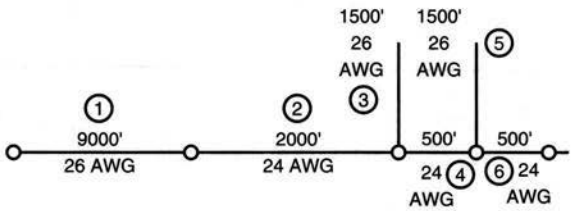
$$ABCD_{tap} = \begin{bmatrix} 1 & 0 \\ \frac{1}{Zin_{tap}} & 1 \end{bmatrix} = \begin{bmatrix} 1 & 0 \\ \frac{1}{Z_{o,tap}\coth(\gamma L_{tap})} & 1 \end{bmatrix}$$

These ABCD parameters do not describe the parameters along the length of the bridged tap but rather the effect of the bridged tap on the main loop. The following section, "Loop Analysis," illustrates how this information can be used to model a loop with any structure.

Loop Analysis

At this point, you can analyze a wide variety of loops by finding the ABCD parameters of each section of the loop and performing matrix multiplications. For example, consider the loop shown in Figure 3.7.

Figure 3.7 An example twisted pair to illustrate the usefulness of ABCD parameters.



This loop consists of 9 kft of #26 gauge cable followed by a total of 3 kft of #24 gauge cable. Because two bridge taps exist on the #24 section (each 1.5 kft of #26 gauge cable), the #24 section is broken into one 2 kft section and two 500 foot sections. The ABCD parameters for the entire cable are found by multiplying the ABCD parameters for the individual sections along the loop. This is shown generically in Eqtn. 3.20.

Eqtn. 3.20

$$ABCD_{tot} = [9kft, \#26][2kft, \#24][BT1][500\,ft, \#24][BT2][500\,ft, \#24]$$

The values shown in each set of brackets represent the ABCD parameters of the listed section. Note that six sets of ABCD parameters are necessary to analyze this loop as labeled in the figure and shown in Eqtn. 3.20. This loop is T1.601 #9 and is analyzed in detail later in the chapter.

The ABCD parameters for each term in Eqtn. 3.20 were discussed in the preceding sections. The information necessary to find the ABCD parameters includes the gauge and length of each section (along with whether the section is part of the main loop or a bridged tap). A cable of this type, with varying gauge and multiple bridged taps, illustrates the usefulness of ABCD parameters.

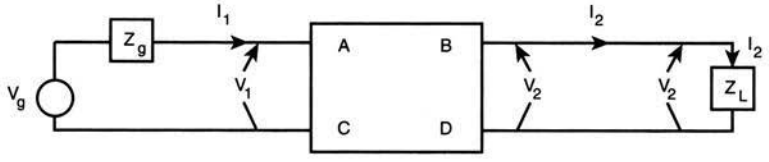
Input Impedance, Transfer Functions, and Insertion Loss

Given that you can characterize any twisted pair in terms of ABCD parameters, you can see how to find three important characteristics about a loop, mainly the *input impedance*, *transfer function*, and *insertion loss*. In each case, an assumption is made that the loop's ABCD parameters have been found.

For analysis of a loop, specific information beyond the ABCD parameters of the loop is necessary. This information includes the impedance of the source providing a signal to the loop and the impedance of the loop termination. These are sometimes referred to as *source*

impedance (or generator impedance) and *termination impedance* (or load impedance). Figure 3.8 shows a generic end-to-end loop model.

Figure 3.8 A generic end-to-end model of a loop including the generator impedance at the modulator and the load or terminating impedance at the receiver.



Z_g is the impedance of the generator, and Z_L is the load impedance (this analysis assumes that both are 100 ohms). Note that in ADSL and VDSL, Z_g would normally be part of the transmitter design and Z_L part of the receiver design. The input impedance will be a function of the impedance of the loop and of the load (but not Z_g). The transfer function will be from V_1 to V_2. The insertion loss will be a function of the loop, the load impedance, and the generator impedance.

The input impedance of the loop is simple to derive. Given the ABCD parameter equations as shown in Eqtn. 3.1, the input impedance is found by simply dividing the first equation by the second. Regarding Figure 3.8, by Ohm's law, it follows that $V_2=I_2Z_L$. Thus, the input impedance can be found as in Eqtn. 3.21.

Eqtn. 3.21

$$Z_{in} = \frac{V_1}{I_1} = \frac{AV_2 + BI_2}{CV_2 + DI_2}$$
$$= \frac{AI_2Z_L + BI_2}{CI_2Z_L + DI_2} = \frac{AZ_L + B}{CZ_L + D}$$

The transfer function of a loop can be found from the first ABCD equation. Once again, using Ohm's law, the equation can be written as in Eqtn. 3.22.

Eqtn. 3.22

$$V_1 = AV_2 + BI_2 = AV_2 + B\frac{V_2}{Z_L}$$

Ohm's law was used to replace I_2 by V_2/Z_L.

Eqtn. 3.22 can be solved algebraically for the transfer function, V_2/V_1 yielding the simple expression in Eqtn. 3.23.

Eqtn. 3.23

$$T = \frac{V_2}{V_1} = \frac{1}{A + \frac{B}{Z_L}} = \frac{Z_L}{AZ_L + B}$$

The insertion loss of the loop is the ratio of power delivered to the load to the power that would have been delivered to the load without the loop present. Essentially, this is the loss caused by inserting the loop between the source and termination. Insertion loss is normally expressed in dB.

If no loop were present (Z_G was connected directly to Z_L), the voltage across the load could be found by a simple voltage divider as shown in Eqtn. 3.24.

Eqtn. 3.24

$$V_L = V_G \frac{Z_L}{Z_G + Z_L}$$

The power delivered to the load in this case would then follow simply as in Eqtn. 3.25.

Eqtn. 3.25

$$P_{\text{No Loop}} = \frac{V_L^2}{Z_L} = \frac{V_G^2 Z_L^2}{Z_L (Z_G + Z_L)^2}$$

When the loop is present, the voltage V_1 can be written as in Eqtn. 3.26.

Eqtn. 3.26

$$V_1 = AV_2 + BI_2 = V_G - I_1 Z_G$$

The last part of this equation follows from simple circuit theory (taking into account the voltage drop across Z_G). Substituting in the second generic ABCD equation for I_1 then yields Eqtn. 3.27.

Eqtn. 3.27

$$AV_2 + BI_2 = V_G - (CV_2 + DI_2)Z_G$$

The entire equation can be written in terms of voltages by substituting V_2/Z_L in for the two I_2 terms. This is done in Eqtn. 3.28.

Eqtn. 3.28

$$AV_2 + B\frac{V_2}{Z_L} = V_G - \left(CV_2 + D\frac{V_2}{Z_L}\right)Z_G$$

Finally, algebraic manipulation can be used to solve Eqtn. 3.28 for V_2. The result is shown in Eqtn. 3.29.

Eqtn. 3.29

$$V_2 = \frac{V_G Z_L}{AZ_L + B + Z_G(CZ_L + D)}$$

Now that V_2 is known, the power delivered to the load with the loop present can be found as shown in Eqtn. 3.30.

Eqtn. 3.30

$$P_{\text{With Loop}} = \frac{V_2^2}{Z_L} = \frac{V_G^2 Z_L^2}{Z_L\left(AZ_L + B + Z_G(CZ_L + D)\right)^2}$$

The insertion loss of the loop is then defined by Eqtn. 3.31.

Eqtn. 3.31

$$IL = 10\log\left(\left|\frac{P_{\text{No Loop}}}{P_{\text{With Loop}}}\right|\right)$$

$$= 10\log\left(\left|\frac{\dfrac{V_G^2 Z_G^2}{Z_L(Z_G + Z_L)^2}}{\dfrac{V_G^2 Z_L^2}{Z_L\left(AZ_L + B + Z_G(CZ_L + D)\right)^2}}\right|\right)$$

The results of Eqtn. 3.25 and Eqtn. 3.30 have been used in Eqtn. 3.31 for the power expressions. The insertion loss expression in Eqtn. 3.31 can be algebraically simplified and results in Eqtn. 3.32.

Eqtn. 3.32

$$IL = 20\log\left(\left|\frac{AZ_L + B + Z_G(CZ_L + D)}{(Z_G + Z_L)}\right|\right)$$

This expression for insertion loss will be used extensively later in the book to predict the performance of ADSL and VDSL systems on various loops. For more discussion on ABCD parameters, Appendices C, D, and E of the *Subscriber Loop Signalling and Transmission Handbook* are recommended.[4]

Basic Loop Configurations

To set requirements, compare different modulation proposals, and demonstrate compliance, standards bodies have defined fixed loops for ADSL and VDSL. (VDSL loops are still being defined. Discussed here are what have been agreed on at the present time.) The following sections present these loops and show the input impedance, transfer function, and insertion loss of each. A generator impedance and load impedance of 100 ohms is assumed throughout.

Note

A null loop, often called CSA #0, which is less than 10 feet of #26 gauge cable, is not discussed. It is sometimes used to show basic operational capability.

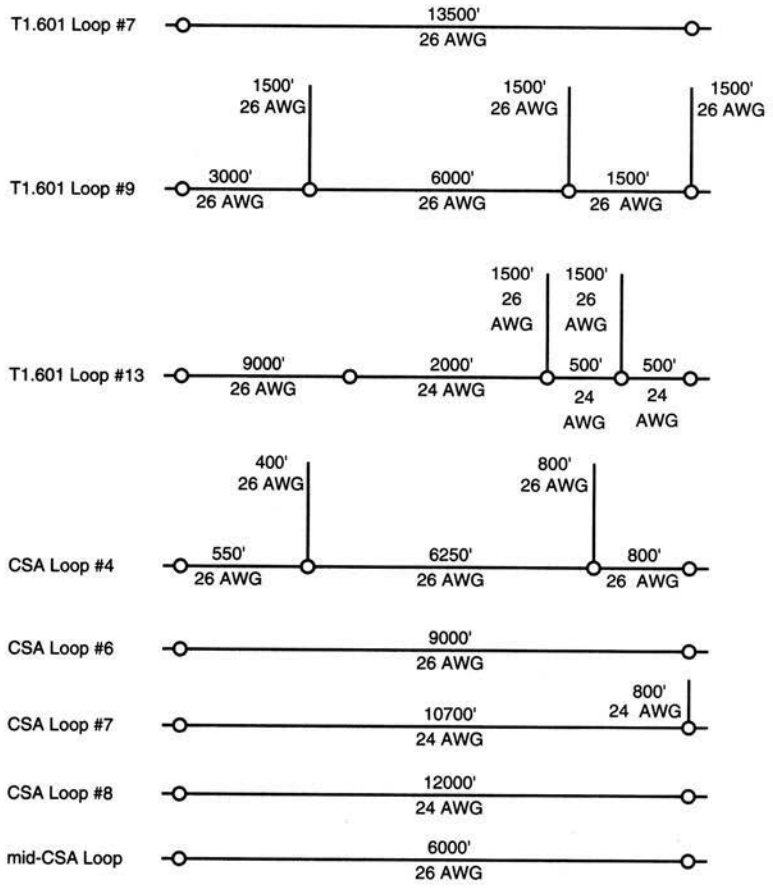
ADSL Loops

Figure 3.9 shows the loops used for ADSL.$_1$ The variety of different loop topologies and gauges lends weight to the value of the previous discussions on ABCD parameters. For these loops, only #24 and #26 gauge cables are used.

The numerical models for sections of #24 and #26 gauge twisted pairs were presented in Chapter 2, "Twisted Pair Environment," and will be used when analyzing the loops. Specifically, the characteristic impedances and propagation constants over frequency of each cable will be necessary for the analysis. In addition, the basic concepts of ABCD parameters are needed along with the input impedance, transfer function, and insertion loss results derived in Eqtn. 3.21, Eqtn. 3.23, and Eqtn. 3.32, respectively.

Figures 3.10–3.17 show graphs of impedance over frequency as well as transfer function and insertion loss for all ADSL loops (except the null loop). The responses are shown up to around 1.2 MHz encompassing the entire ADSL band. For the input impedance and insertion loss graphs, a source and load impedance of 100 ohms is assumed. A few notes about the graphs follow Figure 3.9.

Figure 3.9 Test loops specified for ADSL.



NOTES
1 AWG = American Wire Gauge
2 Dustance are in feet(') : 100'

- The real part of the input impedance for all loops converges to around 100 ohms, and the imaginary part to zero as frequency increases.
- The insertion loss for the lines with no bridged taps is monotonically decreasing with frequency. The loops with bridged taps have an insertion loss exhibiting more fluctuation. T1.601 Loop #9 is a good example of the effect that bridged taps can have on insertion loss.

- The transfer function (graphed on a log scale) very much follows the shape of the insertion loss. The insertion loss is dependent on the choice of generator impedance (100 ohms in our case), whereas the transfer function is independent of this impedance. Insertion loss and transfer function curves are notably different when the input impedance strays from 100 ohms. Such behavior can be seen in the CSA Loop #4 graphs.

Figure 3.10 Input impedance, transfer function magnitude, and insertion loss for T1.601 Loop #7.

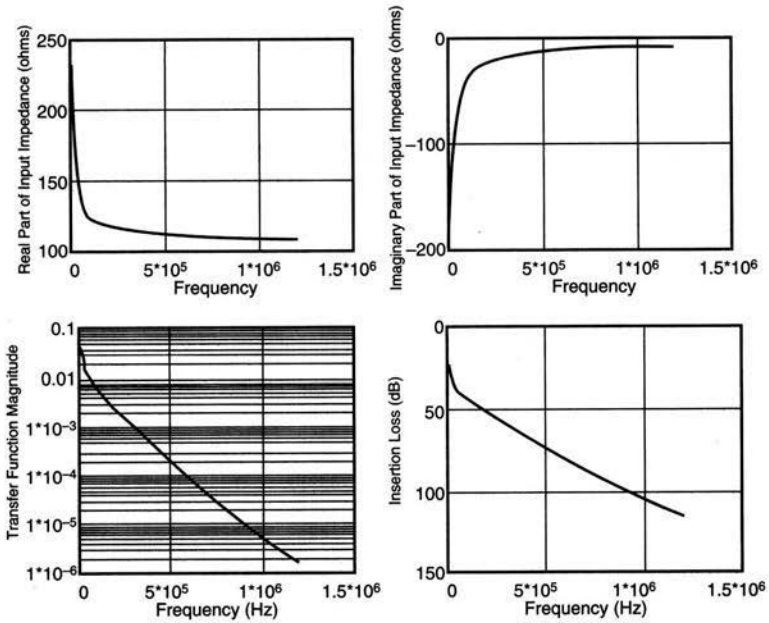


Figure 3.11 Input impedance, transfer function magnitude, and insertion loss for T1.601 Loop #9.

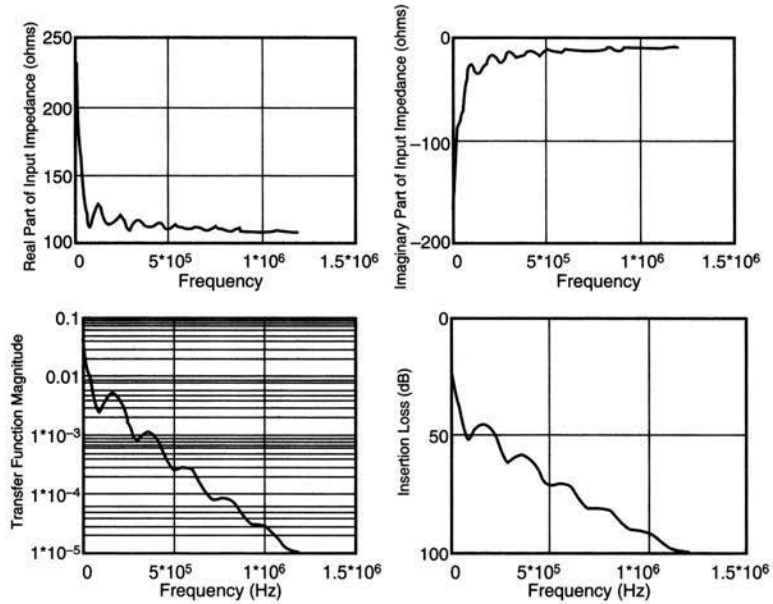


Figure 3.12 Input impedance, transfer function magnitude, and insertion loss for T1.601 Loop #13.

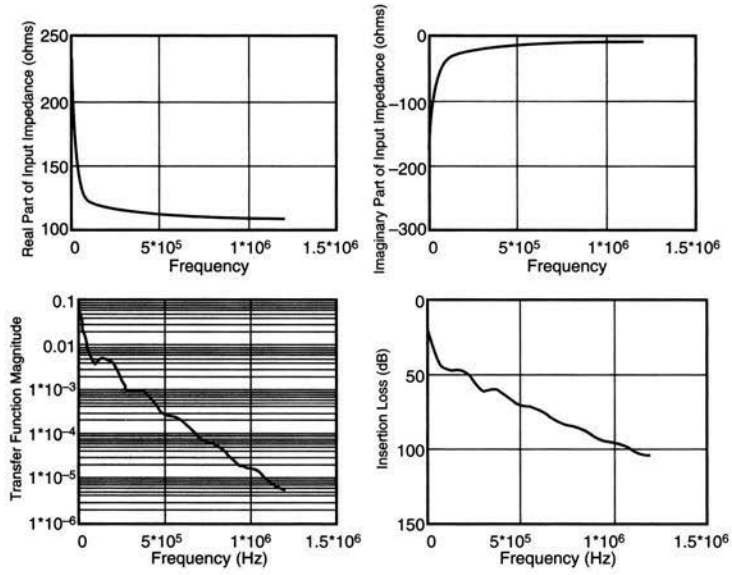


Figure 3.13 Input impedance, transfer function magnitude, and insertion loss for CSA Loop #4.

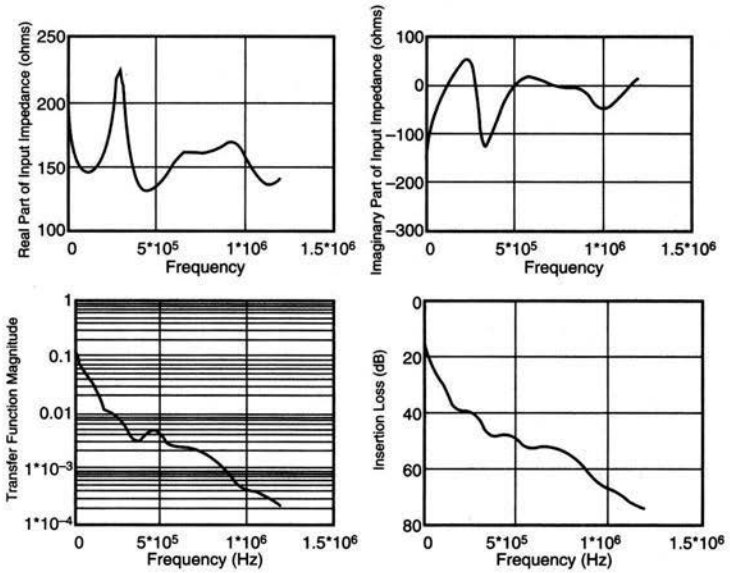


Figure 3.14 Input impedance, transfer function magnitude, and insertion loss for CSA Loop #6.

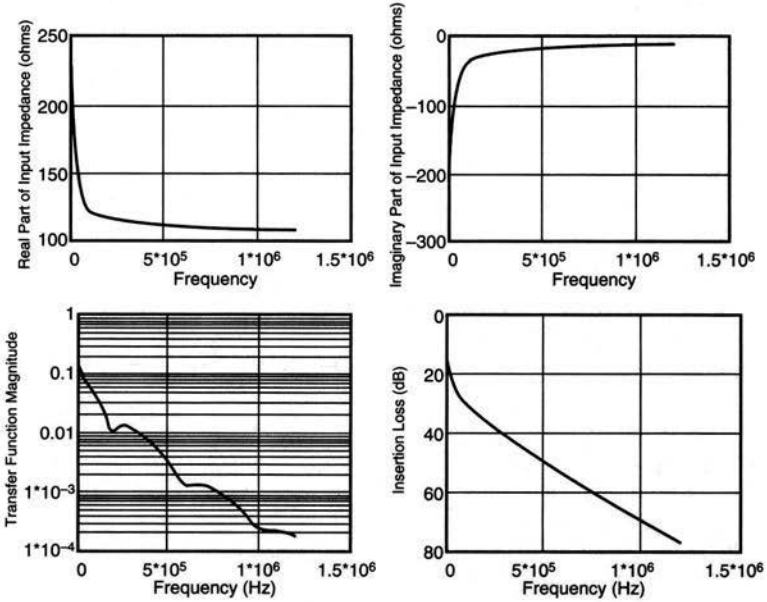


Figure 3.15 Input impedance, transfer function magnitude, and insertion loss for CSA Loop #7.

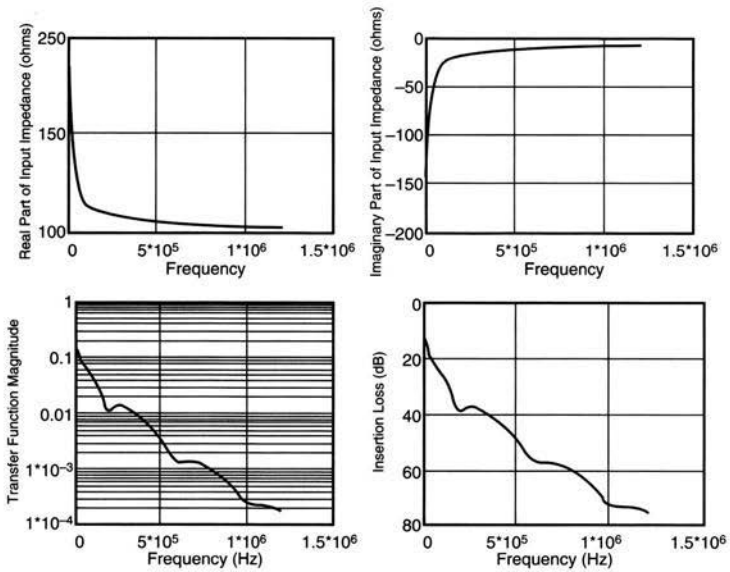


Figure 3.16 Input impedance, transfer function magnitude, and insertion loss for CSA Loop #8.

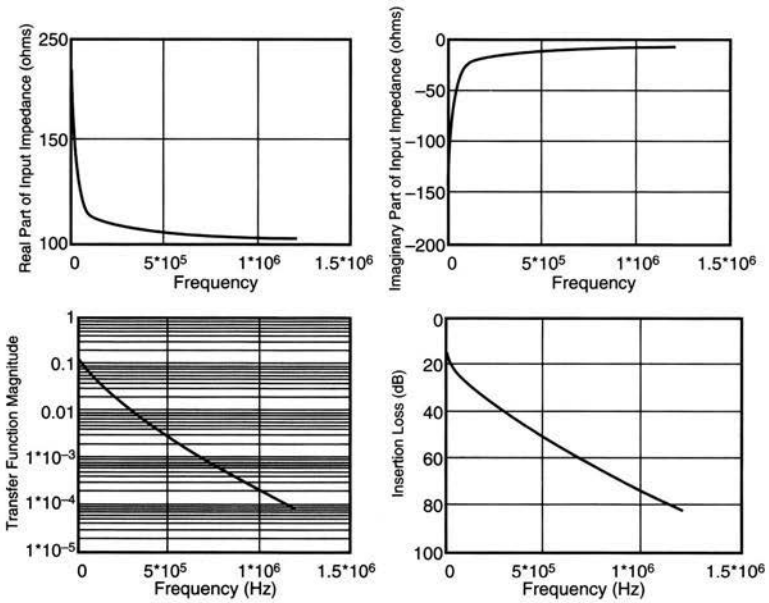
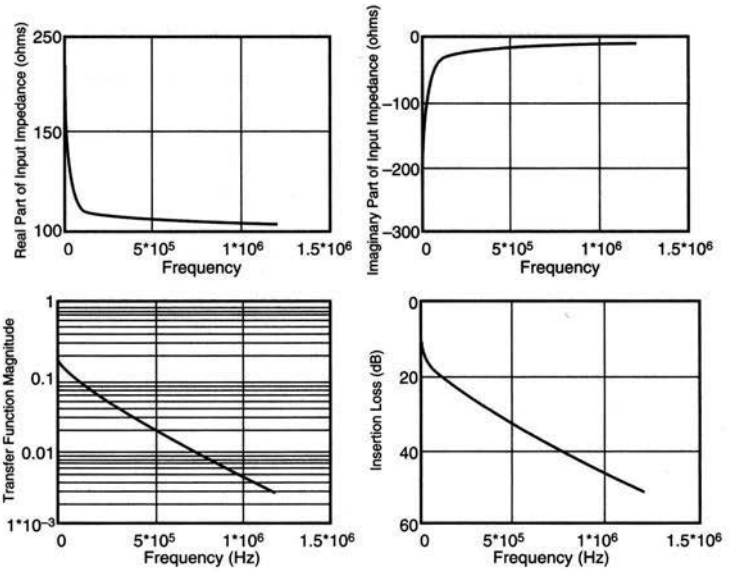


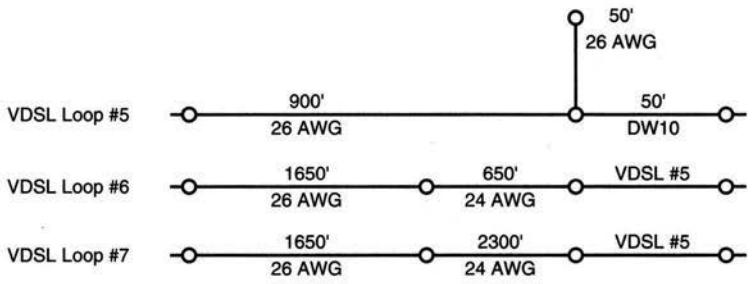
Figure 3.17 Input impedance, transfer function magnitude, and insertion loss for the Mid CSA Loop.



VDSL Loops

Figure 3.18 shows the loops currently designated for VDSL. For these three loops, two new types of cables are shown, called DW10 and FP (DW10 stands for Drop Wire #10). DW10 consists of 0.5 mm untwisted conductors insulated with PVC. FP represents untwisted Flat-Pair wires. Short sections of these wires are often used to connect twisted pairs to homes and buildings. These wires are not included in the ADSL models because their effect is negligible.

Figure 3.18 Test loops specified for VDSL.



For VDSL, these wires are not negligible because VDSL loops are short, and the frequency range of VDSL signals is higher. Table 3.1 provides the numerical parameter models for DW10 and FP wires.

Table 3.1 Parameters for the Numeric Twisted Pair Model for DW10 and Flat-Pair Cable

Parameter	DW10	FP
r_{oc} (ohms/km)	180.93	41.6
r_{os} (ohms/km)	∞	∞
a_c (ohms^4/km^{4}Hz^2)	0.0497223	0.001218
a_s (ohms^4/km^{4}Hz^2)	0	0
l_o (H/km)	728.87*10^{-6}	1000*10^{-6}
l_∞ (H/km)	543.43*10^{-6}	911*10^{-6}
f_m (Hz)	718888	
b	0.75577086	1.195
g_o (Siemen/Hz*km)	89*10[–9]	53*10[–9]
g_e	0.856	0.88
c_∞ (nF/km)	63.8	22.8
c_o (nF/km)	51	31.78
c_e	–0.11584622	0.1109

VDSL Loops #5, #6, and #7 have more than one length defined for them as shown in Figure 3.18. Essentially, the different lengths represent a short, medium, and long length loop for VDSL testing. Note that VDSL Loop #5 and VDSL Loop #6 are similar except for the short section at the end, essentially exercising the different types of end drops. VDSL Loop #7 is meant to test operation in the presence of bridged taps. The other test loops are configurations representing common loop topologies.

Figures 3.19–3.22 show graphs for the selected VDSL loops. Again, for input impedance and insertion loss graphs, the source and load impedances are assumed to be 100 ohms. The graphs are shown up to around 15 MHz, which encompasses most of the usable VDSL band. In some cases (Figure 3.20 and Figure 3.22), more than one loop is shown on a graph to draw a comparison between loops. For loops with a selectable length, the longest length is shown. The following list provides a few notes about the VDSL loop graphs:

- VDSL Loop #2 and VDSL Loop #3 have very similar impedance characteristics, but VDSL Loop #3 is a bit more lossy. This suggests that DW10 is more lossy than FP cable.

- The input impedance of VDSL Loop #6 and VDSL Loop #7 is almost identical. VDSL Loop #7 has more loss because the middle section of #24 gauge twisted pair is almost four times as long as that for VDSL Loop #6.
- Properties similar to the ADSL loops are observed. The real and imaginary parts of the impedances converge similarly. Also, the insertion loss graphs generally decrease with frequency, although they do contain some ripple due to the presence of bridged taps.

Figure 3.19 Input impedance, transfer function magnitude, and insertion loss for the VDSL Loop #1.

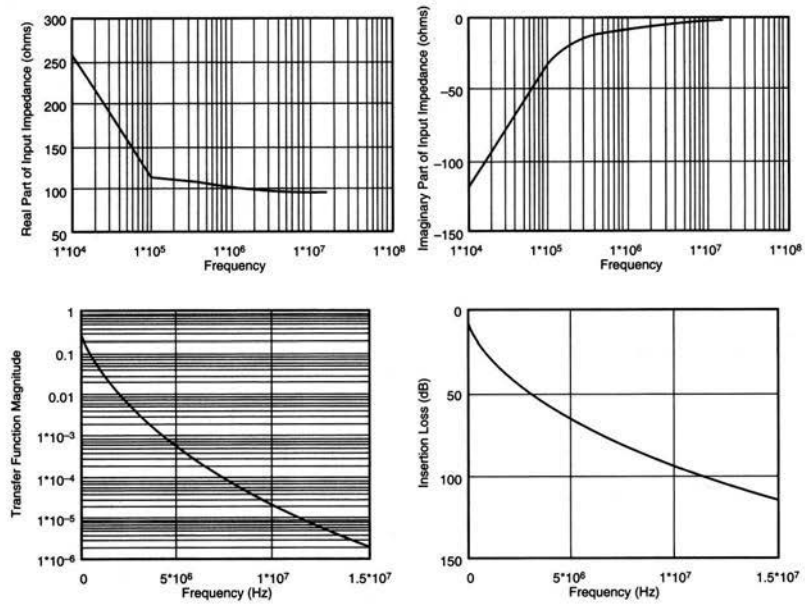


Figure 3.20 Input impedance, transfer function magnitude, and insertion loss for the VDSL Loop #2 and VDSL Loop #3.

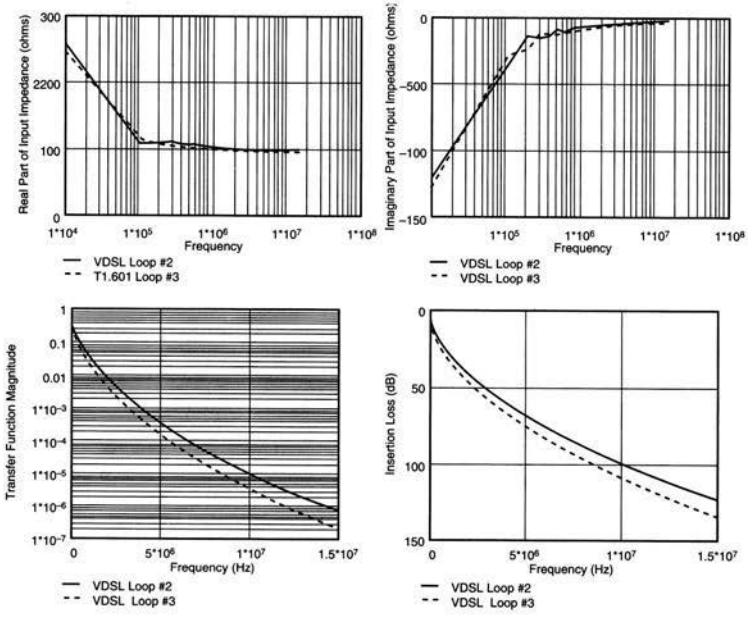


Figure 3.21 Input impedance, transfer function magnitude, and insertion loss for the VDSL Loop #4.

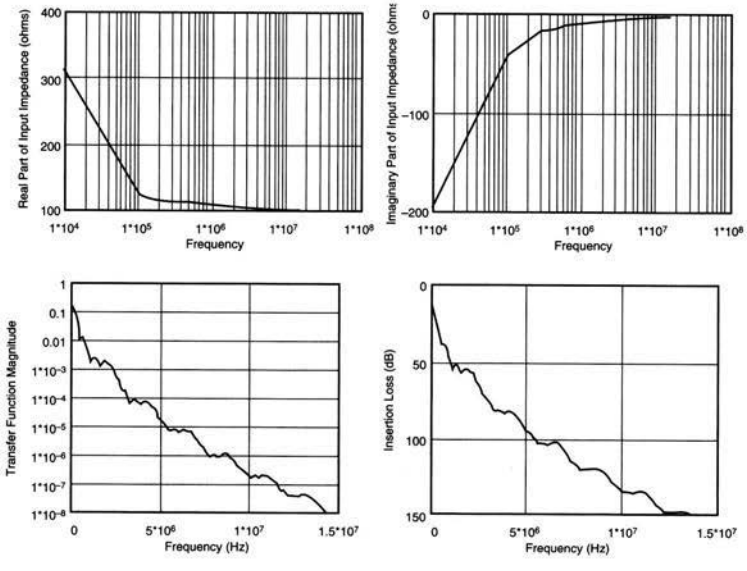
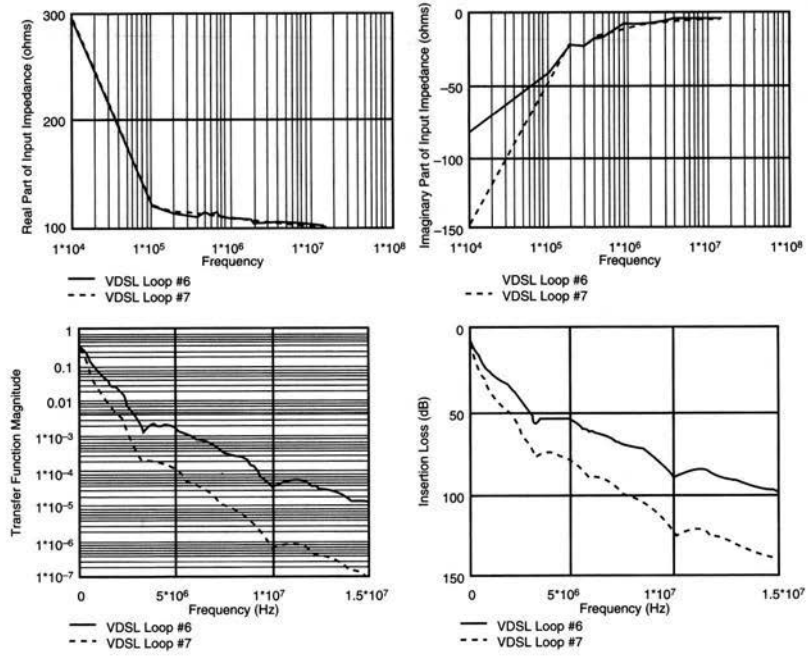


Figure 3.22 Input impedance, transfer function magnitude, and insertion loss for the VDSL Loop #6 and VDSL Loop #7.



Summary

This chapter described a method to analyze loops of many different types using ABCD parameters. Detailed derivations of ABCD parameters for transmission lines were presented, and expressions for input impedance, insertion loss, and transfer function were derived. Test loops used to benchmark ADSL systems and VDSL systems were presented, and ABCD parameters used to examine their characteristics were described in detail. These results are used in later chapters to derive the theoretical performance limits of ADSL and VDSL.

Exercises

1. Prove the relationship given in Eqtn. 3.2 by writing out ABCD equations for each of the networks and solving them for the total network output.
2. Prove the relationship given in Eqtn. 3.15.

3. Simplify Eqtn. 3.14 for the special case where $Z_o=Z_L$.
4. Find the input impedance, transfer function magnitude, and insertion loss of a 9 kft, #26 gauge cable and a 9 kft, #26 gauge cable with a 2 kft, #26 gauge bridged tap located at 8 kft.
5. Find the transfer function phase response of CSA Loop #6. Why does the slope of the phase increase with increasing frequency?
6. Find the input impedance of CSA Loop #7 in the reverse direction (looking in from the subscriber's location). Assume a termination at the other end of 100 ohms. How does the input impedance behave when the bridged tap's length is varied? How does this compare with the input impedance for this loop looking in from the central office?
7. Consider a source generating a signal occupying the band from 0 Hz to 1.0 MHz with a flat power spectral density of ñ40 dBm/Hz. What is the total output power of the source? Compare the total power of the received signal if such a source were the transmitter on each of the ADSL loops. Compare the total power received in only the 0 Hz to 500 kHz range.
8. Consider a source generating a signal occupying the band from 0 Hz to 10 MHz with a flat power spectral density of –60 dBm/Hz. What is the total output power of the source? Compare the total power of the received signal if such a source were the transmitter on each of the VDSL loops. Compare the total power received in only the 0 Hz–500 MHz range.

Endnotes

1. American National Standards Institute, *Asymmetric Digital Subscriber Line Metallic Interface Standard T1.431.* August 1995.
2. John Cioffi, *VDSL System Requirements Document.* T1E1.4 Contribution 96–153, November 1996.
3. J. David Irwin, *Basic Engineering Circuit Analysis.* New York: Macmillan, 1987.
4. Whitham D. Reeve, *Subscriber Loop Signalling and Transmission Handbook.* New York: IEEE Press, 1992.

CHAPTER 4

Power Spectral Densities and Crosstalk Models

In this chapter:

- Explanation of a complete crosstalk model for DSLs
- Method of determining power spectral density (PSD)
- PSD derivations for many DSLs
- NEXT and FEXT models for common DSL disturbers

This chapter discusses crosstalk noises present on digital subscriber lines (DSLs) and applies the mathematical models for near-end crosstalk (NEXT) and far-end crosstalk (FEXT) for a general disturber (see Chapter 2, "Twisted Pair Environment") to specific types of common ADSL and VDSL disturbers. Chapter 5, "DSL Theoretical Capacity in Crosstalk Environments," combines these concepts with the analysis tools presented in Chapter 3, "Loop Analysis," to analyze the theoretical capabilities of any type of twisted pair under any type of environment.

This chapter also discusses power spectral density (PSD). The PSD of a line code defines the distribution of the line code's power in the frequency domain. A *PSD mask* is a template that specifies the maximum PSD allowable for a line code. PSD masks are used as both guidelines for the design and implementation of a DSL technology as well as for crosstalk modeling (as described in the next section) to simulate and benchmark performance.

The crosstalk derivations in this chapter are only statistical models and thus do not imply that every DSL will be corrupted by the predicted amounts of crosstalk. Instead, the models and the different types of crosstalk tests for ADSL and VDSL are meant to be

reasonable as they are based on actual empirical data, yet somewhat pessimistic in that they assume near worst-case conditions. Designers hope that a system's positive performance in the presence of the crosstalk specified in the models will ensure adequate performance in the highly variable and diverse environment of the outside loop plant.

Introduction

Chapter 2 gave the crosstalk loss function for both NEXT and FEXT. Eqtn. 4.1 repeats this function for NEXT.

Eqtn. 4.1

$$H_{Next}(f) = K_{NEXT} f^{3/2}$$

Here K_{NEXT} is a constant that depends on the quality of the twisted pair type. Eqtn. 4.2 repeats the loss equation for FEXT.

Eqtn. 4.2

$$H_{FEXT}(f) = K_{FEXT} f^2 e^{-2\alpha(f)L} L$$
$$= K_{FEXT} f^2 \left|H_{channel}(f)\right|^2 L$$

Here K_{FEXT} is a constant, and L is the length of the line.

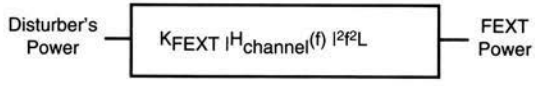
For analysis, Eqtn. 4.1 and Eqtn. 4.2 allow crosstalk to be modeled as a signal on a disturbing line, coupling onto the disturbed line through either a NEXT or FEXT transfer function (depending on whether the crosstalk is NEXT or FEXT). Figure 4.1 shows a simple model for NEXT, and Figure 4.2 shows a simple model for FEXT. In each case, the power of the interference depends on both the spectrum of the disturbing signal and the crosstalk loss function.

Note
Common disturbers include ISDN, HDSL, T1, ADSL, and VDSL lines that may be nearby.

Figure 4.1 A simple model of a NEXT disturber.



Figure 4.2 A simple model of a FEXT disturber.



In general, you need be concerned only with the expected crosstalk power and not with the crosstalk voltage. The reason is simply that a statistical model of crosstalk power allows the prediction of signal-to-noise ratio (SNR) on the disturbed twisted pair. Chapter 5 shows that knowledge of the SNR enables engineers to predict the performance limit on the loop.

Crosstalk Equations

The equations that describe crosstalk consist of three basic terms. The first term describes the PSD of the disturber. The PSD of the disturber is the expected power on the disturbing line and thus includes all transmitter filtering associated with the disturber. PSD is a function of frequency.

The second term of the crosstalk equations is the coupling term. This term is simply the NEXT or FEXT equation (Eqtn. 4.1 and Eqtn. 4.2) and depends on whether the crosstalk being described is NEXT or FEXT.

The final term of the crosstalk equations is derived from and reflects the number of crosstalkers being considered; this term is described in the next section.

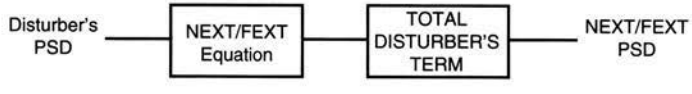
Eqtn. 4.3 gives the general form of a crosstalk equation for some disturber.

Eqtn. 4.3

$$PSD_{xtalk} = [\text{Disturber PSD}][\text{NEXT/FEXT Equation}][\text{Total Disturbers Term}]$$

A model to illustrate the block diagram is shown in Figure 4.3. Note that Eqtn. 4.3 is valid for crosstalkers of the same type (for example, a number of ISDN crosstalkers). If more than one type of crosstalker exists, Eqtn. 4.3 would also have to be calculated for the second type, using the second crosstalker's PSD as well as the number of disturbers of that type.

Figure 4.3 A simple model for multiple NEXT or FEXT disturbers.



Number of Crosstalkers

At first glance, adjusting crosstalk for different numbers of disturbers by simply multiplying the total crosstalk for one disturber by the total number of disturbers may seem trivial. Such a method is incorrect, however, and will lead to an overly pessimistic crosstalk model in that the predicted crosstalk power will be too high. The reason is that crosstalk between twisted pairs has been statistically modeled. The value used for K_{NEXT} (or K_{FEXT}) for a cable type is empirically determined so that for a single crosstalker, sometimes called "pair-to-pair crosstalk," the crosstalk power predicted is worse than 99% of any measured pair-to-pair crosstalk power. Put another way, for pair-to-pair crosstalk, the actual crosstalk is worse than that predicted by the mode only 1% of the time.

As more crosstalkers are included in the model, however, to assume that they are also worse than 99% of all lines is overly pessimistic. They are certainly more likely to be better (have less effect) than the first crosstalker. Thus as the number of disturbers increases, the cumulative effect of each additional disturber should be less than that of the previous disturber. For NEXT, the model for incorporating the number of disturbers is normally combined with the NEXT coupling equation (dependence on $f^{3/2}$) and is given by Eqtn. 4.4

Eqtn. 4.4

$$x_N = [\text{NEXT Equation}][\text{Number of Disturbers Model}]$$
$$= 0.882 \times 10^{-14} \times N^{0.6} \times f^{3/2}$$

In Eqtn. 4.4, N is the total number of disturbers. Thus two of the three terms needed for finding the PSD of crosstalk are known.

Types of Disturbers

Two methods are available for finding the PSDs of common disturbers for ADSL and VDSL. The first method, used on the more "classical" baseband disturbers including ISDN, HDSL, and T1, entails using the autocorrelation function. In this method, the PSD is given by Eqtn. 4.5.

Eqtn. 4.5

$$PSD = \frac{2\Im[R_{xx}(\tau)]}{ZT}$$

Here T is the length of the baseband symbol, Z is the reference impedance across which the signal is measured, R_{xx} is the autocorrelation function of the line code, and the fourier transform function is shown in Eqtn. 4.6.

Eqtn. 4.6

$$\Im[R_{xx}(t)] = \int_{-\infty}^{\infty} R_{xx}(\tau) e^{-j2\pi ft} dt$$

The factor of two in Eqtn. 4.5 reflects the use of the single-sided PSD, as opposed to the double-sided PSD (which is defined over both positive and negative frequencies). Thus the PSDs obtained from Eqtn. 4.5 are valid only on (0, ∞). The proper unit for PSD is Watts/Hz, and the power in any frequency region is found by integrating the PSD between the edges of the region. The autocorrelation of a wide-sense stationary waveform x is given by Eqtn. 4.7.

Note

You can also talk about a PSD having units of dBm/Hz. This terminology tends to be convenient in graphically showing PSD as well as when comparing crosstalk PSD with received-signal PSDs.

Eqtn. 4.7

$$R_{xx}(\tau) = E[x(t)x(t-\tau)]$$

Here x(t–τ) is simply x delayed by time τ, and E[*] is the expected value operator.

The second method for defining the PSD of a disturber is to simply specify a PSD mask for the disturber type. A PSD mask is a template defining the maximum value of the technology's PSD at each frequency. Sometimes a mask is used because the PSD of certain technologies is not mathematically convenient. Other times the mask allows for flexibility in the implementation of DSL designs while ensuring that all designs adhere to the same PSD restrictions. ADSL and VDSL PSD specifications for both CAP- and DMT-based line codes use this method. In this case, the PSD is again the single-sided PSD, the unit is still Watts/Hz, and the power in any frequency band is found by the same method described previously.

Note that it is possible to use both methods to bound a PSD. Often the in-band PSD (the energy in the main part of the PSD) is bounded by the first method , and the out-of-band energy (sometimes called the side lobes) is bounded by the second method. In practical DSL systems, it is customary to use analog filtering to comply with out-of-band PSD requirements.

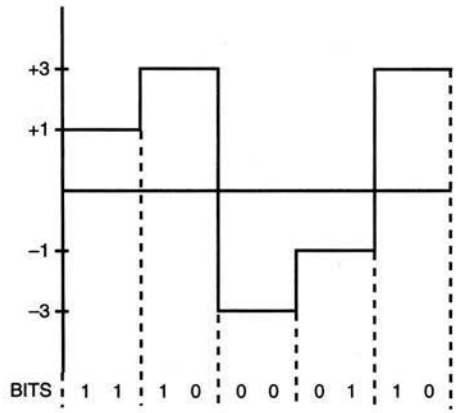
ISDN and HDSL

ISDN and HDSL use the *2B1Q line code* in which two bits are encoded into a pulse that can take on one of four levels. The pulse, also called a *quat,* is then sent over the twisted pair. The method in which two bits are coded into a quat is shown in Table 4.1. An example of a 2B1Q line code for a string of bits appears in Figure 4.4. Each quat is independent of the preceding and succeeding quats, which simplifies the calculation of R_{xx} for 2B1Q.

Table 4.1 Method of Encoding Two Bits into One Quat for 2B1Q Line Codes

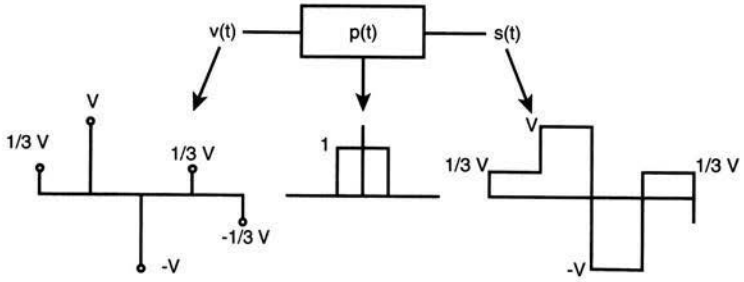
First Bit	Second Bit	Normalized Level
0	0	-3
0	1	-1
1	0	+3
1	1	+1

Figure 4.4 An example of a 2B1Q line code; two bits make up one quat, and each quat takes one of four discrete levels.



A 2B1Q data stream is best viewed as a sequence of impulses, v_k sent at the system's baud rate and passed through a filter with impulse response p. The impulse response of p forms the pulses of the line code. Such an implementation appears in Figure 4.5.

Figure 4.5 A simple 2B1Q modulator.



The height of each impulse can be modeled as a random variable that can take on one of four values: +V, –V, +1/3V, and –1/3V.

The second moment of an impulse is given by Eqtn. 4.8.

Eqtn. 4.8

$$E[v^2] = \frac{1}{4}\left(V^2 + \left(\frac{1}{3}V\right)^2 + (-V)^2 + \left(-\frac{1}{3}V\right)^2\right)$$
$$= \frac{1}{4}\left(\frac{20}{9}V^2\right) = \frac{5}{9}V^2$$

Note that with the assumption of equal probabilities over all four possible values of v, the mean of v is zero and thus the variance of v is the same as the second moment given in Eqtn. 4.8.

A train of impulses is then given by v as in Eqtn. 4.9.

Eqtn. 4.9

$$v(t) = \sum v_k \partial(t - kT)$$

Here T is the period of the line code quats. Eqtn. 4.10 gives the autocorrelation function of such a train of impulses, assuming the random variable v_k, as being independent of one another.

Eqtn. 4.10

$$R_w(\tau) = E[v(t)v(t-\tau)]$$
$$= \frac{5}{9}V^2\partial(\tau)$$

Now if the string of impulses v is passed though a filter with impulse response p, the output s is given by the convolution of the two quantities as in Eqtn. 4.11.

Eqtn. 4.11

$$s(t) = \int_{-\infty}^{\infty} v(t-\alpha)p(\alpha)d\alpha$$

The autocorrelation function of s is given by Eqtn. 4.12.

Eqtn. 4.12

$$R_{ss}(\tau) = E[s(t)s(t-\tau)]$$
$$= E\left[\int_{-\infty}^{\infty} v(t-\alpha)p(\alpha)d\alpha \int_{-\infty}^{\infty} v(t+\tau-\alpha)p(\alpha)d\alpha\right]$$
$$= E\left[\int_{-\infty}^{\infty}\int_{-\infty}^{\infty} v(t-\alpha)v(t+\tau-\beta)p(\alpha)p(\beta)d\alpha d\beta\right]$$
$$= \int_{-\infty}^{\infty}\int_{-\infty}^{\infty} E[v(t-\alpha)v(t+\tau-\beta)]p(\alpha)p(\beta)d\alpha d\beta$$
$$= \int_{-\infty}^{\infty}\int_{-\infty}^{\infty} R_w(\tau+\alpha-\beta)p(\alpha)p(\beta)d\alpha d\beta$$

The fourier transform of Eqtn. 4.12 is given by Eqtn. 4.13.

Eqtn. 4.13

$$S(f) = \int_{-\infty}^{\infty} R_{ss}(\tau)e^{-j2\pi f\tau}d\tau$$
$$= \int_{-\infty}^{\infty}\left(\int_{-\infty}^{\infty}\int_{-\infty}^{\infty} R_w(\tau+\alpha-\beta)p(\alpha)p(\beta)d\alpha d\beta\right)e^{-j2\pi f\tau}d\tau$$
$$= \int_{-\infty}^{\infty}\int_{-\infty}^{\infty}\int_{-\infty}^{\infty} R_w(\tau+\alpha-\beta)p(\alpha)p(\beta)e^{-j2\pi f\tau}d\alpha d\beta d\tau$$

If you change the variables, let $t=\tau+\alpha-\beta$, and recognize that $dt=d\tau$, then Eqtn. 4.13 can be simplified to Eqtn. 4.14.

Eqtn. 4.14

$$\begin{aligned}
S(f) &= \int_{-\infty}^{\infty} R_{ss}(\tau)e^{-j2\pi f\tau}d\tau \\
&= \int_{-\infty}^{\infty}\left(\int_{-\infty}^{\infty}\int_{-\infty}^{\infty} R_w(t)p(\alpha)p(\beta)d\alpha d\beta\right)e^{-j2\pi f(t+\alpha-\beta)}d\tau \\
&= \int_{-\infty}^{\infty} R_w(t)^2\,\partial(t)e^{-j2\pi ft}dt\int_{-\infty}^{\infty} p(\alpha)e^{-j2\pi f\alpha}d\alpha\int_{-\infty}^{\infty} p(\beta)e^{j2\pi f\beta}d\beta \\
&= \int_{-\infty}^{\infty}\frac{5}{9}V^2\partial(t)e^{-j2\pi ft}dt\int_{-\infty}^{\infty} p(\alpha)e^{-j2\pi f\alpha}d\alpha\int_{-\infty}^{\infty} p(\beta)e^{j2\pi f\beta}d\beta \\
&= \frac{5}{9}V^2\int_{-\infty}^{\infty} p(\alpha)e^{-j2\pi f\alpha}d\alpha\int_{-\infty}^{\infty} p(\beta)e^{j2\pi f\beta}d\beta
\end{aligned}$$

Note that last line in Eqtn. 4.14 resulted from the sifting property. The first integration in the last line is the fourier transform of the impulse response of the pulse filter. The second is the complex conjugate of the pulse filter impulse response fourier transform (the exponent is positive instead of negative). Thus Eqtn. 4.14 can be rewritten as in Eqtn. 4.15.

Eqtn. 4.15

$$\begin{aligned}
S(f) &= V(f)P(f)P^*(f) \\
&= \frac{5}{9}V^2|P(f)|^2
\end{aligned}$$

Assuming a square pulse impulse response for p, Eqtn. 4.15 can be written as shown in Eqtn. 4.16.

Eqtn. 4.16

$$S(f) = \frac{5}{9}V^2\left|\frac{\sin(\pi fT)}{\pi f}\right|^2$$

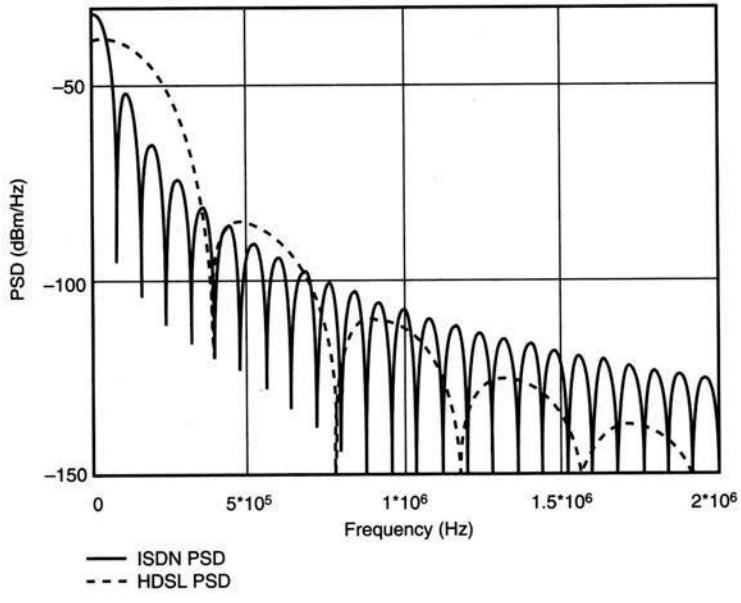
Using Eqtn. 4.5, the PSD of the 2B1Q signal is given as Eqtn. 4.17.

Eqtn. 4.17

$$S_{PSD}(f) = \frac{2S(f)}{ZT}$$
$$= \frac{10}{9}\frac{V^2}{ZT}\frac{\sin^2(\pi fT)}{\pi^2 f^2}$$

For an ISDN system, Z is assumed to be 135 ohms, and T, the pulse period, is $1/80*10^3$ s. For an HDSL system, Z is 100 ohms, and T is $1/392*10^3$ s. The resulting PSDs appear in Figure 4.6.

Figure 4.6 ISDN and HDSL PSDs.



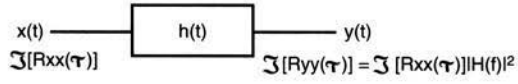
Along the way to deriving Eqtn. 4.17, an important result has been illustrated. If a signal x with autocorrelation function R_{xx} is passed through a linear, time-invariant filter with impulse response h, the fourier transform of the autocorrelation at the output of the filter will provide the results given by Eqtn. 4.18.

Eqtn. 4.18

$$\Im[R_{yy}(\tau)] = \Im[R_{xx}(\tau)]|H(f)|^2$$

Figure 4.7 illustrates this result, which will be helpful later in the chapter.

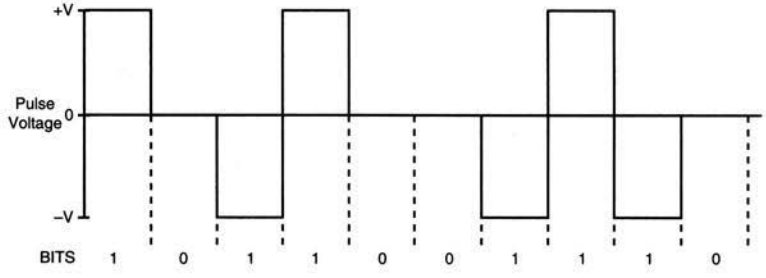
Figure 4.7 The effect of passing a signal through a linear, time-invariant filter on the signal's PSD; the input and output PSD expressions are shown.



T1 Lines

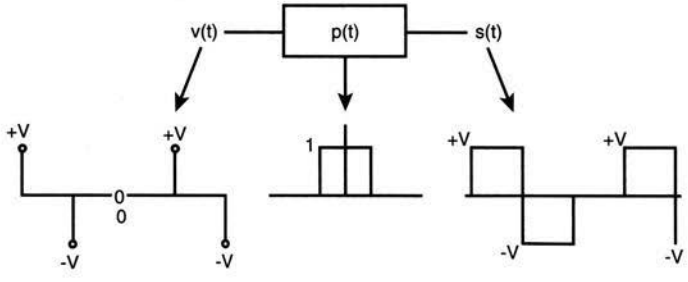
T1 lines use a binary return to zero (RZ) *alternate mark inversion* (AMI) line code. In this scheme, a binary 1 is encoded as a pulse with either a positive or negative level, and a binary 0 is encoded as a 0 V symbol (in other words, no pulse at all). An example of an AMI line code is shown in Figure 4.8. Note that the polarity of each pulse representing a binary 1 is opposite of the previous binary 1. This condition gives rise to the name "alternate mark inversion."

Figure 4.8 An example of an AMI line codes such as that used by a T1 line.



Similar to the 2B1Q line code, the T1 line code can be viewed as a sequence of impulses fed through a pulse filter with impulse response p. This is shown in Figure 4.9.

Figure 4.9 A simple T1 line modulator using a bipolar AMI line code.



In this case, the impulses can have a height of +V, –V, or 0. The first two impulse heights represent binary 1s, and the third represents a binary 0. (It is assumed that the network element producing the impulses encodes the proper polarity pulse for a binary 1.) The final two impulses represent binary 1s. In contrast to ISDN and HDSL, T1 lines typically do not employ scrambling at the transmitter and descrambling at the receiver. As a result, the relative density of ones and zeros being encoded is not necessarily uniform. The interference models for both ADSL and VDSL assume that the density is uniform; this discussion proceeds on that assumption. If v_k is the sequence of impulse, the probability density function (pdf) of each impulse is given by Eqtn. 4.19.

Eqtn. 4.19

$$f_v(v) = \begin{cases} \frac{1}{4} & v = -V \\ \frac{1}{2} & v = 0 \\ \frac{1}{4} & v = +V \\ 0 & \text{otherwise} \end{cases}$$

A continuous time representation of the impulse train v_k can be represented by Eqtn. 4.20.

Eqtn. 4.20

$$v(t) = \sum v_k \partial(t - kT)$$

Here T is the bit period of the line code. The waveform v is then passed through the pulse filter to form the T1 waveform. Using the convolution method similar to what was done when analyzing 2B1Q, the actual line code waveform is given by Eqtn. 4.21.

Eqtn. 4.21

$$s(t) = \int_{-\infty}^{\infty} v(t - \alpha) p(\alpha) d\alpha$$

Eqtn. 4.21 is identical to Eqtn. 4.11 though the process v is certainly different. The line code PSD is then given by the fourier transform of the autocorrelation function of s. The analysis is identical to that done in the previous section for 2B1Q, and the two main quantities necessary for the result include the fourier transform of the autocorrelation function of v and the fourier transform of the impulse response p. The resulting power spectrum of s is then given by Eqtn. 4.22.

Eqtn. 4.22

$$\begin{aligned} S(f) &= \Im(R_w(\tau))P(f)P^*(f) \\ &= V(f)P(f)P^*(f) \\ &= V(f)|P(f)|^2 \end{aligned}$$

Finding V first requires finding the autocorrelation of v, which is given by Eqtn. 4.23.

Eqtn. 4.23

$$R_w(\tau) = \begin{cases} \frac{-V^2}{4} & \tau = \text{-T} \\ \frac{V^2}{2} & \tau = 0 \\ \frac{-V^2}{4} & \tau = \text{T} \\ 0 & \text{otherwise} \end{cases}$$

The value at τ=0 is simply the second moment of discrete random variable v, and the values at τ=–T and τ=T result in shifting the waveform by one symbol. The nonzero values of the autocorrelation function at shifts of one symbol are a result of the memory in the encoding of AMI. (The derivation of Eqtn. 4.23 is left as an exercise for the end of this chapter.) The fourier transform of R_w is given by Eqtn. 4.24.

Eqtn. 4.24

$$\begin{aligned} V(f) &= \int_{-\infty}^{\infty} R_w(\tau)e^{-j2\pi f\tau}d\tau \\ &= \int_{-\infty}^{\infty}\left(\frac{-V^2}{4}\partial(\tau+T)+\frac{V^2}{2}\partial(\tau)+\frac{-V^2}{4}\partial(\tau-T)\right)e^{-j2\pi f\tau}d\tau \\ &= \frac{-V^2}{4}e^{j2\pi fT}+\frac{V^2}{2}+\frac{-V^2}{4}e^{-j2\pi fT} \\ &= \frac{V^2}{2}(1-\cos(2\pi fT)) \end{aligned}$$

The last line in Eqtn. 4.24 results simply from Euler's formula and some factorization.

Now that the fourier transform of R_{vv} is known, the fourier transform of p is necessary. Because p is again a pulse of width T (as was the case for 2B1Q), its spectrum is given by Eqtn. 4.25.

Eqtn. 4.25

$$P(f) = \frac{\sin(\pi f T)}{\pi f}$$

The spectrum of s is given by Eqtn. 4.26.

Eqtn. 4.26

$$\begin{aligned} S(f) &= V(f)P(f)P^*(f) \\ &= V(f)|P(f)|^2 \\ &= \frac{V^2}{2}(1-\cos(2\pi f T))\left|\frac{\sin(\pi f T)}{\pi f}\right|^2 \end{aligned}$$

The PSD of s is then given by Eqtn. 4.27.

Eqtn. 4.27

$$\begin{aligned} S_{PSD}(f) &= \frac{2S(f)}{ZT} \\ &= \frac{2V^2}{2ZT}(1-\cos(2\pi f T))\left(\frac{\sin(\pi f T)}{\pi f}\right)^2 \\ &= \frac{V^2}{ZT}\frac{\sin^2(\pi f T)}{\pi^2 f^2}(1-\cos(2\pi f T)) \end{aligned}$$

For T1 lines, the termination reference impedance Z is 100 ohms, and the bit period is $1/1.544*10^6$ s. The voltage magnitude V of an AMI pulse is typically 3.6V for a T1 line. ADSL and VDSL interference models make two extra assumptions about a T1 disturber. First, they assume that a T1 transmitter has a low-pass shaping filter to limit higher-frequency components on the line. The shaping filter is modeled as a third-order Butterworth filter with a 3.0 MHz, 3 dB point. The magnitude of the transfer function of this filter is given by Eqtn. 4.28.

Eqtn. 4.28

$$\left|H_{shaping}(f)\right|^2 = \frac{1}{1+\left(\frac{f}{3\times10^6}\right)^6}$$

Second, the T1 transmitter is coupled through a transformer that can be modeled as a high-pass filter with a 40 kHz, 3 dB point. Eqtn. 29 gives the magnitude of the transfer function of the transformer model.

Eqtn. 4.29

$$\left|H_{transformer}(f)\right|^2 = \frac{f^2}{f^2+\left(40\times10^3\right)^2}$$

By passing the T1 signal through the shaping filter and transformer, the resultant PSD becomes (using Eqtn. 4.28 and Eqtn. 4.29) Eqtn. 4.30.

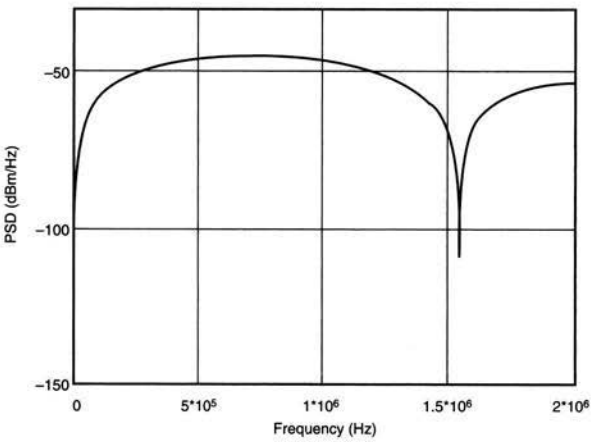
Eqtn. 4.30

$$PSD_{T1}(f) = S_{PSD}(f)\left|H_{shaping}(f)\right|^2\left|H_{transformer}(f)\right|^2$$

$$= \frac{V^2}{ZT}\frac{\sin^2(\pi fT)}{\pi^2 f^2}(1-\cos(2\pi fT))\left(\frac{1}{1+\left(\frac{f}{3\times10^6}\right)^6}\right)\left(\frac{f^2}{f^2+\left(40\times10^3\right)^2}\right)$$

Here T and Z are the same as those defined in Eqtn. 4.27. The PSD of a T1 signal with a binary 1's density of 50% is shown in Figure 4.10.

Figure 4.10 PSD of an AMI T1 line with a binary 1's density of 50%.



DMT ADSL (Downstream)

For ADSL separate models are necessary for the upstream and downstream directions as a result of different data rates and modulation parameters for each direction. Several methods can be used to find the downstream PSD of a DMT-based ADSL system. One reasonable method is to simply find the theoretical PSD for DMT modulation. A second method is to make an assumption about how the transmitter is implemented and create a mathematical model similar to those for 2B1Q and T1. Both of these methods have some shortcomings. The former is not always applicable to practical implementations. The latter assumes a type of implementation that can vary depending on the actual design. Neither method adequately addresses out-of-band energy. The value, however, of these models is that they form a good basis on which to specify a generic PSD mask. An implementation can then be engineered to keep the actual output power spectrum within the PSD mask. This section looks at and compares these two methods and then compares the standard DMT PSD mask for the downstream direction to the models.

Later chapters show that an ADSL DMT symbol is merely a number of sign and cosine waves at different frequencies being sent at a baud rate of 4.3125 kHz. The lowest frequency usable is 34.5 kHz, and the highest is 1.104 MHz. All frequency multiples of 4.3125 kHz between these limits are also used. Mathematically, it is correct to say that a sine and cosine wave are sent having a frequency of nx4.3125 kHz with n=8,9...256. A theoretical way to create a DMT symbol is to create the cosine and sine waves at all the necessary frequencies and then sum them. Eqtn. 4.31 gives the summation for f_o=4.3125 kHz.

Eqtn. 4.31

$$s(t) = \sum_{n=8}^{256} \left(a_n \cos(2\pi n f_o t) + b_n \sin(2\pi n f_o t)\right) \quad \text{for } 0 \le t < \frac{1}{f_o} \qquad (4.31)$$

For a single cosine and sine summation in Eqtn. 4.31 (say, for n=m), the expression for the power spectrum is derived later in the chapter in detail. Eqtn. 4.32 gives a generalized version of this PSD, representing the PSD due to term m of Eqtn. 4.31.

Eqtn. 4.32

$$PSD_m = \frac{4V^2 \sin^2(\pi T(f - mf_o))}{\pi^2 ZT(f - mf_o)^2}$$

$$= K_m \frac{\sin^2(\pi T(f - mf_o))}{\pi^2 (f - mf_o)^2}$$

If the sine and cosine waves are independent for a DMT symbol, the total PSD is equal to the sum of the PSDs due to each term in Eqtn. 4.31. Thus the theoretical PSD for a downstream DMT symbol is given in Eqtn. 4.33.

Eqtn. 4.33

$$PSD_{DS} = \sum_{i=8}^{256} K_i \frac{\sin^2(\pi T(f - if_o))}{\pi^2(f - if_o)^2}$$
$$= K_{DS} \sum_{i=8}^{256} \frac{\sin^2(\pi T(f - if_o))}{\pi^2(f - if_o)^2}$$

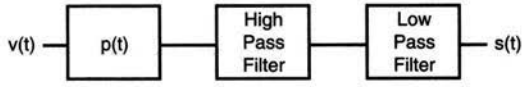
In Eqtn. 4.33, K_{DS} represents the expected value of all scalar terms in a typical PSD equation (termination impedance, expected voltage level, and so on). For a typical DSL system, this value is approximately 10^{-7}.

A design that produces a PSD in accordance with the theoretical PSD given in Eqtn. 4.33 may not be in the best interest of DSL technology. In some areas, the mask may be too difficult to achieve (for example, near the edges of the pass band). In the out-of-band regions, the mask may not be stringent enough. These regions could be attenuated more with reasonable filters, reducing the amount of crosstalk coupled into other DSLs. Under the circumstances, basing the PSD model of a downstream DMT ADSL symbol solely on this model is not very wise. As a second point of reference, a basic implementation can be assumed for the front end of a DMT modulator. A DMT symbol can be formed by passing an impulse train v_k though a pulse filter p, just as in the 2B1Q and T1 case. The resulting waveform is then high-pass and low-pass filtered and sent out of the transmitter. A block diagram of this process appears in Figure 4.11. The impulses are assumed to be independent and Gaussian distributed with a mean of zero and a variance of V^2. Common notation for each v_k would be $N(0,V^2)$.

Note

The interpreted impulse heights for this model are not the same as those for T1 and 2B1Q line codes. That is, the height of a single impulse does not correspond to a single bit or set of bits, and further processing is necessary to decode bits from sequences of samples. This topic is discussed again in Chapter 6, "DSL Modulation Basics."

Figure 4.11 A common method of producing an ADSL signal.



As in the previous cases, the continuous time function v, describing the train of impulses, can be written as in Eqtn. 4.34.

Eqtn. 4.34

$$v(t) = \sum_{\infty} v_k \partial(t - kT)$$

Assuming an independent v_k, Eqtn. 4.35 gives the autocorrelation function, R_{vv}, of v.

Eqtn. 4.35

$$R_{vv}(\tau) = V^2 \partial(\tau)$$

As previously shown, the PSD at the output of the transmitter is simply the fourier transform of Eqtn. 4.35 multiplied by the squared magnitude spectrums of each of the filters between the v and the output. Given that the filters are the pulse filter, the high-pass filter (HPF), and the low-pass filter (LPF), the PSD of a downstream ADSL signal is given by Eqtn. 4.36.

Eqtn. 4.36

$$PSD_{ADSL}(f) = \frac{2\Im[R_{vv}(\tau)]P(f)|^2 |HPF(f)|^2 |LPF(f)|^2}{ZT}$$

A reasonable LPF used to filter the ADSL downstream PSD is a fourth-order Butterworth filter with a cutoff frequency of 1.104 MHz. The square of its magnitude spectrum is given by Eqtn. 4.37.

Eqtn. 4.37

$$|LPF(f)|^2 = \frac{1}{1 + \left(\frac{f}{1.104 \times 10^6}\right)^8}$$

A reasonable HPF used to filter the ADSL downstream PSD is a fourth-order filter with a 3 dB point at 20 kHz. This filter would serve the purpose of limiting the low end of the ADSL spectrum to separate ADSL from normal Plain Old Telephone Service (POTS) traffic. The squared magnitude of its spectrum is provided by Eqtn. 4.38.

Note

Do not interpret the specific transfer functions for the HPF and LPF necessities to use for any ADSL implementation. These functions are chosen for PSD-modeling purposes only.

Eqtn. 4.38

$$|HPF(f)|^2 = \frac{f^8}{f^8 + (20\times 10^3)^8}$$

All together, the PSD of a downstream ADSL signal then becomes Eqtn. 4.39.

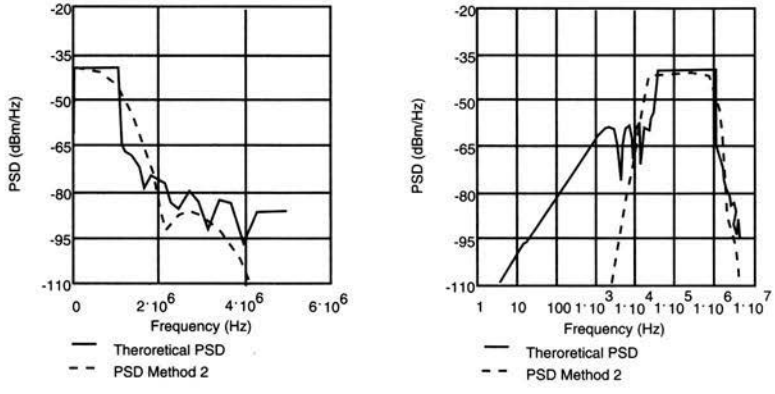
Eqtn. 4.39

$$PSD_{ADSL}(f) = \frac{2\Re[R_w(\tau)]P(f)|^2|HPF(f)|^2|LPF(f)|^2}{ZT}$$

$$= \frac{2V^2}{ZT}\left(\frac{\sin(\pi fT)}{\pi f}\right)^2\left(\frac{1}{1+\left(\frac{f}{1.104\times 10^6}\right)^8}\right)\left(\frac{f^8}{f^8+(20\times 10^3)^8}\right)$$

For ADSL, Z—the reference impedance—is assumed to be 100 ohms, and T is given by 1/(2.208 MHz). The theoretical PSD of a downstream DMT ADSL line code as well as the PSD calculated in this model appear in Figure 4.12.

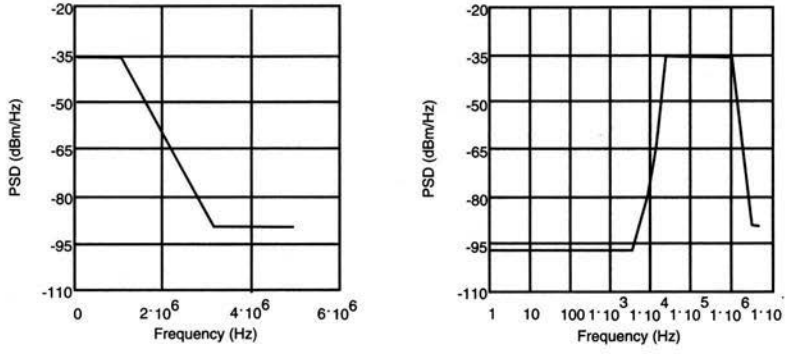
Figure 4.12 Theoretical and implementable ADSL downstream PSDs with a linear frequency scale and a logarithmic frequency scale.



Note that in some areas the theoretical PSD is the higher (primarily outside of the passband) of the two; at other times it is lower (primarily near the edge of the passband). A tighter specification in the out-of-band regions is desired to reduce crosstalk into other DSLs.

These two masks provide insight to the theoretical downstream PSD and to an achievable PSD due to a feasible implementation. These two masks lead to the PSD mask specified by ANSI for an ADSL downstream implementation. This mask is shown in Figure 4.13.

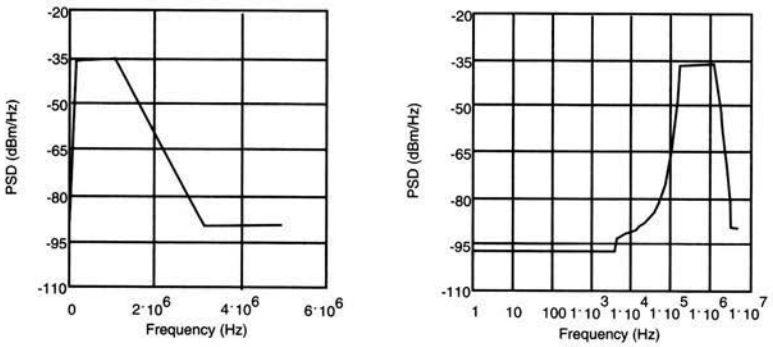
Figure 4.13 PSD mask of a downstream DMT ADSL signal in an echo-canceled system with a linear frequency scale and a logarithmic frequency scale.



Basically, the mask is a piecewise continuous function. Conforming to this mask should not cause unreasonably complex designs for ADSL implementation, but should minimize interference in the out-of-band region.

The PSD mask in Figure 4.13 is for downstream ADSL employing echo cancellation. A second downstream mask, called the "reduced NEXT mask" is defined for systems not using echo cancellation. This mask reduces the power allowed in the lower passband region. The mask is illustrated in Figure 4.14. An ADSL system operating in frequency division multiplexing (FDM) mode would use this PSD mask. See Chapter 7, "ADSL Modulation Specifics," for additional information of the two types of downstream ADSL modes for DMT.

Figure 4.14 PSD mask of a downstream DMT ADSL signal in an FDM system with a linear frequency scale and a logarithmic frequency scale.



DMT ADSL (Upstream)

Normally, the ADSL upstream signal occupies a frequency range from 25 kHz to 138 kHz. For an echo-canceled system, the upstream PSD overlaps the downstream PSD in this region. If you use the same type of analysis to find the theoretical PSD as you used for downstream ADSL, the expression results in Eqtn. 4.40.

Note

In some FDM systems, the upper frequency may be less than 138 kHz if those frequencies are to be used by the downstream ADSL signal.

Note

If POTS does not reside on the twisted pair, some engineers have suggested using some of the bandwidth between DC and 25 kHz for upstream ADSL (and downstream ADSL in the case of an echo-canceled system), which would then extend the frequency range down.

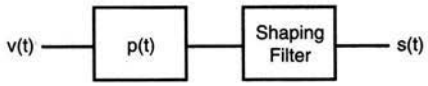
Eqtn. 4.40

$$PSD_{US} = \sum_{i=8}^{32} K_i \frac{\sin^2(\pi T(f - if_o))}{\pi^2(f - if_o)^2}$$
$$= K_{US} \sum_{i=8}^{32} \frac{\sin^2(\pi T(f - if_o))}{\pi^2(f - if_o)^2}$$

The expression in Eqtn. 4.40 has the same basic components as the expression in Eqtn. 4.32, and K_{US} is given by approximately 10^{-7}.

Because of the deficiencies associated with using the theoretical PSD expression as the PSD mask specification, the PSD from an experimental implementation is again helpful. An upstream DMT symbol can be created by passing an impulse train through a pulse filter at the rate of 276 kHz. The output of the pulse filter is then sent through a shaping filter. Figure 4.15 shows such a system.

Figure 4.15 A method of producing an ADSL upstream signal.



If the impulses are Gaussian with statistics given by $N(0,V^2)$, then Eqtn. 4.34 and Eqtn. 4.35 apply as the train of impulses and autocorrelation function, respectively. Following the treatment of a signal passed through a filter used in the previous sections, the output PSD of Figure 4.15 can be written as Eqtn. 4.41.

Eqtn. 4.41

$$PSD_{ADSL,US}(f) = \frac{2\Im[R_w(\tau)]P(f)|^2|H_{US}(f)|^2}{ZT}$$
$$= \frac{2V^2}{ZT}\left(\frac{\sin(\pi fT)}{\pi f}\right)^2|H_{US}(f)|^2$$

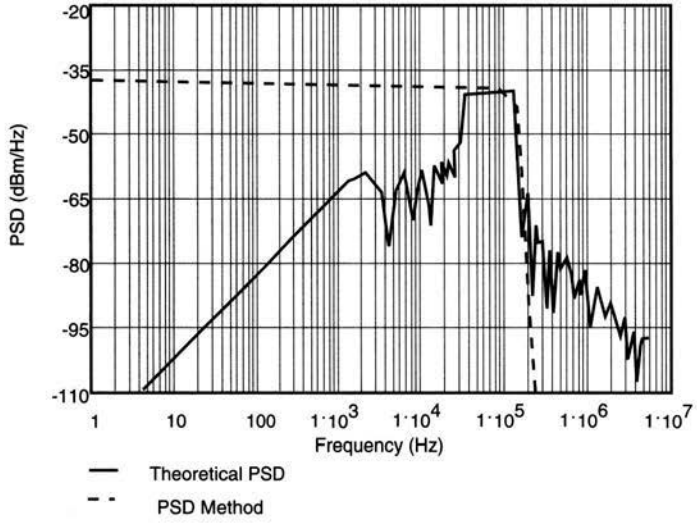
In Eqtn. 4.41, Z is given by 100 ohms, and T is $1/(276*10^3)$ s. For a downstream disturber, the shaping filter was explicitly defined so that calculation of the downstream PSD was straightforward. In the original ADSL upstream PSD specification, a generic mask was used as the upstream shaping filter magnitude. Mathematically, this mask is given in Eqtn. 4.42.

Eqtn. 4.42

$$|H_{US}(f)|^2 = \begin{cases} 10^{\frac{-38-30}{10}} & f < 138\,\text{kHz} \\ 10^{\frac{-38-24\left(\frac{f-13800}{43125}\right)-30}{10}} & f > 138\,\text{kHz} \end{cases}$$

The resulting PSD due to the implementation along with the mask defined in Eqtn. 4.42 is shown in Figure 4.16. Overlaid on this figure is the theoretical expression from Eqtn. 4.40.

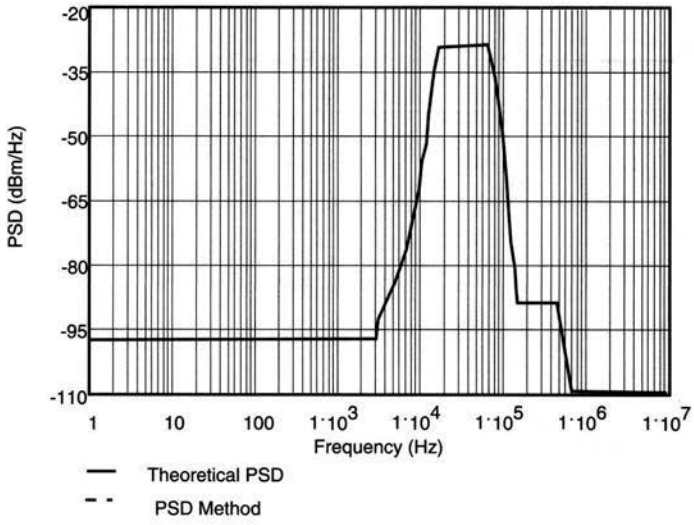
Figure 4.16 Theoretical and implementation ADSL upstream PSDs with a linear frequency scale and a log frequency scale.



To more fully specify the upstream ADSL PSD, a piecewise continuous mask was created. This mask is based on the masks shown in Figure 4.16 and adds more complete out-of-band specifications. The piecewise continuous mask is shown in Figure 4.17.

One caution about the ADSL upstream and downstream masks is that they continue to evolve. As new services are studied, requests made for the out-of-band PSD regions may be tightened. In some cases, because of implementation problems, loosening of the requirements is proposed. These activities may continue for many years to come.

Figure 4.17 Piecewise continuous PSD for an upstream DMT ADSL signal.



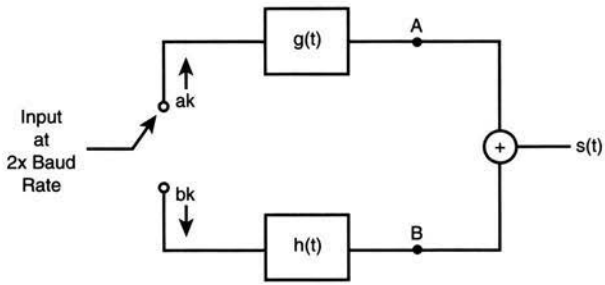
CAP/QAM ADSL

Carrierless Amplitude Modulation/Phase Modulation (CAP) and Quadrature Amplitude Modulation (QAM) technologies have very similar (and in some cases identical) time-domain and frequency-domain representations. For that reason, CAP and QAM are treated together from a PSD and crosstalk point of view. All further discussion in this section is applicable to both CAP and QAM. Both an unshaped (unfiltered) CAP signal and a shaped (filtered) CAP signal are discussed. Normal implementations use a shaped signal; however, discussing unshaped CAP first is valuable for in-depth understanding.

An unshaped CAP signal can be produced by combining the outputs of two filters, g and h, each excited by an input impulse at the baud rate of the CAP system. See Figure 4.18.

The input impulse trains a_k and b_k have independent and identically distributed heights. The impulse height probability density function has zero mean and variance V^2 for both a_k and b_k. If the continuous time waveforms for the two pulse trains are given by a and b, then the autocorrelation functions are as shown in Eqtn. 4.43 and Eqtn. 4.44.

Figure 4.18 Block diagram for a CAP/QAM modulator.



Eqtn. 4.43

$$R_{aa}(\tau) = V^2\delta(\tau)$$

Eqtn. 4.44

$$R_{bb}(\tau) = V^2\delta(\tau)$$

Because all a_k and b_k are independent, the cross-correlation function between a and b is given by Eqtn. 4.45.

Eqtn. 4.45

$$R_{ab}(\tau) = 0$$

For an unfiltered system, the impulse responses of the two filters consist of either a cosine wave or a sine wave for a length of time T. Eqtn. 4.46 and Eqtn. 4.47 show these impulse responses.

Eqtn. 4.46

$$g(t) = \begin{cases} \cos(2\pi f_c t) & |t| \le \dfrac{T}{2} \\ 0 & |t| > \dfrac{T}{2} \end{cases}$$

Eqtn. 4.47

$$h(t) = \begin{cases} \sin(2\pi f_c t) & |t| \le \dfrac{T}{2} \\ 0 & |t| > \dfrac{T}{2} \end{cases}$$

In Eqtn. 4.47, T is the period of a CAP symbol. The fourier transform is used to find the frequency-domain response of a time-domain impulse response. The fourier transform of g is given by Eqtn. 4.48.

Eqtn. 4.48

$$
\begin{aligned}
G(f) &= \int_{-\frac{T}{2}}^{\frac{T}{2}} \cos(2\pi f_c t) e^{-j2\pi ft} dt \\
&= \int_{-\frac{T}{2}}^{\frac{T}{2}} \left(\frac{e^{j2\pi f_c t} + e^{-j2\pi f_c t}}{2} \right) e^{-j2\pi ft} dt \\
&= \frac{1}{2} \int_{-\frac{T}{2}}^{\frac{T}{2}} e^{j2\pi t(f_c - f)} + e^{-j2\pi t(f_c + f)} dt \\
&= \frac{1}{2} \left(\frac{e^{j2\pi t(f_c - f)}}{j2\pi(f_c - f)} + \frac{e^{-j2\pi t(f_c + f)}}{-j2\pi(f_c + f)} \right)_{\frac{-T}{2}}^{\frac{T}{2}} \\
&= \frac{1}{2} \left(\frac{e^{j\pi T(f_c - f)} - e^{-j\pi T(f_c - f)}}{2j\pi(f_c - f)} + \frac{e^{-j\pi T(f_c + f)} - e^{j\pi T(f_c + f)}}{-2j\pi(f_c + f)} \right)
\end{aligned}
$$

Here Euler's formula was used to get to the second line. Note that in the last line of Eqtn. 4.48, each term inside the parenthesis has an embedded sine term. Thus the result of Eqtn. 4.48 can be simplified as in Eqtn. 4.49.

Eqtn. 4.49

$$
\begin{aligned}
G(f) &= \frac{1}{2} \left(\frac{e^{j\pi T(f_c - f)} - e^{-j\pi T(f_c - f)}}{2j\pi(f_c - f)} + \frac{e^{-j\pi T(f_c + f)} - e^{j\pi T(f_c + f)}}{-2j\pi(f_c + f)} \right) \\
&= \frac{1}{2} \left(\frac{\sin(\pi T(f - f_c))}{\pi(f - f_c)} + \frac{\sin(\pi T(f + f_c))}{\pi(f + f_c)} \right)
\end{aligned}
$$

Euler's formula was again used to get the second line in Eqtn. 4.49. Note that the terms in the subtraction and sine of the first term were interchanged. The resulting sign change in both the numerator and denominator cancel out each other. Note also that the result is the addition of two sinc functions, one centered at f_c and one centered at $-f_c$. Because G will be used to help find the PSD of a CAP signal, the single-sided magnitude squared of the transfer function G is of concern. Assuming that the frequency f_c, sometimes called the *center frequency*, is much larger than 1/T, then the tails of each sinc function are negligible

near the peak of the other sinc function. With this assumption, the single-sided response squared magnitude response of G is given by Eqtn. 4.50.

Eqtn. 4.50

$$|G(f)|^2 \approx \left| \frac{\sin(\pi T(f - f_c))}{\pi(f - f_c)} \right|^2$$

With the knowledge of the autocorrelation of a, as well as the transfer function G, the PSD at point A in Figure 4.18 is given by Eqtn. 4.51.

Eqtn. 4.51

$$PSD_A(f) = \frac{2\Im(R_{aa}(\tau))|G(f)|^2}{ZT} = \frac{2V^2 \sin^2(\pi T(f - f_c))}{\pi^2 ZT(f - f_c)^2}$$

The PSD at point B in Figure 4.18 is identical to that given in Eqtn. 4.51. This result should not be very surprising given that the autocorrelations of the inputs are identical and the filters, g and h, are just phase-shifted versions of one another (and phase does not contribute the squared magnitude response). Because the inputs a and b are uncorrelated, the outputs at points A and B of Figure 4.18 are also uncorrelated. Thus the PSD at the output of the modulator, point C, is simply the sum of the PSDs at points A and B. Therefore, the PSD of an unfiltered CAP signal is given by Eqtn. 4.52.

Eqtn. 4.52

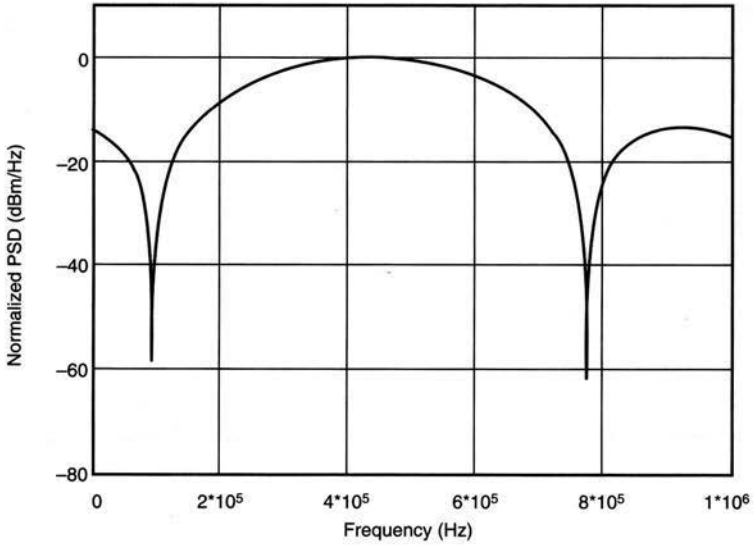
$$PSD_{CAP,un} = PSD_A(f) + PSD_B(f) = \frac{4V^2 \sin^2(\pi T(f - f_c))}{\pi^2 ZT(f - f_c)^2}$$

The normal reference impedance for CAP and QAM on a twisted pair is 100 ohms. The symbol period T and the center frequency f_c have purposely been left unspecified until now. Different combinations of T and f_c can be implemented to achieve different bit rates on the twisted pair. Also, different values will change the frequency band being used. For illustration purposes, an unfiltered CAP signal centered at 435.5 kHz with a baud rate of 340 ksymbols/s ($T=1/340*10^3$ s) is shown in Figure 4.19.

Note

One normally does not talk about center frequency with a CAP signal. Nevertheless, it is intuitive to the current discussion and is therefore used for illustrative purposes only.

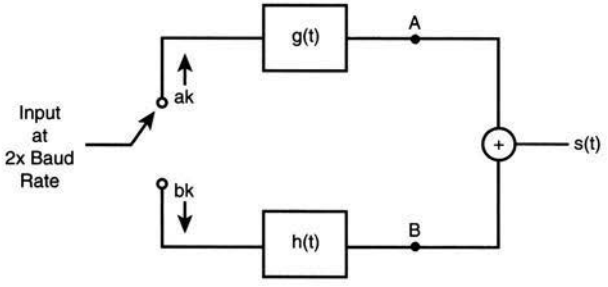
Figure 4.19 A normalized PSD for an unfiltered 340 kbaud CAP/QAM signal centered at 435.5 kHz.



In Figure 4.19, the width of the center lobe is approximately twice the symbol baud rate. Shaping can reduce this wide bandwidth by a factor of two. Note also the level of the center lobe in Figure 4.19 compared to the side lobes. The side lobes, representing the out-of-band energy of the line code, are less than 20 dB below the center lobe, or in band energy. It is more desirable to have the sidebands attenuated more so that they do not cause severe crosstalk into other lines. Sideband reduction can also be obtained by using shaping.

A shaped CAP signal can be achieved by adding shaping, or windowing, to the impulse response g and h in the CAP modulator. The new filters are labeled r_I and r_Q and are shown in Figure 4.20.

Figure 4.20 Block diagram for a CAP/QAM modulator with shaping.



The main purpose of shaping is to reduce bandwidth of the signal's main lobe to approximately the symbol baud rate and to reduce the out-of-band energy in the CAP signal. *Out-of-band energy* refers to the frequency components outside the main lobe of the PSD that ripple away on either side.

Note that the impulse responses g and h in Figure 4.18 can be considered to have rectangular shaping given by Eqtn. 4.53.

Eqtn. 4.53

$$m(t) = u\left(t + \frac{T}{2}\right) - u\left(t - \frac{T}{2}\right)$$

More simply put, in this rectangular window the symbol baud rate is the width. Such a window tends to have poor properties in the frequency domain (which results in the wide bandwidth and high sidebands in Figure 4.19). The most commonly used shaping filter for DSL-based CAP and QAM is the square root raised cosine filter. A baseband normalized square root raised cosine filter has an impulse response given by Eqtn. 4.54.

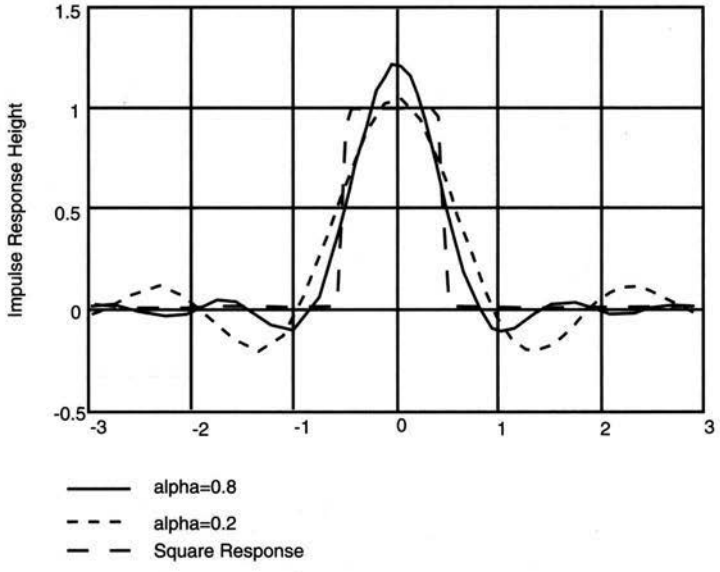
Eqtn. 4.54

$$r_{srrc}(t) = \frac{\sin\left(\pi(1-\alpha)\frac{t}{T}\right) + 4\alpha\frac{t}{T}\sin\left(\pi(1+\alpha)\frac{t}{T}\right)}{\pi\frac{t}{T}\left(1-\left(4\alpha\frac{t}{T}\right)^2\right)}$$

In Eqtn. 4.54, the parameter α represents the excess bandwidth that the signal will occupy in the frequency domain due to shaping. A larger α implies more bandwidth. For α=0, the signal bandwidth is equal to exactly half the baud rate. This type of filter is difficult to

implement, and so some bandwidth expansion is normally used. Typical values of α are 0.15 and 0.2, implying that 15% and 20% extra bandwidth, respectively, above the baud rate of the system is needed. The extra bandwidth is normally considered a fair trade-off for the reduced side-band energy. The impulse response for a square root raised cosine filter for various values of α along with a rectangular window used in an unshaped CAP modulator is shown in Figure 4.21.

Figure 4.21 Examples of square root raised cosine impulse response for various values of a.



Note that impulses passed through the square root raised cosine filter at baud rate T produce symbols that overlap in time. The receiver can handle this overlap with equalization. When the square root raised cosine response is combined with the CAP modulator filters, the resulting filters become Eqtn. 4.55 and Eqtn. 4.56.

Eqtn. 4.55

$$r_I(t) = \frac{\sin\left(\pi(1-\alpha)\frac{t}{T}\right) + 4\alpha\frac{t}{T}\sin\left(\pi(1+\alpha)\frac{t}{T}\right)}{\pi\frac{t}{T}\left(1-\left(4\alpha\frac{t}{T}\right)^2\right)}\cos(2\pi f_c t)$$

Eqtn. 4.56

$$r_Q(t) = \frac{\sin\left(\pi(1-\alpha)\frac{t}{T}\right) + 4\alpha\frac{t}{T}\sin\left(\pi(1+\alpha)\frac{t}{T}\right)}{\pi\frac{t}{T}\left(1-\left(4\alpha\frac{t}{T}\right)^2\right)}\sin(2\pi f_c t)$$

Normally, the impulse response is several symbols long. Each filter will have the same squared magnitude frequency response. For an infinitely long impulse response, the response of r_I can be approximated by Eqtn. 4.57.

Eqtn. 4.57

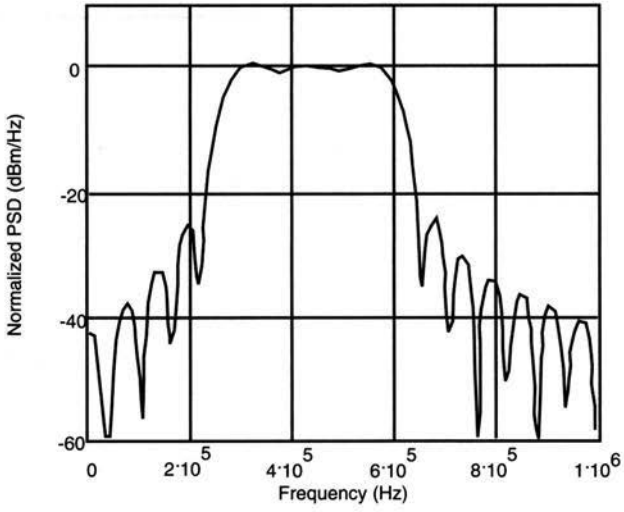
$$R_I(f) = \begin{cases} T & |f - f_c| < \frac{1}{2T}(1-\alpha) \\ \frac{T}{\sqrt{2}}\sqrt{1-\sin\left(\frac{\pi T}{\alpha}\left(|f-f_c| - \frac{1}{2T}\right)\right)} & \frac{1}{2T}(1-\alpha) \le |f-f_c| \le \frac{1}{2T}(1+\alpha) \\ 0 & |f-f_c| > \frac{1}{2T}(1+\alpha) \end{cases}$$

The expression in Eqtn. 4.57 has three parts. The first part is the in-band signal with an amplitude of T (normally, this would be scaled to the proper signal level desired). The second part of Eqtn. 4.57 is the bandwidth expansion region. The final part of the equation represents the out-of-band region and is approximated as zero.

For a truncated window, a closed-form solution to the frequency-domain template of the shaping is not possible. However, the numeric approximation in Figure 4.22 uses the same parameters as the unshaped example (Figure 4.19) uses.

Note the level of the sidebands in this figure as compared to Figure 4.19. Also note that the out-of-band energy is not zero (negative infinity on a dB scale) as predicted in Eqtn. 4.57. Given the response of r_I and the autocorrelation function of a, the PSD at point A in Figure 4.20 is given by Eqtn. 4.58.

Figure 4.22 Approximation of the normalized spectrum of a QAM signal with square root raised cosine shaping.



Eqtn. 4.58

$$PSD_A(f) = \frac{2\Im(R_{aa}(\tau))|R_I(f)|^2}{ZT} = \frac{2V^2|R_I(f)|^2}{ZT}$$

Once again, because of the independence of a and b, the output PSD of the shaped CAP modulator is simply the sum of the PSDs of each modulator leg. Thus the output PSD is given by Eqtn. 4.59.

Eqtn. 4.59

$$PSD_{CAP}(f) = \frac{2V^2|R_I(f)|^2}{ZT} + \frac{2V^2|R_Q(f)|^2}{ZT} = \frac{4V^2|R_I(f)|^2}{ZT}$$

In Eqtn. 4.59, the terminating impedance Z is 100 ohms, and T is purposely left unspecified. The center frequency f_c is also not specified. The CAP/QAM modem developers have not yet finalized the exact parameters for ADSL lines.

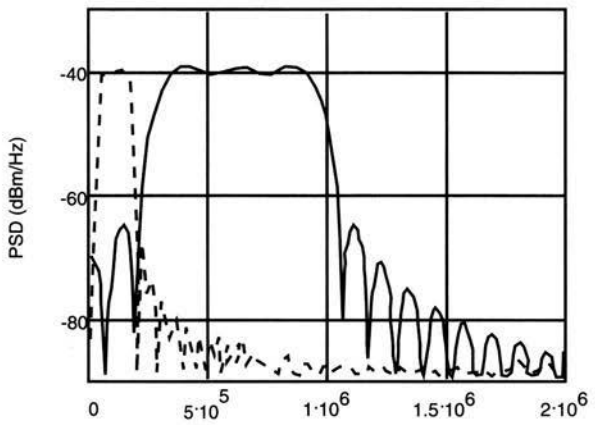
Some candidate values are shown in Table 4.2.

Table 4.2 Candidate Symbol Rates and Bandwidths for CAP/QAM ADSL Signals

Symbol Rate 1/T (ksymbols/s)	Excess Bandwidth (α)	Center Frequency (kHz)	Low-End 3 dB Point (kHz)	High-End dB Point (kHz)
84	0.20	84.0	42.0	126.0
136	0.15	113.2	45.2	181.2
340	0.15	435.5	265.5	605.5
680	0.15	631.0	291.0	971.0
952	0.15	787.4	311.4	1263.4

The first two entries in Table 4.2 are for upstream ADSL, and the rest are for downstream. The PSDs for two of the CAP/QAM implementations shown are given in Figure 4.23.

Figure 4.23 PSDs for various CAP/QAM signals.



VDSL PSDs

Standards for VDSL are still under development; although a PSD requirement has been agreed upon, it is likely to evolve as times goes on. The mask may change drastically depending on the modulation type chosen for VDSL (several modulation candidates exist, including a variation of DMT called "synchronous DMT(SDMT)," a variation of DMT called "zipper," and also CAP- and QAM-based techniques).

One major difference between ADSL and VDSL is that VDSL signals overlap the amateur radio bands as well as several other allocated frequency regions. Even though a VDSL signal is confined to a twisted pair and not radiated from an antenna, at high frequencies the emissions from the twisted pair can be large enough to interfere with receivers of these other services.

This type of emission is commonly referred to as radio frequency interference (RFI) egress. Depending on the region and type of VDSL installation, the RFI egress may or may not be a problem. When it is a problem, to reduce RFI egress, the VDSL PSD will have notches at identified frequency bands. A list of the frequency bands at which the VDSL PSD will need reduction appears in Table 4.3.

Table 4.3 Internationally Recognized Bands That Require PSD Reduction for VDSL

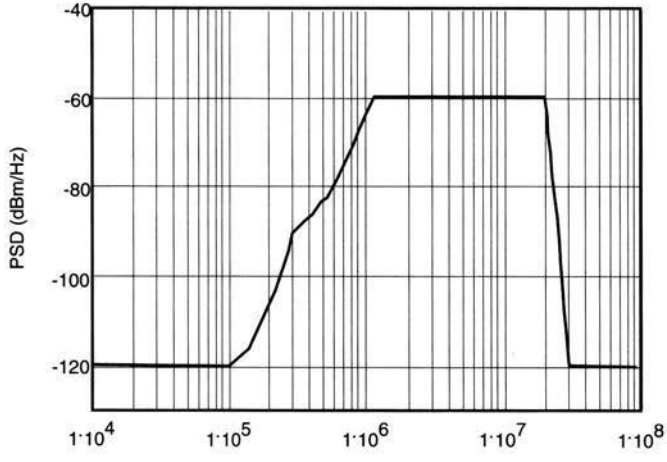
Start Frequency (MHz)	Stop Frequency (MHz)
1.8	2.0
3.4	4.0
7.0	7.3
10.1	10.15
14.0	14.35
18.068	18.168
21	21.45
24.890	24.990
28.0	29.7

Other possible bands needing PSD reduction are under study and may be added to those listed in Table 4.3.

Any type of VDSL modulation must be able to reduce the PSD to acceptable levels in these bands. The PSD mask requirement for VDSL is shown in Figure 4.24.

Similar to the ADSL masks, this mask is piecewise continuous. A requirement to reduce the PSD in the RFI regions given in Table 4.3 is also imposed (but not shown in Figure 4.24). The PSD in these regions must be reduced to –80 dBm/Hz (or lower if desired). Note that the VDSL band is much wider than the bands of any other DSL technology and that the starting point of the passband is above the highest frequency used in ADSL. This arrangement would allow ADSL and VDSL to coexist in a binder group without major interference. An option to allow the VDSL band's lower limit to extend down into the ADSL band is being discussed for situations in which VDSL is deployed, but ADSL is not.

Figure 4.24 PSD mask for VDSL.



Summary of PSDs

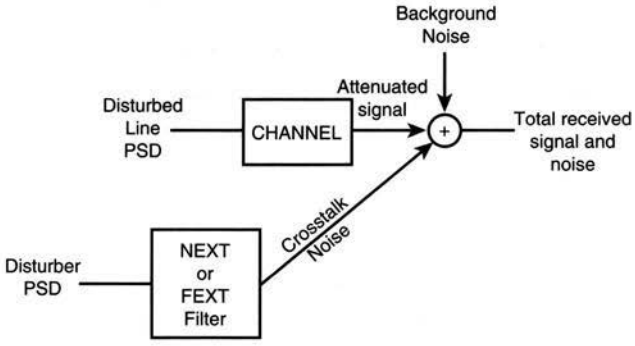
In the previous sections, PSDs of most of the common types of signals in the DSL environment were derived. These PSDs, along with channel transfer functions, are useful for finding the received signal power of a signal that propagates along a twisted pair. Also, the PSDs are the basis for finding NEXT and FEXT expressions for different types of disturbers. The former quantity defines the signal power at a receiver; the latter defines the noise power at a receiver. Together they define the SNR at a receiver. This quantity predicts system performance, including the maximum data rate achievable or the SNR margin for a fixed data rate.

PSDs are also useful for finding the total power in a given frequency band. Integration of the PSD over the band of interest yields the total power in that band due to the signal. Integrating over all frequencies gives the total power of the signal.

NEXT and FEXT Expressions

In previous sections, the PSDs of various types of DSL line codes were derived. The PSDs of the line codes are different from the PSD of a disturber coupled onto a disturbed DSL. The latter PSD is often called the NEXT PSD or the FEXT PSD, depending on the type of crosstalk. NEXT and FEXT PSDs are found by simply passing the disturbing line's PSD (as derived previously) through the NEXT or FEXT transfer functions derived in Chapter 2. Figure 4.25 shows the combination of this crosstalk model with the channel transfer function of the disturbed line. The NEXT and FEXT PSDs must also be adjusted for the number of disturbers present, as discussed earlier in this chapter.

Figure 4.25 Additive model for NEXT and FEXT into the disturbed line's signal.



NEXT Disturbers

The general expression for a NEXT disturber, based on the disturbing systems PSD, is given by Eqtn. 4.60.

Eqtn. 4.60

$$PSD_{NEXT}(f) = PSD_{DIST}(f) \times X_N f^{3/2}$$

Here X_N is given by Eqtn. 4.61.

Eqtn. 4.61

$$X_N = 0.882 \times 10^{-14} \times N^{0.6}$$

Here N is the number of disturbers having a PSD given by PSD_{DIST}. Note that as the number of disturbers increases, the effect of each additional disturber decreases. This outcome takes into account worst-case modeling and the fact that all disturbers will not be on the worst-case disturbing line.

It is generally assumed that all crosstalk comes from inside the binder group of the disturbed twisted pair; the coupling values in Eqtn. 4.61 are based on this assumption. For some DSL technologies, common practice prohibits T1 disturbers from being in the same binder group as the DSL line. However, T1 lines do tend to be in the vicinity of many DSL technologies and so some adjustment to Eqtn. 4.60 is necessary to account for T1 disturbances from outside the DSL binder group.

The adjustment is a reduction by 15.5 dB of the T1 NEXT calculated using Eqtn. 4.60. This is equivalent to multiplying Eqtn. 4.60 by 0.0282. Graphs of the NEXT PSD for ISDN, HDSL, and T1 disturbers are shown in Figure 4.26 and Figure 4.27.

Figure 4.26 10 ISDN, HDSL, and T1 NEXT disturbers.

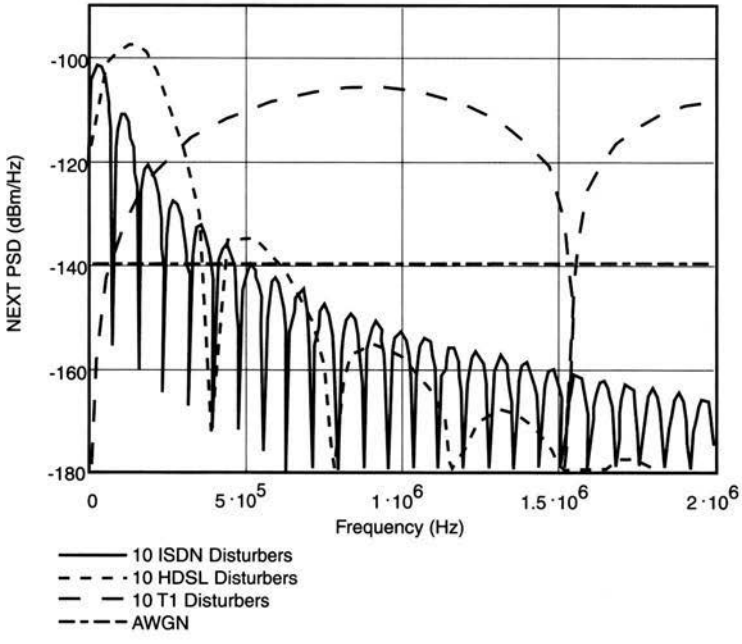
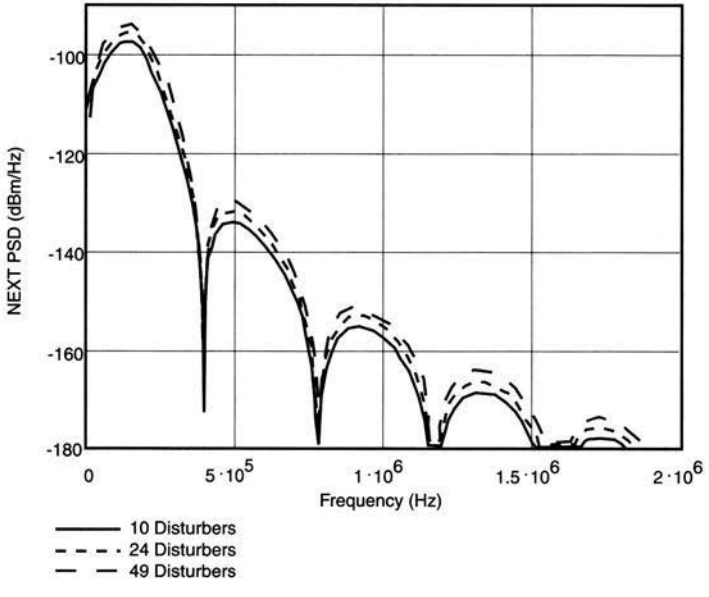


Figure 4.27 10, 24, and 49 HDSL NEXT disturbers.



In Figure 4.26, 10 NEXT disturbers exist for each type of disturber. Figure 4.27 compares 10, 24, and 49 disturbers for HDSL. In addition, the normally assumed *additive white Gaussian noise* (AWGN) floor for a DSL line of –140 dBm/Hz is shown.

Figure 4.28 shows NEXT curves for upstream and downstream ADSL signals (both DMT based and CAP/QAM based).

Figure 4.28 10 DMT and CAP/QAM NEXT disturbers.

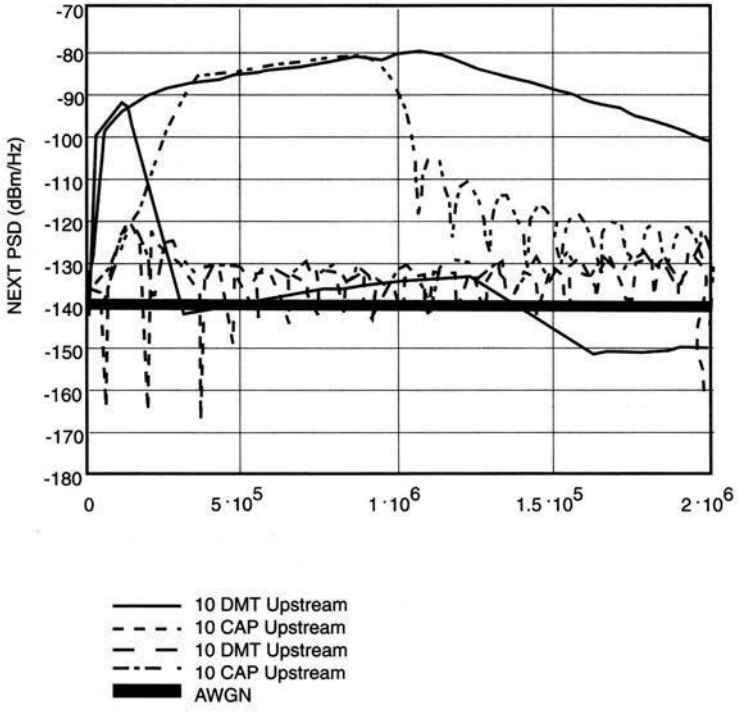
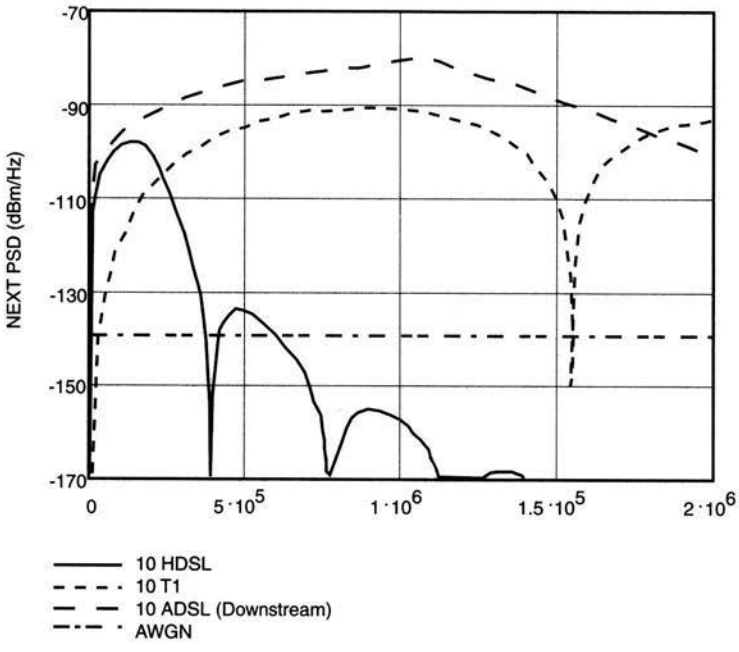


Figure 4.29 compares the NEXT from DMT-based ADSL to HDSL crosstalk. The next chapter looks at the effect of NEXT disturbers on the data rate achievable over the DSL.

Figure 4.29 Comparison of DMT downstream NEXT to HDSL NEXT.



FEXT Disturbers

The general expression for a FEXT disturber, based on the PSD of the disturbing signal, is given by Eqtn. 4.62.

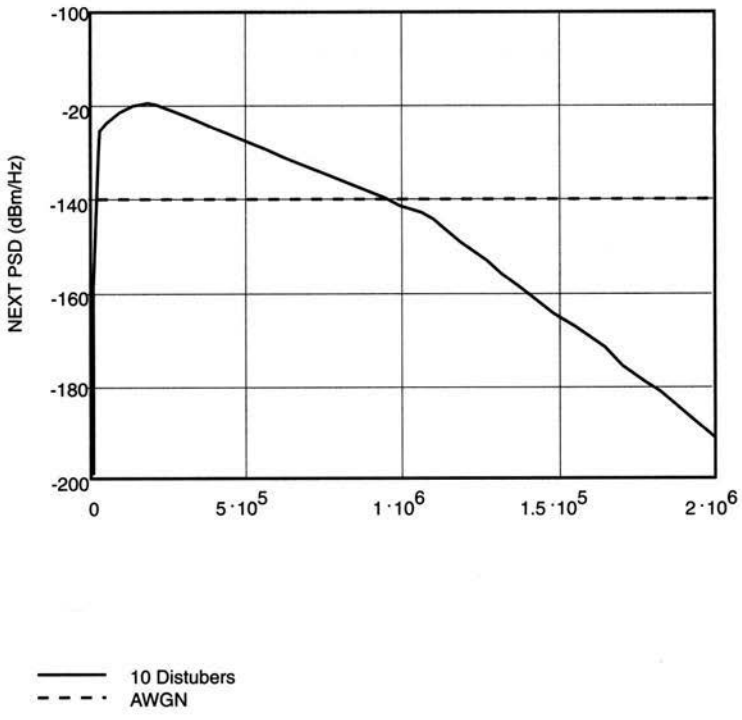
Eqtn. 4.62

$$PSD_{FEXT}(f) = PSD_{DIST}(f) \times \left|H_{channel}(f)\right|^2 \times K_{FEXT} \times l \times f^2$$

Here $H_{channel}$ is the response of the channel, K_{FEXT} is a coupling constant, and l is the coupling path length. Normally, NEXT is much greater than FEXT, and so FEXT is often ignored.

However, FEXT from other ADSL signals (ADSL self-FEXT) is used in some performance benchmarking. Specifically, FEXT from downstream ADSL is often used. FEXT for 10 downstream ADSL disturbers assuming a CSA #6 Loop is shown in Figure 4.30. The coupling constant K_{FEXT} for 10 disturbers is given by $3.083*10^{-20}$. Also shown is the –140 dBm/Hz AWGN noise floor.

Figure 4.30 10 DMT ADSL FEXT disturbers on CSA #6 Loop.



Summary

This chapter discussed complete crosstalk models, both NEXT and FEXT, for DSLs, and the PSDs of ISDN, HDSL, T1, and both CAP/QAM and DMT-based ADSL and VDSL were derived. These PSDs can be "dropped" into a generic NEXT or FEXT equation that, along with the coupling coefficient and the number of disturbers, gives the PSD of the crosstalk. This PSD is noise to an ADSL or VDSL receiver. The treatment of NEXT is a bit more in-depth than that of FEXT because NEXT is usually a more dominant source of crosstalk noise.

Chapter 3 derived channel transfer functions for various types of twisted pairs. Passing the PSDs derived in this chapter through the twisted pair transfer functions derived in previous chapters results in the signal PSD at the DSL receiver. Given that signal PSD and the noise PSD due to crosstalk, the performance of the DSL can be predicted.

Exercises

1. Derive the general result given in Eqtn. 4.17 for the autocorrelation of the output of a linear, time-invariant filter. Assume the input autocorrelation to be R_{xx}.
2. Derive the autocorrelation result given in Eqtn. 4.19. Use the probability density function given in Eqtn. 4.18.
3. Approximate the total power for an ISDN signal by integrating the PSD. Compare this value to the average power of the time-domain ISDN waveform.
4. Assume that the binary 1's density on a T1 line is 100%. What will the time-domain waveform look like? Calculate the PSD for this scenario.
5. Verify that the PSD at point B in Figure 4.18 is identical to the PSD given in Eqtn. 4.51.
6. Another common shaping pulse is the raised cosine pulse. Its baseband time-domain waveform is given by Eqtn. 4.63.

Eqtn. 4.63

$$g_{rc}(t) = \frac{\sin\left(\frac{\pi t}{T}\right)}{\frac{\pi t}{T}} \frac{\cos\left(\alpha \frac{\pi t}{T}\right)}{1-\left(2\alpha \frac{\pi t}{T}\right)^2}$$

Plot this pulse for various values of α. For α=0, compare this pulse to a sinc pulse. Plot passband versions of the raised cosine pulse.

7. Plot the passband versions of the square root raised cosine pulse. For various values of α, compare these the passband plots of the raised cosine pulse.
8. Plot all of the upstream and downstream candidate PSDs for CAP/QAM based VDSL. Which upstream/downstream combinations would effectively eliminate NEXT (assuming that all lines in the binder group were using the same parameters)?
9. Find the total power for 10 NEXT HDSL disturbers and compare to the total power of 24 HDSL disturbers.
10. Find the NEXT PSD of a line having 10 T1 NEXT disturbers and 10 ISDN NEXT disturbers. Why is this assumption overly pessimistic?
11. Compare the PSD of NEXT due to 10 ADSL downstream signals with the FEXT due to 10 ADSL downstream signals on a CSA #6 Loop.

12. A downstream ADSL DMT signal is passed through a CSA #6 Loop. Find the PSD at the ADSL receiver. Find the NEXT PSD of 20 HDSL disturbers. Using the received PSD and the NEXT PSD, find the SNR over frequency at the receiver.

13. Repeat the previous exercise for a mid-CSA loop with 10 T1 NEXT disturbers. Repeat with a T1.601 Loop #13 and 24 ISDN disturbers.

CHAPTER 5

DSL Theoretical Capacity in Crosstalk Environments

In this chapter:

- Review and discussion of channel capacity
- Evaluation of channel capacity for ADSL loops
- Evaluation of channel capacity for VDSL loops
- Case study highlighting channel capacity over frequency

This chapter examines the potential of a twisted pair channel to carry information—better known as the channel capacity of a twisted pair channel. The discussion here applies much of the information presented in Chapters 2, "Twisted Pair Environment," and 3, "Loop Analysis," regarding twisted pair loss, and in Chapter 4, "Power Spectral Densities and Crosstalk Models," regarding crosstalk between twisted pairs. This chapter also reviews the basic concepts of capacity and the derivation of capacity under different channel conditions. In addition, this chapter presents a method for finding capacity in channels with intersymbol interference and colored noise and applies that method to many ADSL and VDSL scenarios. For further reading, refer to "Achievable Information Rates on Digital Subscriber Loops: Limiting Information Rates with Crosstalk"[1] and "Asynchronous Multiple-Access Channel Capacity"[2] for well-written discussions on capacity, as well as for discussions on the methods of calculating capacity used in this chapter.

Chapters 2 and 3 discussed the loss on a twisted pair channel as well as the crosstalk coupling between two twisted pairs that are physically located near one another. Both of these conditions are factors in determining the amount of information that a twisted pair channel can reliably carry. Simply put, these factors determine the data rate capability of the twisted pair. It makes sense that twisted pair channels with more loss support lower data rates than

do twisted pairs with less loss. Similarly, a twisted pair with more crosstalk disturbance supports a lower data rate than a twisted pair with little or no crosstalk. Mathematically bounding channel capacity provides a benchmark for the performance of various types of coding and modulation techniques. This chapter sets the benchmarks; later chapters compare the performance of modulation techniques, namely, DMT- and CAP/QAM-based systems, to the benchmarks.

A Review of Capacity

For a continuous time channel, capacity is a function of signal power and noise power at the receiver of the channel. If a specific application uses only a certain frequency band on the channel, the frequency band used (the bandwidth) also affects capacity.

Truly understanding channel capacity begins with an understanding of entropy and mutual information, two topics often discussed by information theory texts.[3,4] The following sections review the mathematical specifics of capacity.

Entropy and Information

Information theory defines the capacity of a channel as the maximum mutual information between a channel's output and a channel's input, or I(X;Y), where X is the input and Y the output. Written in terms of entropy for discrete random variables X and Y, this definition is equivalent to Eqtn. 5.1.

Eqtn. 5.1

$$\max\left(I(X;Y)\right) = \max\left(H(X) - H(X/Y)\right)$$

In Eqtn. 5.1, H is the entropy, or uncertainty, of input X, and H(X/Y) is the entropy or uncertainty of input X given output Y. A trivial example is best used to demonstrate the relationship between information and uncertainty.

Consider the following situation: A person flips a coin (a fair one) and tells the result to another person. In this example, the input can be either a head or a tail; each is equally likely. The uncertainty of the input H is one bit. The output of the channel Y is what the listener hears. At one extreme, the listener clearly hears what the "flipper" says is the result of the coin toss. In this case, H(X/Y)=0 because no uncertainty about the outcome of the toss remains. Thus the speaker conveyed one bit of information over the channel.

Note

A *bit* is one basic unit of information. You will see later that it involves using base 2 logarithms to define entropy. Another common unit of information is *nat*, which uses base e logarithms (or natural logs). All entropy and information expressions in this book use bits as units.

At the other extreme, the listener cannot hear what the speaker is saying. In this case, H(X/Y)=1 bit. In other words, the listener received no indication of whether a head or tail resulted and thus still has one bit of uncertainty. The information conveyed over the channel by the speaker is zero bits because uncertainty about the coin toss outcome was not reduced (there was one bit of uncertainty before the speaker spoke and one bit after). Between the extremes, the listener may have faintly understood or heard the speaker, and somewhere between zero and one bit of uncertainty was removed. The more clearly the speaker was heard, the more uncertainty was removed.

Returning to a more analytical treatment H, the entropy of the input in Eqtn. 5.1 is given by Eqtn. 5.2.

Eqtn. 5.2

$$H(X) = \sum_{x' \in \Gamma} \Pr(x') \log_2 \left(\frac{1}{\Pr(x')} \right)$$

Here Γ represents a set of all values that X can take on, and Pr(x') represents the probability that X takes on the value of x'. Likewise, H(X/Y), the uncertainty of the input given the output, can be written as Eqtn. 5.3.

Eqtn. 5.3

$$H(X/Y) = \sum_{x' \in \Gamma} \sum_{y' \in \Psi} \Pr[(x', y')] \log_2 \left(\frac{1}{\Pr[(x'/y')]} \right)$$

Here Γ represents a set of all possible values of X, and ψ represents a set of all possible values of Y. Note that if X and Y are independent, then the uncertainty of X given Y is the same as the uncertainty of X as illustrated in Eqtn. 5.4.

Eqtn. 5.4

$$H(X/Y) = H(X)$$

This equation is true because knowledge of Y clears up no uncertainty of X.

The expression for capacity given in Eqtn.5.1 can be equivalently written as Eqtn. 5.5.[3,4]

Eqtn. 5.5

$$\max\big(I(X;Y)\big) = \max\big(H(Y) - H(Y / X)\big)$$

Whereas Eqtn. 5.1 allows for an intuitive understanding of capacity, Eqtn. 5.5 derives an analytical expression for the capacity of a channel with noise.

For a continuous random variable, the concepts of entropy and information can be extended, and the entropy of some continuous random variable Z defined as in Eqtn. 5.6.

Note

The extension of entropy to the continuous case is not so straightforward. In this context, it is not truly uncertainty, as uncertainty would be infinite for a continuous random variable, but rather as a quantity analogous to uncertainty. This condition is sometimes referred to as *differential entropy*.

Eqtn. 5.6

$$h(Z) = \int_{-\infty}^{\infty} p(z)\log_2\left(\frac{1}{p(z)}\right)dz$$

Here p is the probability density function of random variable Z. If Z is Gaussian and characterized by a zero mean and a variance σ_z^2 of $N_o/2$ (denoted by $(0,N_o/2)$), then h can be written as shown in Eqtn. 5.7.

Eqtn. 5.7

$$\begin{aligned} h(Z) &= \int_{-\infty}^{\infty} p(z)\log_2\left(\frac{1}{(p(z))}\right)dz \\ &= \int_{-\infty}^{\infty} p(z)\left(\log_2(\sqrt{2\pi\sigma_z^2}) + \frac{z^2}{2\sigma_z^2}\right)dz \\ &= \frac{1}{2}\log_2\left(2\pi\sigma_z^2\right) + \frac{1}{2} \\ &= \frac{1}{2}\log_2\left(2\pi N_o\right) \end{aligned}$$

The final expression in Eqtn. 5.7 will be useful in calculating the capacity of an additive white Gaussian noise (AWGN) channel.

Gaussian Channels

Consider an AWGN channel now with input X, output Y, and additive noise Z, where Z is independent of X. Eqtn. 5.8 gives the output of the channel.

Eqtn. 5.8

$$Y = X + Z$$

The capacity of the channel can then be written as Eqtn. 5.9.

Eqtn. 5.9

$$C = \max\big(I(X;Y)\big) = \max\big(h(Y) - h(Y \,/\, X)\big)$$
$$= \max\big(h(Y) - h((X+Z) \,/\, X)\big)$$

Because all uncertainty about X can be cleared up if X is known, the h(X+Z/X) term in Eqtn. 5.9 can be simplified and the equation can be rewritten as Eqtn. 5.10.

Eqtn. 5.10

$$C = \max\big(h(Y) - h(Z \,/\, X)\big)$$

Remember that the AWGN term Z and the input signal X are independent by assumption. As discussed previously, no uncertainty can be cleared with knowledge of an independent entity. Thus knowledge of X resolves no uncertainty about Z, and Eqtn. 5.10 becomes Eqtn. 5.11.

Eqtn. 5.11

$$C = \max\big(h(Y) - h(Z)\big)$$

If Z is AWGN with statistics $(0, \sigma_z^2)$, Eqtn. 5.7 can be substituted for the second entropy term in Eqtn. 5.10, yielding Eqtn. 5.12.

Eqtn. 5.12

$$C = \max\big(h(Y)\big) - \frac{1}{2}\log_2\left(4\pi\sigma_z^2\right)$$

Maximizing Eqtn. 5.11 is equivalent to maximizing h, which is a function of the probability distribution of X, namely, p. For a given variance, it can be shown that the Gaussian distribution with zero mean will maximize entropy. [3] Because Z is Gaussian and Y=X+Z, if X is Gaussian, then Y is also Gaussian (the sum of two Gaussian random variables is also a

Gaussian random variable). Assuming a Gaussian distributed X with statistics $(0,\sigma_x^2)$, Y then has statistics $(0,\sigma_x^2+\sigma_z^2)$ and h can be written as Eqtn. 5.13.

Eqtn. 5.13

$$h(Y)=\frac{1}{2}\log_2\left(4\pi\left(\sigma_x^2+\sigma_z^2\right)\right)$$

And Eqtn. 5.13 can be simplified to Eqtn. 5.14.

Eqtn. 5.14

$$\begin{aligned}C&=\frac{1}{2}\log_2\left(4\pi\left(\sigma_x^2+\sigma_z^2\right)\right)-\frac{1}{2}\log_2\left(4\pi\sigma_z^2\right)\\&=\frac{1}{2}\log_2\left(\frac{4\pi\left(\sigma_x^2+\sigma_z^2\right)}{4\pi\sigma_z^2}\right)\\&=\frac{1}{2}\log_2\left(1+\frac{\sigma_x^2}{\sigma_z^2}\right)\\&=\frac{1}{2}\log_2\left(1+\frac{E\left[x^2\right]}{E\left[z^2\right]}\right)\\&=\frac{1}{2}\log_2\left(1+SNR\right)\end{aligned}$$

Here SNR is the average signal-to-noise ratio at the receiver. Thus the channel capacity of an AWGN channel increases logarithmically with the average SNR at the receiver of the channel.

Channels with Memory and Interference

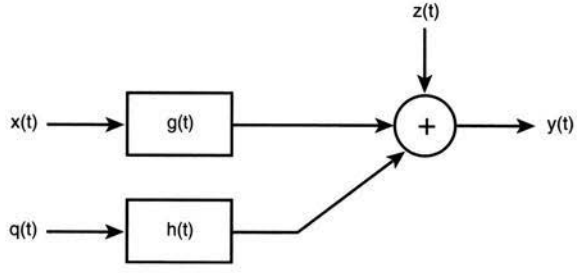
When a channel is not "memoryless," that is, the channel has some impulse response that is nonzero at more than one point in time, the analysis of channel capacity is a bit more involved. Furthermore, if colored noise rather than white noise is added to the channel, the AWGN channel results are not easily applied. A channel model including memory and colored noise is representative of a twisted pair channel with crosstalk noise. This transfer function over frequency of the twisted pair gives rise to the memory of the channel. The presence of crosstalk that varies with frequency gives rise to the colored-noise model. Note that a channel with memory is also called a channel with *intersymbol interference* or ISI.

This discussion considers a channel with input x, output y, a colored-noise component representing crosstalk resulting from AWGN source q passed through a linear time invariant

system (LTI) with impulse response h, and an AWGN noise component z. It is also assumed that x, q, and z are mutually independent and that the channel itself has an impulse response given by g. The channel model appears in Figure 5.1.

At first glance, the channel in Figure 5.1 may seem very different from the AWGN channel. Through transformations, however, it is possible to create an equivalent series of independent AWGN channels. Then you can use Eqtn. 5.14 to find the capacity of each AWGN channel. Because the channel is independent, the sum of the capacities of the individual channels is equivalent to the capacity of the original, colored, ISI channel.

Figure 5.1 Block diagram for system with ISI, AWGN, and colored-noise corruption.



Assuming that the channel shown in Figure 5.1 is sampled, we can write the output at time n as Eqtn. 5.15.

Eqtn. 5.15

$$y_n = \sum_{j=0}^{kg-1} g_j x_{n-j} + \sum_{j=0}^{kh-1} h_j q_{n-j} + z_n$$

Eqtn. 5.15 also assumes that the impulse response g_j of the twisted pair channel is kg samples long and that of the noise coupling function h_j is kh samples long.

Given Eqtn. 5.15, for a block of data beginning at n=0, some of the channel outputs may require knowledge of inputs x or n at indexes less than zero (past values of the inputs). Strictly for analysis, Verdu showed that the memory of the system could be assigned arbitrarily for analysis.[5] By assigning memory properly, the summations in Eqtn. 5.15 can be written as circular convolutions, and the N block output can be written as Eqtn. 5.16.

Note

Memory assigned in this manner is sometimes called a *cyclic prefix*. For very large blocks, the length of the assigned prefix will be negligible compared to the block length.

Eqtn. 5.16

$$y^N = g^N \otimes x^N + h^N \otimes q^N + z^N$$

Here ⊗ represents the circular convolution operator superscript, and superscript N represents N length sample vectors of each quantity. It is assumed that N is larger than the channel transfer function lengths kg and kh and that zero padding is used to extend the vectors g_j and h_j to length N.

A discrete fourier transform (DFT) of Eqtn. 5.16 can be taken and results in 5.17.

Eqtn. 5.17

$$Y^N = G^N X^N + H^N Q^N + Z^N$$

In Eqtn. 5.17, each capital letter represents the DFT of its respective lowercase time-domain counterpart. In general, each discrete point in Eqtn. 5.17 contains both a real and an imaginary component. Also, if all values in Eqtn. 5.16 are real (real values in the time domain), a DFT has the property that the second half of the transformed sequence will have complex conjugate symmetry with the first half of the sequence.[6] Thus the second half of the quantities after the transform can be dropped, and enough information remains to reconstruct the original untransformed sequence. The truncated version of Eqtn. 5.17 is shown in Eqtn. 5.18.

Note

Depending on whether N is odd or even, the actual symmetry may be around the center point (odd N) or around a point between the two most-center points (even N).

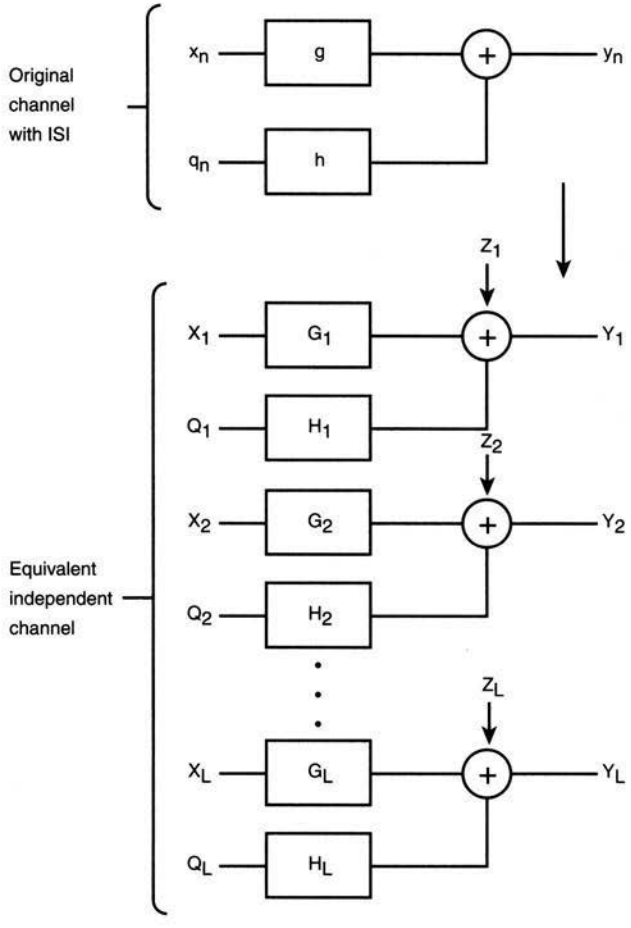
Eqtn. 5.18

$$Y^L = G^L X^L + H^L Q^L + Z^L$$

Here L represents half the length of the original transformed sequence. Hereafter, for notation convenience only, the superscript L will be dropped when referring to each quantity in Eqtn. 5.18.

Where we originally had a sequence of correlated samples, we now have a sequence of independent samples. (Each discrete frequency point is one channel; thus L independent channels exist.)[7] In a sense, each point in the sequence represents the output of one channel. The transformed set of channels appears in Figure 5.2.

Figure 5.2 Original channel with ISI (top) and a transformed set of independent channels with no ISI (bottom).



For channel m, the received signal is denoted by Y_m as shown in Eqtn. 5.19.

Eqtn. 5.19

$$Y_m = G_m X_m + (H_m Q_m + Z_m)$$
$$= \text{Signal} + (\text{Noise})$$

In Eqtn. 5.19, $G_m X_m$ represents the received signal on channel m, and $H_m Q_m + Z_m$ represents the received noise on channel m. Thus the SNR for channel m at the receiver is given by Eqtn. 5.20.

Eqtn. 5.20

$$SNR_m = \frac{|G_m X_m|^2}{|H_m Q_m + Z_m|^2}$$

If the power allotted to channel m is S_m, then from Eqtn. 5.14 the capacity on channel m is given by Eqtn. 5.21.

Eqtn. 5.21

$$\begin{aligned} C_m &= \frac{1}{2}\log_2(1 + SNR_m) \\ &= \frac{1}{2}\log_2\left(1 + \frac{|G_m X_m|^2}{|H_m Q_m + Z_m|^2}\right) \\ &= \frac{1}{2}\log_2\left(1 + \frac{|G_m|^2 S_m}{|H_m Q_m + Z_m|^2}\right) \end{aligned}$$

Because the subchannels are independent of one another, the total capacity of the system is the sum of the capacities of the individual subchannels. Thus the total capacity is given by Eqtn. 5.22.

Eqtn. 5.22

$$\begin{aligned} C &= \sum_{i=1}^{L} C_i = \sum_{i=1}^{L} \frac{1}{2}\log_2(1 + SNR_i) \\ &= \sum_{i=1}^{L} \frac{1}{2}\log_2\left(1 + \frac{|G_i|^2 S_i}{|H_i Q_i + Z_i|^2}\right) \end{aligned}$$

In this equation, S_i is the power allotted to channel i. Note that the capacity expression given in Eqtn. 5.22 makes no assumption about bandwidth. The units of Eqtn. 5.22 are bits per channel usage. If the original channel has a bandwidth of B Hz, then each subchannel will have a bandwidth of B/L Hz. For such a channel, it is possible to send a symbol over the channel 2B/L times per second. By sending symbols at this rate, the maximum rate of the channel R_{max} is given by Eqtn. 5.23.

Eqtn. 5.23

$$R_{max} = \sum_{i=1}^{L} \frac{B}{L}\log_2\left(1 + \frac{|G_i|^2 S_i}{|H_i Q_i + Z_i|^2}\right)$$

At this point, if S_i is known for all i subchannels, the total capacity of the channel is given by Eqtn. 5.23. This condition is true for most DSL technologies and is known as the power spectral density (PSD) limited channel. For the PSD limited channel, the sum of power on all the subchannels, as well as the power on each individual subchannel, is constrained. Both ADSL and VDSL fall under this category. The analysis in this chapter is based on Eqtn. 5.23.

For completeness, a derivation is given (see Appendix 5A) to find the capacity for the total power limited case also. In the total power limited case, the sum of power on all of the subchannels is constrained, but how the power is distributed among the channels is not constrained. This approach allows for one additional level of optimization.

Note

Optimization of this type in an environment prone to crosstalk would make performance prediction quite difficult. This situation is investigated later in the chapter.

Framework for Capacity Calculations for ADSL and VDSL

The result of Eqtn. 5.23, along with the results from Chapter 3 and Chapter 4, allow capacity calculations for any loop with any combination DSL crosstalk disturbers. Table 5.1 relates the quantities in Eqtn. 5.23 to the entities they represent.

Table 5.1 Description of Each Term in Eqtn. 5.23 for Calculating the Capacity of a Twisted Pair Channel

Quantity	Description
B	The entire bandwidth of the modulation scheme—1.1 MHz for ADSL and 15 MHz for VDSL. If L is the number of subchannels, then B/L is the bandwidth of each subchannel.
S_i	The signal power for each subchannel at the transmitter.
G_i	The loss between the transmitter and receiver for each subchannel. (ABCD parameters are used to find this quantity.)
Q_i	The signal power at a disturbers transmitter.
H_i	The transfer function for a disturber given by the NEXT or FEXT equations in Chapter 4.
Z_i	The background AWGN on a subchannel.

For ideal calculations, the number of subchannels would approach infinity, and the summation in Eqtn. 5.23 would become an integration. For practical performance calculations, however, the summation is adequate. For ADSL, capacity is found with the following variations:

- Different loops with the same noise and interference
- A single loop with different types of crosstalk
- Loop and noise called out in the ADSL standard

For VDSL, a slightly less vigorous examination will be carried out, focusing on the capacity of different VDSL loops under some limited crosstalk noises.

Also, a case study on a loop shows the SNR as a function of frequency and the information-carrying ability at different points in the frequency band of the channel. Note that capacity is independent of the type of modulation scheme used on the twisted pair. How close each modulation method comes to operating at the maximum theoretical rate (capacity) is investigated in later chapters.

ADSL Capacities

For ADSL, the signal power at the input to the channel is simply given by the PSD derived for ADSL. The capacity will be found for both the upstream and the downstream directions of data transmission. For the downstream direction, the capacity summation uses 1,000 points evenly spaced between 30 kHz and 1.106 MHz. These frequencies correspond to the actual usable band of an ADSL signal. Frequencies below 30 kHz are typically not used because of the Plain Old Telephone Service (POTS) underlay, and above 1.106 MHz the PSD for a downstream ADSL signal drops off quickly.

For the upstream direction, the capacity summation uses 1,000 points between 30 kHz and 138 kHz. The PSD of the upstream signal is specified to fall off above 138 kHz, and most usable signal energy is within this frequency range.

Loop Capacities with Identical Crosstalk

To compare the different types of loops, a single crosstalk will be applied to a variety of different loops, and the capacities calculated. In general, the crosstalk will consist of 24 HDSL disturbers and a background AWGN of -140 dBm/Hz. The capacity for each case will be found as well as the theoretical maximum rate of each line with a 6 *SNR margin.* The SNR margin, or simply margin, is similar to a cushion given for performance. With a 6 dB margin specified, the maximum achievable rate is equivalent to the capacity of a line having noise 6 dB greater than the actual noise (or equivalently, multiplying the SNR by

0.251). When calculating the actual operating rate of an ADSL modem given some crosstalk configuration, a 6 dB margin is prudent to use because small changes in the channel transfer function or crosstalk noise will not affect the quality of the ADSL link. The loop performances are shown in Table 5.2.

Note

The changes in the channel transfer function can be the result of weather (heat, cold, rain, and so on) or of other types of DSL lines being added or removed from the binder group.

Table 5.2 Loop Performance with Fixed Crosstalk and Noise

	Channel Capacity		Achievable Rate with 6 dB Margin	
Loop	**Upstream (kbit/s)**	**Downstream (Mbit/s)**	**Upstream (kbit/s)**	**Downstream (Mbit/s)**
T1.601 #7	591	3.91	396	2.45
T1.601 #13	554	5.05	370	3.35
CSA #4	1113	12.5	899	10.4
CSA #6	1086	12.2	872	10.1
CSA #7	1196	12.2	979	10.5
CSA #8	1156	11.4	941	9.22
Mid CSA	1425	18.4	1208	16.2

Note several things about Table 5.2. First, the T1.601 loops do not support data rates as high as the CSA loops in either the upstream or downstream direction. Second, the data rate reduction varies when a 6 dB margin is imposed. The "costs" in the downstream direction are roughly 1.5 Mbps–2.5 Mbps, and in the upstream direction are in the neighborhood of 200 Kbps. Finally, note the high data rates supported by the mid-CSA loop. Because this loop is shorter than the others, you would expect it to support higher data rates in both directions.

Comparison of Different Types of Crosstalk

This section uses a CSA #6 Loop (9 kft of #26) to compare different types of crosstalk. This loop is good for comparing crosstalk because the loop contains no bridged taps and thus has a monotonically increasing insertion loss. It is often used for benchmarking in xDSL reports and publications.

The capacity of the loop is found with NEXT from ISDN, HDSL, and T1 lines, as well as NEXT and FEXT from other ADSL lines. For the downstream direction, FEXT will be from other downstream ADSL signals and ADSL NEXT will be from upstream ADSL signals. The opposite will be true for the upstream direction. In all cases, 24 disturbers will be present, and again, an AWGN of -140 dBm/Hz will be assumed. As a baseline simulation, the capacity of the loop with only the AWGN source will be given. Table 5.3 gives the resulting capacities, as well as the achievable rates for each scenario with a 6 dB margin.

Table 5.3 Loop Performance with Different Types of Crosstalk

	Channel Capacity		Achievable Rate with 6 dB Margin	
Disturbers	**Upstream (kbit/s)**	**Downstream (Mbit/s)**	**Upstream (kbit/s)**	**Downstream (Mbit/s)**
AWGN Only	2601	16.8	2385	14.7
24 ISDN NEXT	1485	14.4	1271	12.2
24 HDSL NEXT	1089	12.2	872	10.1
24 T1 NEXT	2338	7.29	2124	5.88
24 ADSL NEXT	1126	14.8	910	11.9
24 ADSL FEXT	2072	14.1	1156	12.6
Downstream ADSL NEXT	1109	2.45	894	1.67

Several things are worth highlighting in Table 5.3. First, not including the last line in the table, T1 NEXT is by far the worst disturber for the downstream direction. This result includes the 15.5 dB reduction in the T1 interfering model. This result is due to the fact that the T1 NEXT PSD is significant over the entire downstream ADSL bandwidth.

Note, however, that the T1 NEXT is not as detrimental to the upstream channel as are the other disturbers. HDSL and ADSL are the next most damaging to the upstream ADSL. Both of these disturbers span the entire upstream bandwidth.

Finally, note that ADSL FEXT is not as damaging to the downstream direction as downstream ADSL NEXT. ADSL systems have been designed so that this disturbance does not occur. In fact, this is one of the reasons that the upstream ADSL channel uses a far smaller bandwidth than the downstream channel uses. Put another way, there is no self-NEXT for a downstream ADSL channel. Some proposed "reverse ADSL" schemes in which the symmetry of the channels is reversed would cause self-NEXT to be present and severely impair the "regular" ADSL lines. Because different types of DSLs having varying effects on one another, spectral planning is essential for any major deployment of ADSL.

Industry Standard Loop and Crosstalk Configurations

Some of the standard test loops and test noise configurations appear in Table 5.4. Upstream and downstream theoretical maximum rates with a 6 dB margin are also shown. For the HDSL, ISDN, and T1 NEXT, the crosstalk was injected at the near end for both the upstream and downstream measurements.

Table 5.4 Performance over Different Standard Specified Loops

	Type and Number of Disturbers				Achievable Rates with 6 dB Margin (except where noted)	
Loop	**ADSL NEXT And FEXT**	**HDSL NEXT**	**ISDN NEXT**	**T1 NEXT**	**Upstream (kbit/s)**	**Downstream (Mbit/s)**
T1.601 #7	0	0	24	0	767	4.46
T1.601 #13	0	0	24	0	730	5.39
CSA #4	24	0	24	0	887	10.6
CSA #6	0	20	0	0	889	10.2
Mid CSA (3 dB margin only)	0	0	0	10	2325	12.2
T1.601 #13	0	0	24	0	629	5.80
CSA #4	10	10	24	0	852	9.59
CSA #6	10	10	24	0	824	9.45
CSA #8	10	10	24	0	892	8.85
CSA #6[1]	0	0	0	4	1821	6.88
Mid CSA	0	0	10	24	1981	9.43

[1] 0 dB margin. Originally, if T1 disturbers were detected, a 6 dB power boost in the downstream PSD was recommended to boost the rate of this configuration. The power boost was dropped because of the added complexity it gave to the analog portion of the ADSL modem. The result shown assumes no power boost.

VDSL Capacities

For VDSL, the capacity of different lines will be found with no crosstalk and then with several different types of disturbers. The loops investigated are the VDSL loops discussed in Chapter 3, and the reduction of capacity due to RFI is disregarded for the time being. The PSD used for the VDSL transmitter is that given in Chapter 4. From 1.1 MHz to 20 MHz, 1,000 equally spaced points approximate Eqtn. 5.23. In contrast to the ADSL performance calculations, a single result, rather than an upstream and a downstream capacity, is shown. If VDSL systems employed echo cancellation, one might argue that the calculated rates would be achievable bidirectionally. This discussion assumes, however, that the systems are not echo canceled and that the resultant bit rate must be split between an

upstream and a downstream rate (which could be done by frequency-division techniques or time-division techniques).

Note

The computational complexity of echo-canceled VDSL is much larger than that for ADSL, so VDSL systems are normally not echo canceled. In addition, this complexity may present some serious spectral compatibility problems with other DSLs.

Table 5.5 shows the capacities for VDSL loops given a 6 dB margin. For loops VDSL #1 through VDSL #4, which have a variable length and gauge segments, a 4.5 kft, #24 loop was used. Note the large rate results for VDSL Loop #5 as compared to the others. This result makes sense because the VDSL loop is much shorter than the other two.

Table 5.5 VDSL Loop Performance with Different Types of Crosstalk

	Achievable Rate with 6 dB Margin (Mbit/s)						
Disturber	**Loop #1**	**Loop #2**	**Loop #3**	**Loop #4**	**VDSL Loop #5**	**VDSL Loop #6**	**VDSL Loop #7**
AWGN Only	36.1	30.6	22.4	9.98	306	48.1	15.8
HDSL NEXT	36.1	30.6	22.4	9.98	306	48.1	15.8
ADSL NEXT	16.5	11.6	5.51	1.20	285	28.2	26.6
T1 NEXT	10.3	7.68	4.48	0.69	270	17.2	2.33
VDSL NEXT	0.91	0.69	0.31	0.02	26.6	1.62	0.19
VDSL FEXT	30.0	26.1	20.1	9.74	130	40.0	14.4

Several other points worth mentioning about Table 5.5 are the following:

- HDSL NEXT has a negligible effect on VDSL because the main energy for HDSL is well below the lower edge of the VDSL band. HDSL sidebands that overlap the VSDL band will be sufficiently attenuated so that no performance degradation is realized.
- T1 NEXT severely limits the rate of VDSL. The T1 NEXT includes the 15 dB reduction in coupling discussed in Chapter 4, reflecting binder group and distance separation. In general, T1 and VDSL deployment will have to be carefully coordinated to reduce crosstalk problems.

- ADSL has a large effect on VDSL rates. VDSL Loop #7 is especially limited by ADSL crosstalk.
- VDSL NEXT severely limits the achievable rate. In some cases, the achievable rate is below achievable ADSL rates. This condition drives the requirement for VDSL system designs to have no self-NEXT.

A comparison of achievable rates for the different VDSL Loop #1 possibilities for three different noise configurations appears in Table 5.6. As expected, shorter loops can support higher data rates. Also, loops consisting of #24 gauge twisted pair have higher achievable rates than the same length pair utilizing #26 gauge. Note that for 4.5 kft lengths, the total achievable rates get very low depending on the type of disturber (remember that the achievable rate shown in this table is the aggregate upstream and downstream rates).

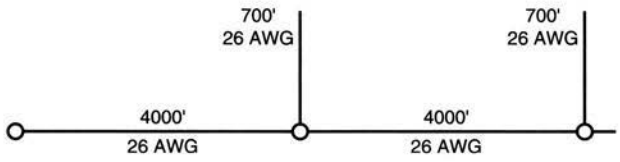
Table 5.6 Performance of VDSL Loop #1 Variations

	Achievable Rate with 6 dB Margin (Mbit/s)					
Disturber	**1.5 kft #24**	**3.0 kft #24**	**4.5 kft #24**	**1.0 kft #26**	**3.0 kft #26**	**4.5 kft #26**
AWGN Only	274	101	36.1	304	57.7	18.3
ADSL NEXT	253	79.6	16.4	283	37.0	3.17
VDSL FEXT	117	69.4	29.9	128	45.4	16.7

Usable Frequencies on Crosstalk Channels

This section focuses on a case study of a single loop with a specified crosstalk disturbance. The SNR at the receiver of the loop as a function of frequency is investigated to show which parts of the band are most capable of carrying information. The loop appears in Figure 5.3.

Figure 5.3 Loop for SNR and channel-capacity case study.



This study assumes that 20 T1 NEXT disturbers and 20 ISDN NEXT disturbers exist. In addition, a background AWGN of -140 dBm/Hz will be added to the crosstalk noise. Assuming that this loop is carrying downstream DMT ADSL, the signal power at the loop's receiver is shown in Figure 5.4.

Figure 5.4 Received signal and noise on case study loop.

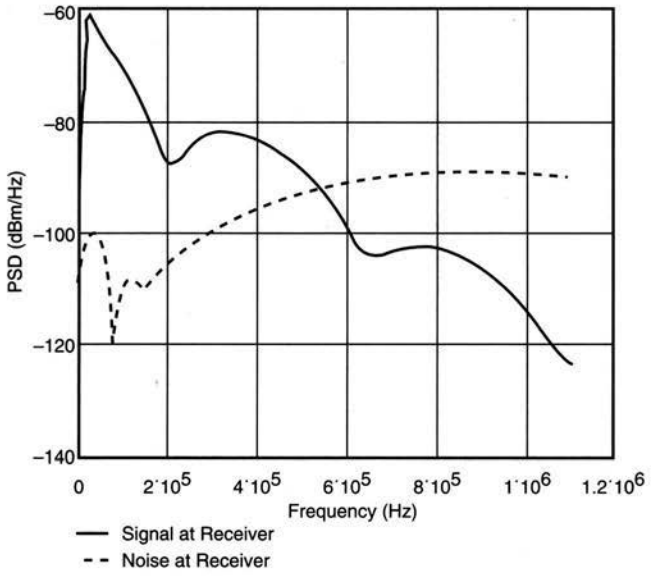


Figure 5.4 also shows the noise due to the crosstalk as well as the AWGN. You might expect areas in the frequency band at which the received signal power is greater than the noise power to be able to carry more information than those areas where the noise is greater.

Figure 5.5 shows the SNR as a function of frequency on the loop. You should be able to verify that the SNR curve is simply the difference of the two curves shown in Figure 5.4.

Note

Recall that when working in mW, you can find the SNR by doing a division, as opposed to a subtraction used when the powers are given in dBm.

Figure 5.5 SNR at the receiver on case study loop.

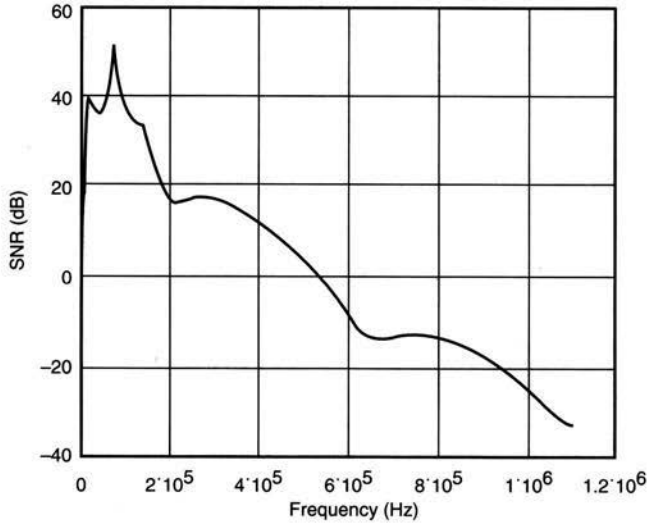
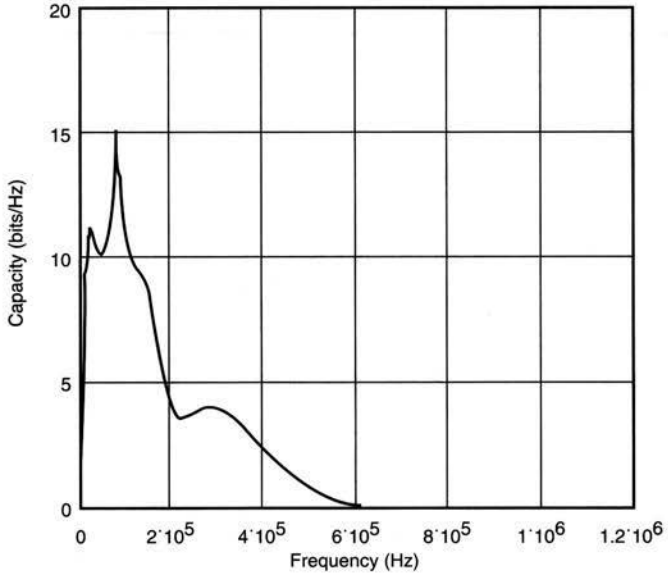


Figure 5.6 shows the information-carrying ability of the channel as a function of frequency. A 6 dB margin is assumed for this graph. The units of the y-axis of this graph are bits/Hz. Notice that the channel is able to carry more bits/Hz at frequencies where the SNR is high. At frequencies where the SNR is very low (including when it is negative), the bits/Hz that the channel can carry approaches zero.

Some systems may not be able to support areas with high information-carrying capability to the limit. For example, in one area the plot in Figure 5.6 can carry about 15 bits/Hz. An implementation may be designed to only send up to 10 bits/Hz (it would still send information at this frequency, but at 10 bits/Hz instead of 15 bits/Hz). Thus although a loop may have a very high capacity, practical implementation will sometimes limit the data rate on the line.

Figure 5.6 shows that a modulation scheme using such a channel must have a very flexible way to heavily use parts of the channel that are "good" and can transmit many bits/Hz. Likewise, the modulation scheme should be able to ignore the parts of the channel that are "bad" and support very close to zero bits/Hz. Later chapters discuss how the various modulation schemes proposed for ADSL and VDSL accomplish this goal.

Figure 5.6 Information-carrying ability as a function of frequency for the case study loop.



Summary

This chapter dealt with the maximum theoretical data rate that can reliably be sent through a channel—often called *channel capacity*. Although practical systems do not operate at capacity, it is a good benchmark for evaluating a modulation and detection system. A derivation of channel capacity, applicable to DSL over twisted pairs, was given. The main constraints for this example include a bandwidth constraint and an average PSD constraint. (A more general derivation is given in Appendix 5A at the end of this chapter.) This chapter also evaluated the capacities of different ADSL and VDSL loops with common crosstalk scenarios and examined the dependence of capacity on SNR over frequency via a case study.

Exercises

1. Find the entropy of a random variable X given that X can take on the value 0 with probability p and the value of 1 with probability 1-p. Graph H with respect to p. Note the point at which X has the greatest entropy.
2. As discussed in Chapter 4, a 2B1Q symbol can have one of four values: -3, -1, +1, and +3. If the four levels are equally likely, find the entropy of a 2B1Q symbol.

How many bits of uncertainty can be cleared up if the 2B1Q symbol is properly received and decoded?

3. Repeat exercise 2 for an 8-PAM signal with equally likely levels.
4. Graph the channel capacity of an AWGN channel according to Eqtn. 5.14 with respect to SNR. Repeat the procedure assuming that the channel has a bandwidth of 1.1 MHz.
5. Find the SNR and bits/Hz with respect to frequency of T1.601 Loop #13. Assume that the signal is downstream ADSL and that 24 ISDN NEXT disturbers exist. Find the channel capacity of this loop.
6. Evaluate the channel capacity for the case in exercise 5 assuming a 6 dB margin. Again assume that the input is an ADSL downstream signal.
7. For this chapter's case study, evaluate the channel capacity assuming a downstream ADSL signal. For the same loop, find the PSD that would achieve capacity assuming no PSD constraint, but rather a total power constraint of 20 dBm into 100 ohms. Find the resultant capacity and compare it to the PSD-constrained case.

Endnotes

1. James Aslanis and John Cioffi, Achievable Information Rates on Digital Subscriber Loops: Limiting Information Rates with Crosstalk. *IEEE Transactions on Communications,* Vol. 40, No. 2, Feb. 1992.
2. Cover, et al, Asynchronous Multiple-Access Channel Capacity. *IEEE Transactions on Information Theory*, Vol. IT-27, No. 4, July 1981.
3. Robert G. Gallager, *Information Theory and Reliable Communication.* John Wiley & Sons, New York, 1968.
4. Thomas Cover and Joy Thomas, *Elements of Information Theory.* John Wiley & Sons, New York, 1991.
5. Roger Cheng and Sergio Verdu, Gaussian Multiaccess Channels with ISI: Capacity Region and Multiuser Water-Filling. *IEEE Transactions on Information Theory*, Vol. 39, No. 3, May 1993.
6. Roman Kuc, *Introduction to Digital Signal Processing.* McGraw-Hill, New York, 1988.
7. Walter Hirt and James Massey, Capacity of the Discrete-Time Gaussian Channel with Intersymbol Interference. *IEEE Transactions on Information Theory*, May 1998.

Appendix 5A

In this chapter, the capacity of a channel was derived with two constraints on the input to the channel:

- The input power is finite and less than some W.
- The input PSD is flat over frequency.

In this appendix, the second constraint is lifted, and the capacity is derived with only the finite power constraint. Thus the treatment of capacity in the appendix is more general than the corresponding treatment in the main chapter.

In Eqtn. 5A.1, the capacity or maximum rate of the channel is given as a summation of the maximum rates of L subchannels. All quantities are given except for the power in each subchannel S_i.

Eqtn. 5A.1

$$R_{\max} = \sum_{i=1}^{L} \frac{B}{L} \log_2 \left(1 + \frac{|G_i|^2 S_i}{|H_i Q_i + Z_i|^2} \right)$$

This discussion assumes that in the original untransformed system, a power constraint W was placed on x such that the average power (normalized to 1 ohm) was Eqtn. 5A.2.

Eqtn. 5A.2

$$\sum_{i=0}^{N-1} |x_i|^2 \leq W$$

Using Parseval's relation, the power constraints of the transformed sequence becomes Eqtn. 5A.3.

Eqtn. 5A.3

$$\sum_{i=0}^{N-1} |X_i|^2 \leq N^2 W$$

Or stated in terms of power, Eqtn. 5A.4.

Eqtn. 5A.4

$$\sum_{i=0}^{N-1} |X_i|^2 \leq N^2 W$$

For notational ease, the substitution Eqtn. 5A.5 will be made:

Eqtn. 5A.5

$$T_i = \frac{|G_i|^2}{|H_i Q_i + Z_i|^2}$$

Thus the expression for capacity, including the substitution of Eqtn. 5A.5, becomes Eqtn. 5A.6.

Eqtn. 5A.6

$$R_{\max} = \sum_{i=1}^{L} \frac{B}{L} \log_2 (1 + T_i S_i)$$

As N approaches infinity, the summation can be converted to an integration and the rate of the total system can be bounded by Eqtn. 5A.7.

Eqtn. 5A.7

$$R \le \int_0^B \log_2 (1 + S(f)T(f)) df$$

The constraints on the power then become Eqtn. 5A.8 and Eqtn. 5A.9

Eqtn. 5A.8

$$S(f) > 0$$

Eqtn. 5A.9

$$\int_0^B S(f) df \le W$$

The first constraint is intuitive, as power cannot be negative, and the second constraint reflects the total power constraint.

To find an S that maximizes Eqtn. 5A.7 under the constraints of Eqtn. 5A.8 and Eqtn. 5A.9, you can use the Lagrange multiplier technique and maximize Eqtn. 5A.10.

Eqtn. 5A.10

$$\log_2 (1 + S(f)T(f)) + \lambda S(f)$$

With respect to S where λ is a Lagrange multiplier. Continuing by differentiating gives Eqtn. 5A.11.

Eqtn. 5A.11

$$0 = \frac{T(f)}{1 + S(f)T(f)} + \lambda$$

Eqtn. 5A.11 can be solved for S as Eqtn. 5A.12.

Eqtn. 5A.12

$$\begin{aligned} S(f) &= \frac{T(f) + \lambda}{\lambda T(f)} \\ &= \frac{1}{\lambda} + \frac{1}{T(f)} \\ &= \left[c - T^{-1}(f)\right]^{+} \end{aligned}$$

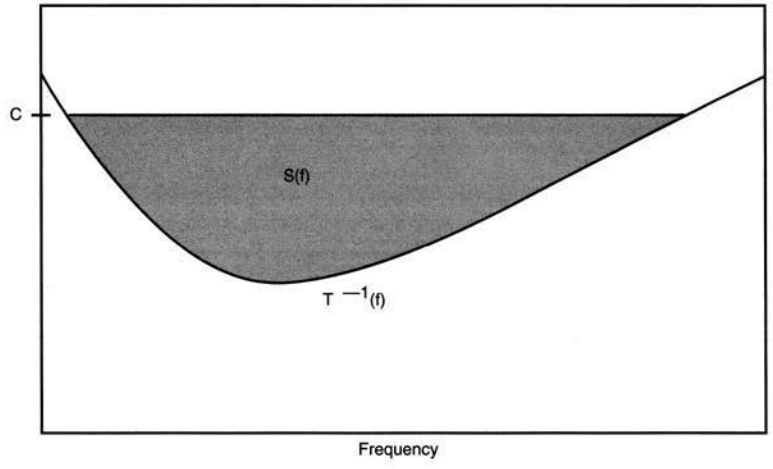
Here c is a constant to be determined by Eqtn. 5A.13.

Eqtn. 5A.13

$$\left[c - T^{-1}(f)\right]^{+} = \begin{cases} c - T^{-1}(f), & c - T^{-1}(f) \geq 0 \\ 0, & c - T^{-1}(f) < 0 \end{cases}$$

Eqtn. 5A.12 specifies the power spectral density necessary on the channel to achieve capacity. When the power spectral density is known, Eqtn. 5A.7 can be used to find the actual capacity. If T^{-1} is plotted as shown in Figure 5A.1, the power spectral density needed to achieve capacity is analogous to the distribution that water would take if poured into an imaginary container with T^{-1} as the container's bottom. For this reason, Eqtn. 5A.12 is often referred to as the "water-filling" solution. The constant c then becomes the level of the "water" such that the total power distributed in the container obeys the power constraints of the signal.

Figure 5A.1 Illustration of the water-filling solution for the capacity-achieving PSD of a channel.



CHAPTER 6

DSL Modulation Basics

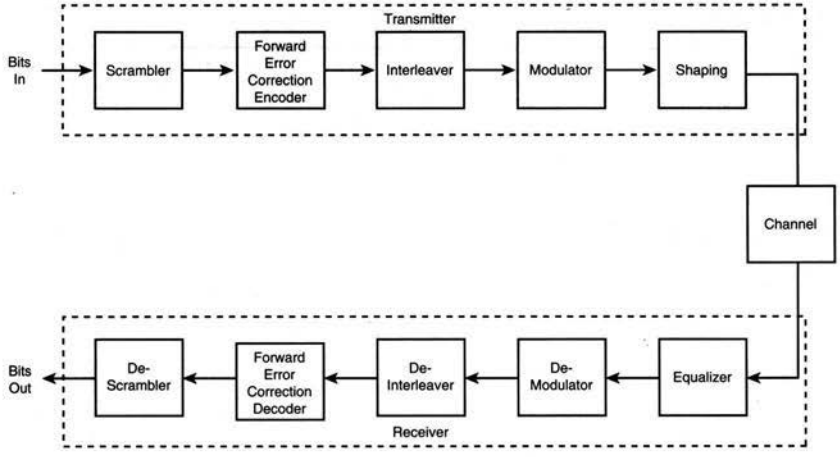
In this chapter:

- Descriptions of the different blocks used in DSL transmitters and receivers
- Basic concepts of single carrier and multicarrier modulation schemes
- Discussion of forward error correction coding and decoding
- Overview of equalization methods and the performance bounds on each

This chapter presents some of the basics of modulation systems as well as other blocks used by DSL communications systems. Subsequent chapters cover ADSL and VDSL in detail and show how the specific implementations of the basic blocks are put together to create a full DSL transmitter and receiver. Many of the topics and blocks in this chapter are also relevant to communication systems other than those used on DSLs, including voice-band modems, cable modems, and magnetic storage channels.

Figure 6.1 shows a generic block diagram of a transmitter and a receiver that is used for reference throughout this chapter. This figure is not specific to either a Carrierless Amplitude and Phase (CAP)/Quadrature Amplitude Modulation (QAM) or a discrete multitone (DMT) system, but rather it illustrates where some of the relevant blocks fit in the "big picture." Notice that most blocks in the transmitter have corresponding sister blocks in the receiver.

Figure 6.1 Transmitter and receiver block diagram for a communications system.



Modulation/Demodulation Blocks

A modulation block typically converts input bits into waveforms to be sent over the channel. A demodulation block in the receiver maps received waveforms back to the bits that most likely generated the waveform. The main idea is to re-create the bits at the demodulator output that were present at the modulator input. The following sections describe three types of modulation common in DSLs: QAM, CAP, and multitone.

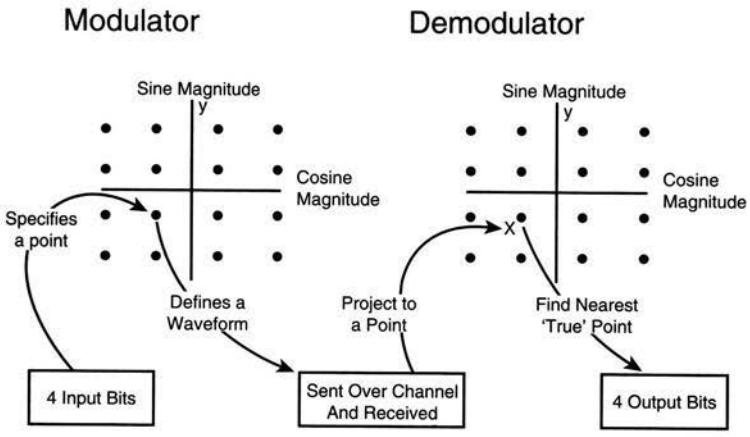
QAM Modulation

QAM utilizes a sine wave and a cosine wave with the same frequency component to convey information. The waves are sent over a single channel simultaneously, and the amplitude (including sign and magnitude) of each wave conveys the information (bits) being sent. At least one period (and sometimes more) of the waves is sent to convey a set of bits before a new set of bits is to be sent (resulting in new magnitudes for the sine and cosine waves). QAM modulation has been used for many years and is the basis for many of the voice-band modem specifications, including V.34.

A Simple QAM Example

An example of a QAM modulation system that can send four bits of information per QAM symbol appears in Figure 6.2.

Figure 6.2 An example of a QAM system sending four bits per symbol over a channel.



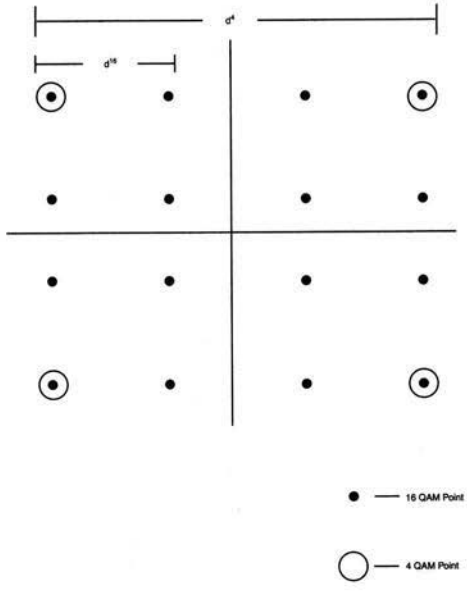
The four bits of information to be transmitted are mapped to 1 of 16 points on a QAM *constellation*. Note that for four bits of information, 16 points allow a unique point for any combination of bits. The x and y components of the point to which the bits were mapped specify the amplitude of the cosine wave and sine wave to be sent over the channel. Both the transmitter and receiver know the predetermined method of mapping between the bits and a point.

After cosine and sine waves are sent over the channel, the receiver recovers and estimates the amplitude of each wave (which normally requires significant equalization and processing as described later in the chapter). These magnitudes are projected on a constellation identical to that used at the transmitter. Again, the cosine wave amplitude is the x component, and the sine magnitude is the y component. Normally, noise and distortion in the channel and compromised electronics in the transmitter and receiver prevent the point projected onto the receiver's constellation from falling directly on top of a "true" point. The receiver, however, selects the closest "true" point to the projected point as the one the transmitter is most likely to use to generate the QAM symbol. This point is then mapped into four bits using the same mapping method employed in the transmitter (but mapping in the opposite direction). If too much noise is present at the receiver, the point projected on the constellation may be closer to the wrong known point than the accurate known point, resulting in an error estimating the recovered symbol.

This example is sometimes called 16-QAM because the constellation has 16 points. In general, other numbers of bits can be transmitted per QAM symbol. For example, if two bits per symbol were transmitted, a four-point constellation would be necessary and the modulation would be called 4-QAM. Figure 6.3 shows a 4-QAM constellation overlaid on

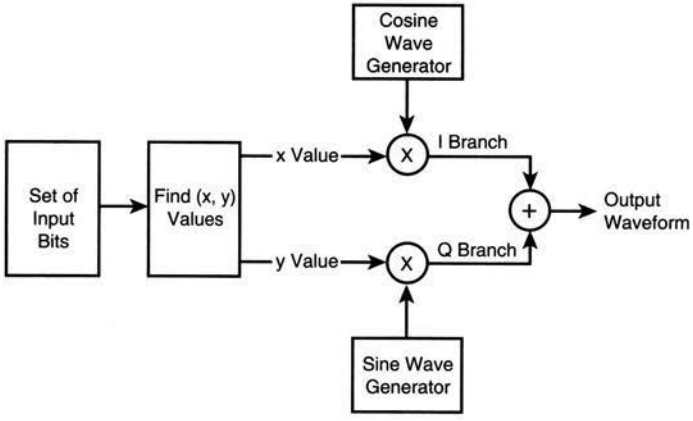
a 16-QAM constellation. The average energy of each signal set is approximately the same. Note that the distance between the points in the 4-QAM constellation (labeled d_4) is greater than the distance between the points in the 16-QAM constellation (labeled d_{16}). Consequently, on the same channel more noise is necessary to cause an error when using 4-QAM than when using 16-QAM. Said differently, 16-QAM requires a greater SNR than 4-QAM requires.

Figure 6.3 An example of a 4-QAM constellation overlaid on a 16-QAM constellation with the same average energy.



A block diagram of a QAM modulator appears in Figure 6.4. The branch of the modulator that carries the cosine wave amplitude is sometimes called the *in phase* branch. The cosine amplitude is called the in phase, or the I, component. The branch of the modulator that carries the sine wave amplitude is sometimes called the *quadrature* branch. The sine amplitude is called the quadrature, or the Q, component.

Figure 6.4 QAM modulator block diagram.



A Mathematical Treatment of QAM

Orthogonality between a sine wave and a cosine wave allows them to transmit data simultaneously over a channel. Considering a single period of each wave, the orthogonality principle can be illustrated by Eqtn. 6.1.

Eqtn. 6.1

$$\int_0^{\tau} \sin\left(\tfrac{2\pi t}{\tau}\right)\cos\left(\tfrac{2\pi t}{\tau}\right)dt = 0$$

In Eqtn. 6.1, τ is the period of the sine and cosine waves. Because of the orthogonality property, the sine and cosine functions are sometimes called *basis functions.*

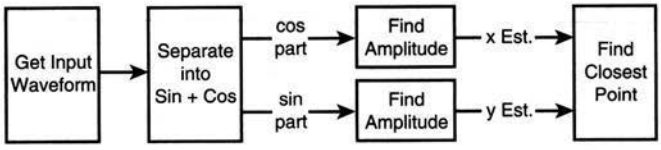
An example of a QAM demodulator appears in Figure 6.5.

The input to this block comes from the channel, and the output projects onto the receiver's constellation. If one assumes that the channel has no loss and that the receiver has perfect phase timing, then it is not difficult to write the equations for each point in Figure 6.5 for some symbol, i. Eqtn. 6.2 gives the input signal at point A.

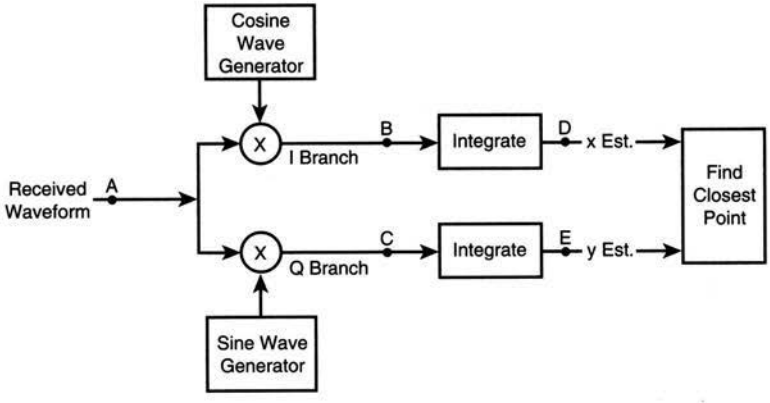
Eqtn. 6.2

$$V_A(t) = X_i \cos(\omega t) + Y_i \sin(\omega t)$$

Figure 6.5 (a) Logical view of a QAM demodulator. (b) Signal-processing view of a QAM demodulator.



(a)



(b)

In Eqtn. 6.2, X_i is the amplitude (sign and magnitude) of the cosine wave encoded at the transmitter, and Y_i is the amplitude (sign and magnitude) of the sine wave encoded at the transmitter. After passing through the multiplication blocks at points B and C, the signals are given by Eqtn. 6.3 and Eqtn. 6.4.

Eqtn. 6.3

$$V_B(t) = X_i \cos^2(\omega t) + Y_i \sin(\omega t)\cos(\omega t)$$

Eqtn. 6.4

$$V_C(t) = X_i \cos(\omega t)\sin(\omega t) + Y_i \sin^2(\omega t)$$

The signals at points B and C then independently pass through integration blocks. These blocks integrate over a single period and reset after each symbol. The switches in Figure

6.5 sample the output of the integrator at the end of each integration period. The signal at points D and E can thus be written as Eqtn. 6.5 and Eqtn. 6.6.

Eqtn. 6.5

$$V_D(t) = \int_0^{\tau} V_B(t)dt$$

$$= \int_0^{\tau} X_i \cos^2(\omega t) + Y_i \sin(\omega t)\cos(\omega t)dt$$

$$= \int_0^{\tau} X_i \cos^2(\omega t)dt + \int_0^{\tau} Y_i \sin(\omega t)\cos(\omega t)dt$$

$$= \frac{\tau X_i}{2} + 0 = \frac{\tau X_i}{2}$$

Eqtn. 6.6

$$V_E(t) = \int_0^{\tau} V_C(t)dt$$

$$= \int_0^{\tau} X_i \cos(\omega t)\sin(\omega t) + Y_i \sin^2(\omega t)dt$$

$$= \int_0^{\tau} X_i \cos(\omega t)\sin(\omega t)dt + \int_0^{\tau} Y_i \sin^2(\omega t)dt$$

$$= 0 + \frac{\tau Y_i}{2} = \frac{\tau Y_i}{2}$$

Note that the terms going to zero in Eqtn. 6.5 and Eqtn. 6.6 do so because of the orthogonality property of sines and cosines. The values at the output of the demodulator then contain a scaled estimate of the magnitudes of the received sine and cosine waves to project onto the receiver's constellation map.

Note

The scale factor can be removed before integrating by scaling the multiplication cosine and sine waves.

This analysis assumes that the baseband pulses in the modulator used to shape the symbols before multiplying by the sine and cosine waves were simple pulses with unity amplitude

during the entire symbol period. In general, a shaping filter may be used to shape the pulse before the mixing function. (The purpose of this step is to reduce the bandwidth of the transmitted signal by filtering out higher-frequency components.) If the shaping filter has a response of p(t), then the transmitted signal for symbol i will be of the form shown in Eqtn. 6.7.

Eqtn. 6.7

$$V(t) = X_i p(t - i\tau)\cos(\omega t) + Y_i p(t - i\tau)\sin(\omega t)$$

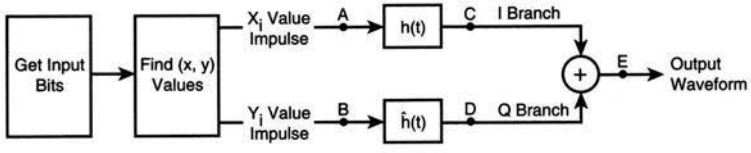
Though the shaping pulse is not very important to the basics of QAM, including the shaping term is more complete and allows comparison to CAP in the next section.

Thus I have shown mathematically how a QAM signal can be received and demodulated. Other methods of demodulation are possible as well, and most take advantage of the orthogonality property discussed in this section.

CAP Modulation

Similar to a QAM modulator, a carrierless amplitude and phase (CAP) modulator uses a constellation to encode bits at the transmitter and decode bits at the receiver. The x and y values resulting from the encoding process are then used to excite a digital filter. A CAP modulator appears in Figure 6.6.

Figure 6.6 A CAP modulator.



The modulator has two branches—one in-phase branch and one quadrature branch. The impulse responses of the digital filters are *hilbert transform pairs* or more simply, a *hilbert pair*. Two functions that form a hilbert pair are orthogonal to one another. In general, any valid hilbert pair can be used to make a CAP modulator; however, today's implementation of CAP uses a cosine wave and a sine wave shaped with a transmit pulse. Typically, CAP modulation is performed with digital filters instead of in-phase and quadrature multipliers.

When comparing a CAP modulator to a QAM modulator, consider voltages at the different points in Figure 6.6. Assume that this modulator uses the same constellation encoding method, the same size constellation, and the same symbol rate as the QAM modulator discussed earlier. The signal at each point can then be written as Eqtn. 6.8 and Eqtn. 6.9.

Eqtn. 6.8

$$V_A(t) = X_i \delta(i\tau)$$

Eqtn. 6.9

$$V_B(t) = Y_i \delta(i\tau)$$

Note that both quantities are simply discrete impulses that will excite the digital filters in the modulator.

Given the impulse responses of the filters in the modulator, the output of the two filters—found by simple convolution—due to the inputs is shown by Eqtn. 6.10 and Eqtn. 6.11.

Eqtn. 6.10

$$\begin{aligned} V_C(t) &= X_i \delta(i\tau) * h(t) \\ &= \int_0^\infty X_i \delta(i\alpha) h(t-\alpha) d\alpha \\ &= X_i h(t - i\tau) \end{aligned}$$

Eqtn. 6.11

$$\begin{aligned} V_D(t) &= Y_i \delta(i\tau) * \hat{h}(t) \\ &= \int_0^\infty Y_i \delta(i\alpha) \hat{h}(t-\alpha) d\alpha \\ &= Y_i \hat{h}(t - i\tau) \end{aligned}$$

In these equations, the sifting property was used to arrive at both results.

The output of the modulator due to symbol i is then given by Eqtn. 6.12.

Eqtn. 6.12

$$V_E(t) = X_i h(t - i\tau) + Y_i \hat{h}(t - i\tau)$$

Comparing Eqtn. 6.12 to the output of a QAM modulator with shaping given in Eqtn. 6.7, note that the two would be identical if Eqtn. 6.13 and Eqtn. 6.14 hold.

Eqtn. 6.13

$$h(t - i\tau) = p(t - i\tau)\cos(\omega t)$$

Eqtn. 6.14

$$\hat{h}(t - i\tau) = p(t - i\tau)\sin(\omega t)$$

If one further designed the system such that $\omega\tau=\pi$, then Eqtn. 6.13 and Eqtn. 6.14 can be written as Eqtn. 6.15 and Eqtn. 6.16.

Eqtn. 6.15

$$h(t - i\tau) = p(t - i\tau)\cos(\omega(t - i\tau))$$

Eqtn. 6.16

$$\hat{h}(t - i\tau) = p(t - i\tau)\sin(\omega(t - i\tau))$$

Both of these equations are valid because i is an integer. The time impulse responses of the filters with no dependence on i then become Eqtn. 6.17 and Eqtn. 6.18.

Eqtn. 6.17

$$h(t) = p(t)\cos(\omega t)$$

Eqtn. 6.18

$$\hat{h}(t) = p(t)\sin(\omega t)$$

These results are important because they show that properly relating the symbol rate and center frequency of a CAP and QAM system allows the time-domain waveforms to be identical. For other relationships of ω and τ—assuming that they are the same across a CAP and QAM system—it can be shown that the modulation systems differ by a rotation. That is, the waveforms will be identical if one of the sets of constellations used for encoding and decoding is rotated about the origin of the plane.[1]

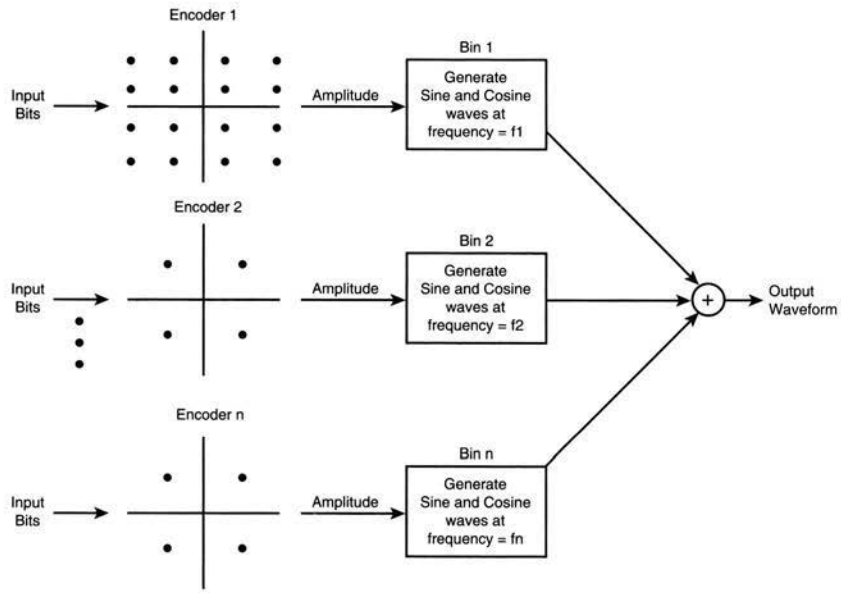
Multitone Modulation

Multitone modulation is the basis of the DMT version of ADSL as well as some multicarrier versions of VDSL. This type of modulation is sometimes called *orthogonal frequency division multiplexing* (OFDM). For simplicity, this book simply refers to multitone modulation as DMT.

DMT builds on some of the ideas of QAM. Imagine having more than one constellation encoder. Each encoder receives a set of bits that are encoded using a constellation encoder as described in the previous sections. The output values from the constellation encoder are

again the amplitudes of cosine and sine waves; however, a different sine and cosine frequency is used for each constellation encoder. All the sine and cosine waves are then summed together and sent over the channel. This waveform is a simple DMT symbol, represented by the diagram in Figure 6.7.

Figure 6.7 Conceptual view of a DMT modulator.



Assuming that one can separate the sines and cosines at different frequencies at the receiver, each set of waveforms can be independently decoded in the same way that a QAM signal can be decoded and the resultant bits output by the constellation decoders.

Note that the idea of using different frequencies to transmit information is not unique to DMT. Television and radio have readily employed such techniques. The difference here is that DMT has a "receiver" tuned to all of the channels at once, whereas the others typically tune to only one channel. Some names used for frequency channels in DMT are *frequency bins* (or *bins*), tones or DMT tones, and subchannels.

Perhaps not obvious in the previous discussion is the assumption that the waveforms in each bin are completely separable from one another. If this is not the case, then decoding for each bin is difficult because the sine and cosine waves in each bin can be corrupted by signals from other bins. One key to DMT is that the sine and cosine frequencies used in each bin should be integer multiples of a common frequency and that the symbol period, τ, be the inverse of that common frequency. (It can also be an integer multiple of the reciprocal of that frequency.)

This common frequency will be referred to as the *fundamental frequency*. From the analysis done for QAM, one can already claim that the sine and cosine waves at the fundamental frequency form basis functions. To ensure that interference does not exist between bins, one must show that sine and cosine waves from any bin are orthogonal to sine and cosine waves in any other bin. Mathematically, this orthogonality can be written as Eqtns. 6.19, 6.20, and 6.21.

Eqtn. 6.19

$$\int_0^{\tau} \cos(n\omega_f t)\cos(m\omega_f t) = 0$$

Eqtn. 6.20

$$\int_0^{\tau} \cos(n\omega_f t)\sin(m\omega_f t) = 0$$

Eqtn. 6.21

$$\int_0^{\tau} \sin(n\omega_f t)\sin(m\omega_f t) = 0$$

Here n and m are different integers, and ω_f is the radian fundamental frequency. Performing the integration in Eqtn. 6.19 yields Eqtn. 6.22.

Note that if n=m, then the first term will converge to $1/2\ \tau$, which follows from the result of Eqtn. 6.5. The relationships in Eqtn. 6.20 and Eqtn. 6.21 can be likewise shown except that in Eqtn. 6.20 the orthogonality holds even for the case of n=m, similar to the discussion around Eqtn. 6.1. Thus the demodulation of a DMT symbol relies on the orthogonality of sine and cosine waves at different frequencies as well as between a sine and cosine wave at the same frequency.

The modulation and demodulation procedures in Figure 6.7 are brute-force methods of creating and detecting a DMT symbol. These methods would be very monotonous on an actual implementation and are generally not the way DMT systems are realized. To better understand how an implementation could be simplified, consider the summation of a sine and cosine of duration τ. Such a waveform could be written as Eqtn. 6.23.

Eqtn. 6.22

$$\int_0^{\tau} \cos(n\omega_f t)\cos(m\omega_f t)$$

$$= \int_0^{\tau} \frac{1}{2}\cos((n-m)\omega_f t) + \frac{1}{2}\cos((n+m)\omega_f t)dt$$

$$= \left[\frac{\sin((n-m)\omega_f t)}{2\omega_f(n-m)} + \frac{\sin((n+m)\omega_f t)}{2\omega_f(n+m)}\right]_0^{\tau}$$

$$= \frac{\sin\left((n-m)\frac{2\pi}{\tau}\tau\right)}{2\omega_f(n-m)} + \frac{\sin\left((n+m)\frac{2\pi}{\tau}\tau\right)}{2\omega_f(n+m)}$$

$$= \frac{\sin((n-m)2\pi)}{2\omega_f(n-m)} + \frac{\sin((n+m)2\pi)}{2\omega_f(n+m)}$$

$= 0$ for n, m integers and $n \neq m$

Eqtn. 6.23

$$s(t) = \begin{cases} X_n \cos(n\omega_f t) + Y_n \sin(n\omega_f t) \text{ for } 0 < t \leq \tau \\ 0 \text{ otherwise} \end{cases}$$

Such a signal is representative of the contribution of a single bin, or simply bin n, to a single DMT symbol. If s(t) is sampled at a rate of $2*N*f_f$, the resulting nonzero values of the signal are given in Eqtn. 6.24.

Eqtn. 6.24

$$s_k = X_n \cos\left(n\omega_f \frac{k}{2Nf_f}\right) + Y_n \sin\left(n\omega_f \frac{k}{2Nf_f}\right)$$

$$= X_n \cos\left(\frac{\pi nk}{N}\right) + Y_n \sin\left(\frac{\pi nk}{N}\right) \text{ for } 0 < k \leq 2N$$

In a DMT system, N would represent the largest bin transmitting a signal. This signal is at a frequency of Nf_f. Because the Nyquist theorem states that the sampling rate for a system must be twice the largest frequency in the system, the rate of $2Nf_f$ was chosen. If we take

the *discrete fourier transform* (DFT) of s_k using 2N points in the transform, the result is Eqtn. 6.25.

Eqtn. 6.25

$$S_m = \sum_{k=0}^{2N}\left(X_n \cos\left(\frac{\pi nk}{N}\right) + Y_n \sin\left(\frac{\pi nk}{N}\right)\right) e^{\frac{-j2\pi km}{2N}}$$

$$= \begin{cases} N(X_n - jY_n) & \text{for m = n} \\ N(X_n + jY_n) & \text{for m = 2N - n} \\ 0 & \text{otherwise} \end{cases}$$

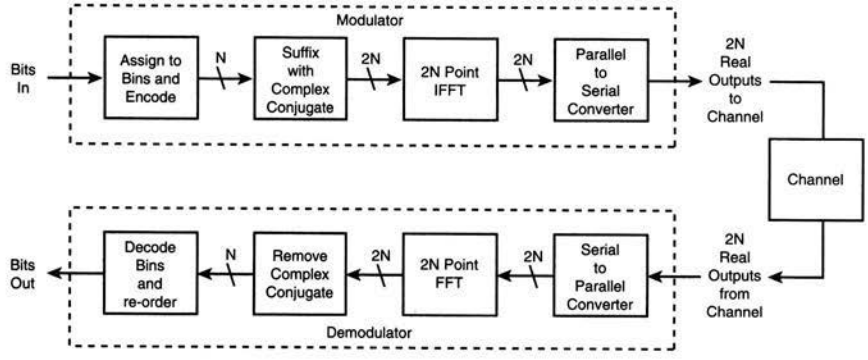
Because the DFT decomposes a signal into its frequency-domain components, the result of Eqtn. 6.25 should not be surprising. Simply put, over the 2N points being transformed, the signal had energy at only one frequency. Nonzero values at two points in the frequency domain arise because, in the frequency domain the frequency represented after the transform represents a two-sided spectrum. For all real values in the time domain (consistent with s_k), the 2N points will exhibit complex conjugate symmetry about the center of the points. This is analogous to having positive and negative frequency components resulting from a fourier transform. The zero values in Eqtn. 6.25 result from no energy being present at the frequencies represented by those points. In essence, Eqtn. 6.25 illustrates orthogonality of sines and cosines at different frequencies, as well as a sine and cosine wave at the same frequency.

The result of Eqtn. 6.25 suggests another way to produce a DMT symbol. Instead of mapping the output of a constellation encoder into a cosine and sine amplitude, the output can be mapped into a complex number in a vector. The value from the X-, or cosine, axis would represent the real part of the complex number, and the Y value, or sine magnitude, would represent the imaginary part. If the outputs of all the constellation encoders are ordered in the vector, then each vector point represents one of the DMT bins. If N bins existed in the DMT system, the complex vector would have N entries. A suffix containing the complex conjugates of the vector's original entries can then be added to this vector such that the new vector has complex conjugate symmetry. An *inverse discrete fourier transform* (IDFT) on this new vector would then produce a real-valued time-domain sequence equivalent to the original DMT modulator in Figure 6.7. Figure 6.8 shows this new method of performing DMT modulation.

Figure 6.8 also shows a method of DMT demodulation. Note that it is basically the reverse of the modulator except that a DFT is used instead of an IDFT. This approach should make sense because the DFT goes from the time domain to the frequency domain. Because the time-domain values are real, the output of the DFT block has complex conjugate symmetry. Only half of the output is then necessary to drive the constellation

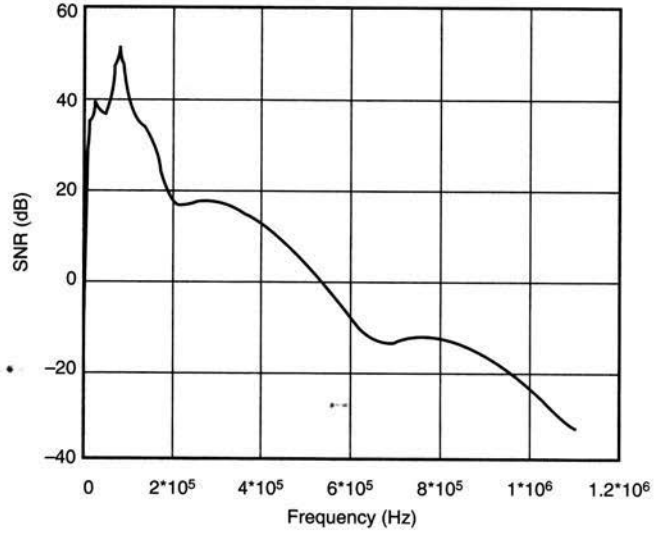
decoders. Implementations often use the fast fourier transform (FFT) and inverse fast fourier transform (IFFT) to realize the modulator and demodulator. These transform algorithms realize the DFT and IDFT with reduced computational complexity.

Figure 6.8 DMT modulation using an IDFT.



DMT allows a communications system to be very flexible and optimally utilize a channel. For example, consider the channel discussed as a case study in Chapter 5, "DSL Theoretical Capacity in Crosstalk Environments." The SNR of the channel, assuming an ADSL downstream PSD at the transmitter, appears in Figure 6.9.

Figure 6.9 SNR with respect to frequency of a sample channel; DMT bins in the areas where the SNR is high can use more dense QAM constellations.



Compared to the bins when the SNR is low, the bins occupying parts of the channel where the SNR is high can be used to transmit more bits. The process involves increasing the number of points used in the constellations of the "good" bins. If you plot the information sent as a function of frequency for this channel using DMT, the resulting curve takes on a shape similar to that shown in Figure 5.6, thus showing the optimal utilization of the channel.

DMT also allows a simple method to increase or decrease the output PSD of a transmitter in selected frequency regions. The process involves scaling the complex valued vector for the bin where power adjustment is desired before performing the IFFT. Such adjustment can boost power in regions where the channel insertion loss is poor, or reduce power in regions where interference with other systems must be avoided. Note that power boosts and reductions can be done in a CAP/QAM system also with external shaping filters, although these tend to be complex and can be difficult to implement for arbitrary shaping requirements.

Note

A classic example is the reduction of VDSL's PSD in certain bands to avoid interference with amateur radio or emergency bands.

Forward Error Correction

A forward error correction (FEC) block adds redundancy to the data to be transmitted. Usually this redundancy is a small fraction of the actual transmitted payload. The value of adding the redundancy is that the FEC block might be able to correct bits that the demodulator decodes incorrectly. The power of a forward error correction technique is often described using the term *coding gain*. A reasonable coding gain for a DSL forward error correction technique may be 3 dB at a bit error rate (BER) of 10^{-7}. Stated another way, adding the FEC to the system makes the system perform as well as a system without coding but with twice the transmit power (3 dB more transmit power). This attribute is indeed formidable.

Two types of forward error correction are common in DSL systems. The first type is a cyclic block code known as a *Reed-Solomon coding*. The second is a *convolution code* known as *trellis-coded modulation* (TCM) and ties in tightly with the constellation encoding used in both CAP/QAM and DMT modulation. The following sections discuss the basics of these two techniques. Detailed treatment of these subjects can be found in various books, including *Digital Modulation and Coding* and *Error Control Coding: Fundamentals and Applications*.[2,3]

Reed-Solomon Coding

Reed-Solomon coding was first described around 1960.[4] This type of coding is a subset of cyclic coding, which in turn is a subset of block coding. Reed-Solomon codes are also a special case of nonbinary BCH codes named for Bose and Ray-Chaudhuri and Hocquenghem who independently discovered them around 1960.[5,6] Many readers may be familiar with *cyclic redundancy check codes* (CRC codes) used in data transmission. Because CRC codes are simple and popular, they will be used as a starting point in describing Reed-Solomon codes that are typical in DSL systems.

CRC codes are typical in almost all types of layer 2 protocols including high-level data link control (HDLC)-based schemes and Ethernet. Normally, these codes operate on bits and are used for error detection but not error correction. Additionally, the number of bits being covered by the check bits is variable.

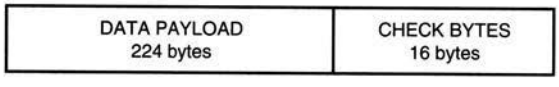
Note

Operating on bits infers that modulo 2 arithmetic is used for coding and checking. It can also be said that the arithmetic is done in GF(2).

Reed-Solomon codes used in DSL systems use *galois field arithmetic*. Specifically, they operate on GF(256), meaning that each symbol can take on one of 256 values (0 through 255). Thus each symbol is made up of eight bits—one byte long. The arithmetic rules in GF(256) define the results when two symbols are added, subtracted, multiplied, or divided. It turns out that in GF(256) carrying is not done in the same way that it is done in the base-10 decimal system.

A Reed-Solomon code produces codewords made up of a fixed number of data bytes and a fixed number of check bytes. When operating in GF(256), the total number of bytes in a codeword must be less than 255. Using different codes can vary the number of data bytes and check bytes making up the codeword. A typical DSL implementation might use a codeword size of 240 bytes, 224 of which are data bytes and 16 of which are check bytes. Figure 6.10 shows a Reed-Solomon codeword with these properties.

Figure 6.10 Example of a Reed-Solomon codeword in GF(256).



Reed-Solomon codes allow for error correction in the receiver. Note that in the receiver, the Reed-Solomon decoder block in the previous example would receive 240 bytes from the demodulator and output 224 bytes (only the data bytes) to the rest of the receiver. In

general, the number of symbols that a Reed-Solomon decoder can correct is half the number of check bytes used. Thus for the example of 16 check bytes, eight byte errors would be correctable even if these bytes all occur in a row (a burst error). This correction is an extremely powerful benefit for very little overhead (6.6% in this example).

Convolution Codes

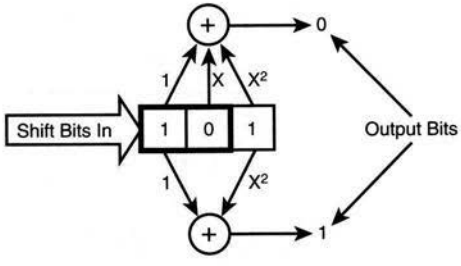
Convolutional coding differs from block coding in that the former does not have codewords made up of distinct data sections and block sections. Instead, redundancy is distributed throughout the coded data. Convolutional codes are sometimes referred to as *trellis codes*. Normally, convolutional encoding is simple, and decoding is a bit more difficult.

Note

Trellis codes can be linear or nonlinear. Convolutional codes are a subset of linear trellis codes.

Figure 6.11 shows a simple convolutional encoder.

Figure 6.11 A simple, rate 1/2 convolutional encoder; note that shifting in one bit produces two output bits.

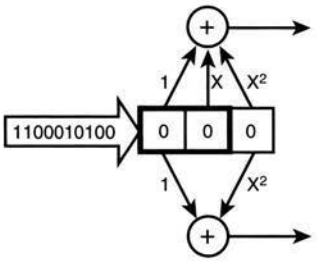


Data bits are shifted into the encoder from the left. Each data bit shifted in produces two data output bits defined by the modulo 2 additions shown. The outputs are defined by generator polynomials. This simple convolutional encoder is said to be a rate 1/2 encoder with a constraint length 2. The rate refers to the ratio of input bits to output bits, and the constraint length refers to the number of delays in the encoder. These parameters, along with the generator polynomials, determine the processing gain of the code.

Note that the first two positions in Figure 6.11 have a darkened outline. The values in these positions are called the *state of the encoder*. The convolutional encoder can be viewed as a finite state machine, changing state based on an input condition and producing an output when it changes state.

Figure 6.12 shows a simple example of using the encoder in Figure 6.11 to encode a set of bits. Note that the initial condition of the encoder is assumed to be all zeros and that the top output is taken before the bottom output.

Figure 6.12 Input and output of the sample convolutional encoder.



Input	0	0	1	0	1	0	0	0	1	1
Output	0 0	0 0	1 1	1 0	0 0	1 0	1 1	0 0	1 1	0 1

Each node in the trellis represents a state. Each line represents a pair of received bits. Note that each state has two lines leading to the state and two lines leaving it. When two bits are received, a transition occurs between the current state and the new state. The type of line connecting the current and new state (solid or dotted) determines whether the decoder will output a zero or a one in response to the two bits received. Note that two bits in produce one bit out—just the opposite of the encoder.

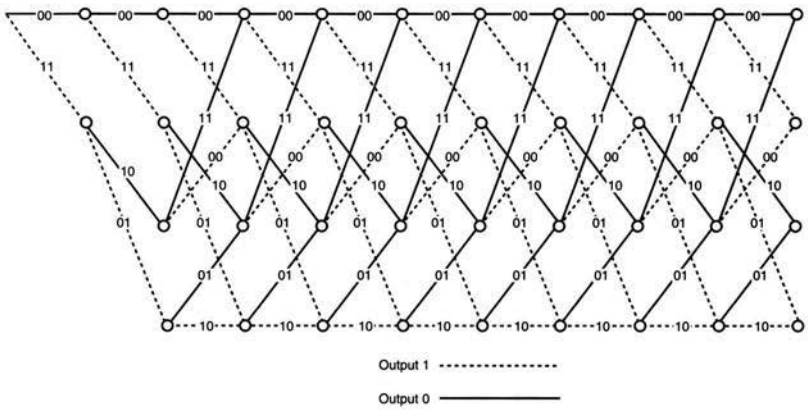
Also in Figure 6.13, note that the numbers on each line represent the input to the receiver that will cause the state transition. The type of line (solid or dotted) represents the decoder output.

Decoding of a convolutional code can be done with a trellis and the *Viterbi algorithm*. The trellis in Figure 6.13 can be used for this encoder example.

If no errors occur, the bits received while in a state correspond to one of the paths leaving the state. When errors occur on the line, the received bits may correspond to neither of the lines leaving the state and knowing which line to follow is unclear. The decoding algorithm allows for multiple paths through the trellis to be kept active. By tallying the number of mismatches (errors) that have occurred along each path, the decoding algorithm terminates those with a high error count. The error count is called a *metric*. As time passes

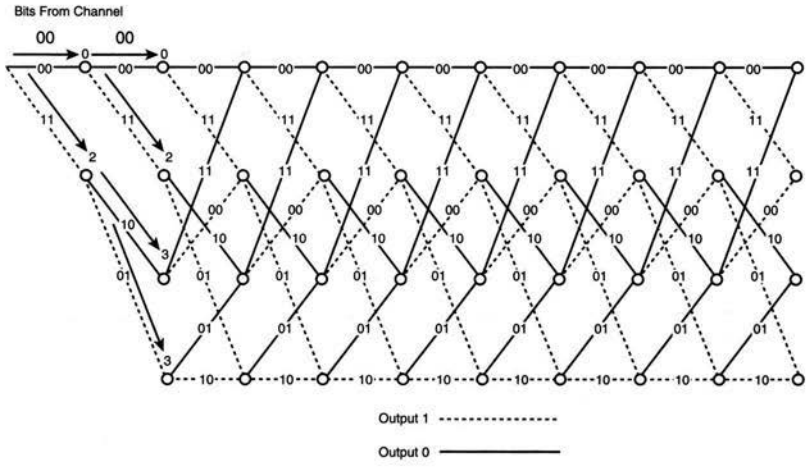
and the decoding process continues, a path with a low metric develops, and all others are terminated. This path is then used to produce the output of the decoder.

Figure 6.13 A trellis that can be used to decode the sample convolutional encoder: each node represents one of the four states.



An example of decoding is the best way to understand the decoding algorithm. Consider the coded output from Figure 6.12. The decoding algorithm for the first four bits is shown in Figure 6.14.

Figure 6.14 Trellis decoding example; the first four received bits are zeros and begin the decoding process.



The received bits are shown above the trellis (00, 00). For these four bits, all paths in the trellis are kept alive (this step is just to get the algorithm started). At each node, a metric is computed that counts the mismatches between the received bits and the path bits. (Note that the metric is a running sum for each path.) At this point, the paths are extended using the following rules:

1. Two lines will lead to each node in the next set of states.
2. For each node, follow only one line to each node, specifically, the line having the lowest metric.

Note

The example being discussed uses hard-decision decoding. Another method, using soft decisions, does not completely decode the received bits before the trellis, but instead assigns a metric to each received bit, indicating how close to a one or zero it is. Soft decoding can outperform hard decoding by several dB.

3. Terminate the other path that would arrive at that node.

Note that four paths always remain active. Ideally, one main path develops through the trellis, and all others terminate. In actual practice, some delay is necessary to identify the correct path.

Turning back to the example, consider the next two bits being received. This situation is shown in Figure 6.15.

Figure 6.15 Example of moving along the trellis—only one of the two lines leading each state is followed.

